Supporting Information for:

Hydrogen Bonds Dictate O_2 Capture and Release within a Zinc Tripod

*Eric W. Dahl,[a] John J. Kiernicki,[a] Matthias Zeller,[b] and Nathaniel K. Szymczak[a]**

[a]Department of Chemistry, University of Michigan, Ann Arbor, Michigan 48109, United States

[b]H.C. Brown Laboratory, Department of Chemistry, Purdue University, West Lafayette, Indiana 44555, United States

Table of Contents:

General Considerations. All manipulations, unless otherwise stated, were performed open to air on the benchtop. Zinc triflate, zinc perchlorate hexahydrate, zinc nitrate hexahydrate, hydrogen peroxide (30%), diisopropylethylamine, trimethylamine, sodium azide, tetrabutylammonium chloride, ceric ammonium nitrate, and reagent grade solvents were purchased from commercial vendors and used as received. L^R (R = OMe, H, CF_3, OPh),[1] tris(2-pyridylmethyl)amine,[2] and tris(6-bromo-2-pyridylmethyl)amine[3] were synthesized according to literature procedures. Caution! Azides and perchlorates present explosion risks and should only be handled on small scales.

NMR spectra were recorded on Varian Vnmrs 700 or Varian MR400 spectrometers. ^1H and ^{13}C chemical shifts are reported in parts per million (ppm) relative to tetramethylsilane and referenced internally to the residual solvent peak. ^{19}F spectra were referenced on a unified scale, where the single primary reference is the frequency of the residual solvent peak of the ^1H NMR spectrum. Multiplicities are reported as follows: singlet (s), doublet (d), triplet (t), quartet (q). Infrared spectra were recorded using a Nicolet iS10 FT-IR spectrometer either as neat solids or in DCM solution. Combustion analysis was performed by Atlantic Microlab, Inc., Norcross, Georgia.

Single crystals of $\mathbf{1^{OMe}}$, $\mathbf{1^{CF3}}$, $\mathbf{2^{H}}$, and $(L^H)Zn(OH)(OTf)$ suitable for X-ray diffraction were coated with poly(isobutylene) oil and mounted on a Rigaku AFC10K Saturn 944+ CCD-based X-ray diffractometer equipped with a low temperature device and Micromax-007HF Cu-target microfocus rotating anode (λ = 1.54187 Å). The data were collected using CrystalClear 2.011 and processed using *CrysAlis PRO* 1.171.38.41. Empirical absorption correction was applied using spherical harmonics, as implemented in the SCALE3 ABSPACK scaling algorithm. Single crystals of $(TPA)Zn(N_3)_2$ suitable for X-ray diffraction were coated with poly(isobutylene) oil and transferred to the goniometer head of a Bruker AXS D8 Quest diffractometer with kappa geometry, an I-μ-S microsource X-ray tube, laterally graded multilayer (Goebel) mirror for monochromatization, a Photon2 CMOS area detector and an Oxford Cryosystems low temperature device. Examination and data collection were performed with Cu Kα radiation (λ = 1.54184 Å). Single crystals of $\mathbf{1^{H}}$, $\mathbf{1^{NMe2}}$, $\mathbf{2^{OMe}}$, $\mathbf{2^{NMe2}}$, $\mathbf{2^{CF3}}$, $[(L^H)ZnCl][OTf]$, and $[(TPA)Zn(N_3)][ClO_4]$ suitable for X-ray diffraction, were coated with poly(isobutylene) oil and transferred to the goniometer head of a Bruker AXS D8 Quest diffractometer with a fixed chi angle, a sealed tube fine focus X-ray tube, single crystal curved graphite incident beam monochromator and a Photon100 CMOS area detector. Examination and data collection were performed with Mo Kα radiation (λ = 0.71073 Å). For both Quest instruments, data were collected, reflections were indexed and processed, and the files scaled and corrected for absorption using APEX3.[4] For all samples, the space groups were assigned and the structures were solved by direct methods using XPREP within the SHELXTL suite of programs[5] and refined by full matrix least squares against F^2 with all reflections using Shelxl2018[6] using the graphical interface Shelxle.[7] If not specified otherwise, H atoms attached to carbon atoms were positioned geometrically and constrained to ride on their parent atoms, with carbon hydrogen bond distances of 0.95 Å for and aromatic C-H, 1.00, 0.99 and 0.98 Å for aliphatic C-H, CH_2, and CH_3 moieties, respectively. Methyl H atoms were allowed to rotate but not to tip to best fit the experimental electron density. $U_{iso}(H)$ values were set to a multiple of $U_{eq}(C)$ with 1.5 for CH_3, and 1.2 for CH_2, C-H and N-H units, respectively. Additional data collection and refinement details, including description of disorder (where present) can be found with the individual structure descriptions, below.

Synthesis of tris(6-(4-dimethylaminophenyl)amino-2-pyridylmethyl)amine (L^{NMe2}). In the air, a 20 mL glass scintillation vial was charged with Br_3tpa (0.200 g, 0.3795 mmol), $Pd(OAc)_2$ (0.0077 g, 0.0342 mmol), BINAP (0.0319 g, 0.0512 mmol), Cs_2CO_3 (0.7421 g, 2.277 mmol), N,N-dimethyl-*p*-phenyldiamine (0.4651 g, 3.4155 mmol), and a Teflon stirbar. 20 mL of N_2-sparged toluene was added and the vial was quickly sealed with a Teflon-lined cap. The solution was heated at 100 °C with vigorous stirring (1300 rpm) for 18 hours. Following heating, the reaction was cooled to room temperature and 20 mL of CH_2Cl_2 was added and stirred for an additional 5 min. The slurry was filtered over Celite and rinsed with CH_2Cl_2 (2 x 10 mL). The filtrate was then dry loaded onto silica gel via rotary evaporation. The dry loaded product was purified by flash chromatography on a Biotage Isolera One using a 25 g self-packed silica gel column. Method: 3 column volumes (CV) of 70% hexane: 30% ethyl acetate, then a gradient of 15 CV to 100% ethyl acetate, then 10 CV of 100% ethyl acetate. Product elutes between 20-26 column volumes. Fractions containing product were evaporated to dryness via rotary evaporation. The brown solid was further purified by recrystallization from 4 mL hot toluene. The light brown powder precipitates at room temperature and was isolated and dried overnight in vacuo to obtain pure L^{NMe2} (0.127 g, 0.183 mmol, 48%). ^{1}H NMR (700 MHz, CD_2Cl_2) δ = 7.41 (dd, *J* = 7.3, 8.2, 3H, pyridine-C*H*), 7.20 (d, *J* = 8.5, 6H, phenyl-C*H*), 7.02 (d, *J* = 7.3, 3H, pyridine-C*H*), 6.73 (d, *J* = 8.5, 6H, phenyl-C*H*), 6.49 (d, *J* = 8.2, 3H, pyridine-C*H*), 6.30 (s, 3H, N*H*), 3.72 (s, 6H, N(CH_2)$_3$), 2.91 (s, 18H, N(CH_3)$_2$). ^{13}C NMR (176 MHz, CD_2Cl_2) δ = 159.2 (pyridine-*C*), 157.5 (pyridine-*C*), 148.2 (phenyl-*C*), 138.2 (pyridine-*C*H), 130.6 (phenyl-*C*), 124.2 (phenyl-*C*H), 113.8 (phenyl-*C*H), 113.0 (pyridine-*C*H), 105.2 (pyridine-*C*H), 60.6 (N(*C*H_2)$_3$), 41.2 (N(*C*H_3)$_2$). HRMS (ESI-TOF) m/z: [L^{NMe2}+H]$^+$ Calc. for $C_{42}H_{49}N_{10}$: 693.4142; Found: 693.4185.

Synthesis of $[(L^H)_2Zn_2O_2][OTf]_2$ from H_2O_2. Open to air, a 20 mL scintillation vial was charged with zinc triflate (0.086 g, 0.237 mmol), L^H (0.134 g, 0.238 mmol), and 4 mL MeCN and stirred for 5 min. To this vial, hydrogen peroxide (30% in H_2O; 54 µL, 0.476 mmol) and diisopropylethylamine (42 µL, 0.241 mmol) was added to the vial in succession and stirred for 5 min. Diethyl ether (15 mL) was added to induce precipitation of an off-white solid. The solution was decanted and the resulting powder washed with diethyl ether (3 x 10 mL) and dried to afford white powder assigned as $[(L^H)_2Zn_2O_2][OTf]_2$ (0.110 g, 0.069 mmol, 58%). The bulk sample was analyzed via elemental analysis: Calc. for $C_{74}H_{66}N_{14}O_8F_6S_2Zn_2$: C, 55.96, H, 4.19, N, 12.35; Found: C, 52.97, H, 4.24, N, 11.63. Single, X-ray quality crystals were obtained by slow diffusion of diethyl ether into an acetonitrile solution at room temperature. ^{1}H NMR (400 MHz, MeCN, 25 °C) δ = 3.96 (d, *J* = 15.6, 6H, N(CH_2)$_3$), 4.11 (d, *J* = 15.6, 6H, N(CH_2)$_3$), 6.03 (d, *J* = 8.6, 6H, pyridine-C*H*), 6.67 (d, *J* = 7.3, 12H, phenyl-C*H*), 6.77 (m, 24H), 7.22 (dd, *J* = 7.2, 8.6, 6H, pyridine-C*H*), 10.21 (s, 6H, N*H*). ^{13}C NMR (125.76 MHz, CD_3CN, 25 °C) δ = 56.02 (N(*C*H_2)$_3$), 110.60 (pyridine-*C*H), 114.76 (pyridine-*C*H), 124.19 (phenyl-*C*H), 126.00 (phenyl-*C*), 129.96 (phenyl-*C*H), 139.02 (pyridine-*C*H), 142.10 (phenyl-*C*), 152.51 (pyridine-*C*), 158.88 (pyridine-*C*). ^{19}F NMR (376.84 MHz, CD_3CN, 25 °C) δ = -79.38.

Synthesis of $[(L^H)_2Zn_2O_2][OTf]_2$ from O_2. In a glovebox, a 20 mL scintillation vial was charged with zinc triflate (0.0068 g, 0.0187 mmol), L^H (0.0105 g, 0.0186 mmol), 4 mL MeCN and a stir bar and stirred for 20 min. The vial was sealed with a 14/20 rubber septum. A separate vial was charged with cobaltocene (0.0035 g, 0.0185 mmol), 2 mL MeCN, and a stir bar and stirred for 20 min and sealed with a 14/20 rubber septum. Both vials were removed from the glovebox. The zinc containing vial was sparged with dry dioxygen for 5 min. The MeCN solution of cobaltocene was withdrawn with a syringe and added rapidly to the zinc containing vial resulting in an immediate color change to yellow (slower addition resulted in greatly diminished conversion to $[(L^H)_2Zn_2O_2][OTf]_2$). The solution was stirred for 15 min then exposed to air. ^{1}H NMR analysis (CH_3CN) revealed 89% conversion to $[(L^H)_2Zn_2O_2][OTf]_2$ by integrating versus a phenyltrimethylsilane standard. The only other species present is $(L^H)Zn(OH)(OTf)$ (independent synthesis described below).

Independent synthesis of (L^H)Zn(OH)(OTf). A 20 mL scintillation vial was charged with zinc triflate (0.018 g, 0.050 mmol), L^H (0.029 g, 0.051 mmol), and 6 mL MeCN and stirred for 10 min. To the solution, KOH (0.004 g, 0.071 mmol) was added and stirred an additional 10 min. Volatiles were removed in vacuo. The residue was extracted into 6 mL DCM, filtered, dried, and washed with 2 x 10 mL diethyl ether to afford an off-white powder (0.024 g, 0.030 mmol, 59%) assigned as (L^H)Zn(OH)(OTf). ^{1}H NMR (500 MHz, MeCN, 25 °C) δ = 4.09 (s, 6H, N(C*H*$_2$)$_3$), 6.70 (d, *J* = 6.0, 3H, pyridine-C*H*), 6.93 (d, *J* = 6.0, 3H, pyridine-C*H*), 7.05 (m, 6H, phenyl-C*H*), 7.08 (t, *J* = 7.0, 3H, pyridine-C*H*), 7.26 (t, *J* = 7.5, 6H, phenyl-*C*H), 7.59 (t, *J* = 8.5, 3H, phenyl-C*H*), 11.30 (s, 3H, N*H*). ^{13}C NMR (125.76 MHz, CD_3CN, 25 °C) δ = 59.38 (N(*C*H$_2$)$_3$), 109.30 (pyridine-*C*H), 113.78 (pyridine-*C*H), 122.78 (phenyl-*C*H), 125.23 (phenyl-*C*), 130.50 (phenyl-*C*H), 140.44 (pyridine-*C*H), 142.16 (phenyl-*C*), 153.50 (pyridine-*C*), 158.39 (pyridine-*C*). ^{19}F NMR (376.84 MHz, CD_3CN, 25 °C) δ = -79.20.

Synthesis of [(L^{OMe})$_2$Zn$_2$O$_2$][OTf]$_2$. Open to air, a 20 mL scintillation vial was charged with zinc triflate (0.0334 g, 0.0919 mmol), L^{OMe} (0.0619 g, 0.0946 mmol), and 2 mL MeCN and stirred for 5 min. To this vial, hydrogen peroxide (30% in H_2O; 19.3 µL, 0.1892 mmol) and diisopropylethylamine (16.5 µL, 0.0946 mmol) was added to the vial in succession and stirred for 10 min. Diethyl ether (2 mL) was added to facilitate precipitation. The white precipitate was collected, washed with diethyl ether (2 x 2 mL) and dried to afford a white powder assigned as [(L^{OMe})$_2$Zn$_2$O$_2$][OTf]$_2$ (0.0700 g, 0.0396 mmol, 86%). The bulk sample was analyzed via elemental analysis: Calc. for $C_{80}H_{78}N_{14}O_{14}F_6S_2Zn_2$: C, 54.33, H, 4.45, N, 11.09; Found: C, 52.25, H, 4.39, N, 10.60. Single, X-ray quality crystals were obtained by slow diffusion of diethyl ether into an acetonitrile solution at room temperature. ^{1}H NMR (400 MHz, MeCN, 25 °C) δ = 3.51 (s, 18H, OC*H*$_3$), 3.92 (d, *J* = 15.6, 6H, N(C*H*$_2$)$_3$), 4.06 (d, *J* = 15.6, 6H, N(C*H*$_2$)$_3$), 6.00 (d, *J* = 8.6, 6H, pyridine-C*H*), 6.31 (d, *J* = 8.9, 12H, phenyl-C*H*), 6.62 (d, *J* = 7.1, 6H, pyridine-C*H*), 6.73 (d, *J* = 8.9, 12H, phenyl-C*H*), 7.23 (dd, *J* = 7.1, 8.6, 6H, pyridine-C*H*), 10.14 (s, 6H, N*H*). ^{13}C NMR (125.76 MHz, CD_3CN, 25 °C) δ = 55.75 (O*C*H$_3$), 55.98 (N(*C*H$_2$)$_3$), 110.10 (pyridine-*C*H), 113.95 (pyridine-*C*H), 115.09 (phenyl-*C*H), 125.89 (phenyl-*C*H), 131.54 (phenyl-*C*), 141.52 (pyridine-*C*H), 152.53 (phenyl-*C*), 157.83 (pyridine-*C*), 159.20 (pyridine-*C*). ^{19}F NMR (376.84 MHz, CD_3CN, 25 °C) δ = -79.37.

Synthesis of [(L^{NMe2})$_2$Zn$_2$O$_2$][OTf]$_2$. Open to air, a 20 mL scintillation vial was charged with zinc triflate (0.0280 g, 0.0770 mmol), L^{NMe2} (0.0534 g, 0.0771 mmol), and 2 mL MeCN and stirred for 5 min. To this vial, hydrogen peroxide (30% in H_2O; 15.7 µL, 0.1542 mmol) and diisopropylethylamine (13.4 µL, 0.0771 mmol) was added in succession and stirred for 10 min. Diethyl ether (5 mL) was added to facilitate precipitation. The off-white precipitate was collected, washed with diethyl ether (3 x 10 mL) and dried to afford an off-white powder assigned as [(L^{NMe2})$_2$Zn$_2$O$_2$][OTf]$_2$ (0.0527 g, 0.0285 mmol, 74%). The bulk sample was analyzed via elemental analysis: Calc. for $C_{86}H_{96}N_{20}O_8F_6S_2Zn_2$: C, 55.93, H, 5.24, N, 15.17; Found: C, 56.06, H, 5.43, N, 14.99. Single, X-ray quality crystals were obtained by slow diffusion of *n*-pentane into 1,2-dichloroethane solution at room temperature. ^{1}H NMR (400 MHz, MeCN, 25 °C) δ = 2.66 (s, 36H, N(C*H*$_3$)$_2$), 3.86 (d, *J* = 15.5, 6H, N(C*H*$_2$)$_3$), 4.00 (d, *J* = 15.5, 6H, N(C*H*$_2$)$_3$), 6.00 (d, *J* = 8.6, 6H, pyridine-C*H*), 6.11 (d, *J* = 9.0, 12H, phenyl-C*H*), 6.52 (d, *J* = 7.1, 6H, pyridine-C*H*), 6.66 (d, *J* = 9.0 Hz, 12H, phenyl-C*H*), 7.13 (t, *J* = 7.5, 6H, pyridine-C*H*) 10.14 (s, 6H, N*H*). ^{13}C NMR (125.76 MHz, CD_3CN, 25 °C) δ = 40.64 (N(*C*H$_3$)$_2$), 56.04 (N(*C*H$_2$)$_3$), 109.89 (pyridine-*C*H), 113.19 (pyridine-*C*H), 113.44 (phenyl-*C*H), 125.52 (phenyl-C*H*), 127.71 (phenyl-*C*), 141.26 (pyridine-*C*H), 149.24, 152.28, 159.33 (pyridine-*C*). ^{19}F NMR (376.84 MHz, CD_3CN, 25 °C) δ = -79.10.

Synthesis of $[(L^{CF3})_2Zn_2O_2][OTf]_2$. Open to air, a 20 mL scintillation vial was charged with zinc triflate (0.0347 g, 0.0955 mmol), L^{CF3} (0.0722 g, 0.0940 mmol), and 2 mL MeCN and stirred for 5 min. To this vial, hydrogen peroxide (30% in H_2O; 19.2 µL, 0.1882 mmol) and diisopropylethylamine (16.4 µL, 0.0941 mmol) was added in succession and stirred for 10 min. Volatiles were removed in vacuo. The resulting solid was redissolved in 1 mL MeCN followed by 4 mL diethyl ether to facilitate precipitation. The white precipitate was collected, washed with diethyl ether (2 x 2 mL) and dried to afford a white powder assigned as $[(L^{CF3})_2Zn_2O_2][OTf]_2$ (0.0546 g, 0.0274 mmol, 58%). The bulk sample was analyzed via elemental analysis: Calc. for $C_{80}H_{60}N_{14}O_8F_{24}S_2Zn_2$: C, 48.13, H, 3.03, N, 9.82; Found: C, 46.36, H, 3.34, N, 9.09. Single, X-ray quality crystals were obtained by slow diffusion of diethyl ether into an acetonitrile solution at room temperature. ^{1}H NMR (400 MHz, MeCN, 25 °C) δ = 4.08 (d, *J* = 15.9, 6H, N(C*H*$_2$)$_3$), 4.22 (d, *J* = 15.9, 6H, N(C*H*$_2$)$_3$), 6.12 (d, *J* = 8.5, 6H, pyridine-C*H*), 6.86 (d, *J* = 7.2, 6H, pyridine-C*H*), 6.89 (d, *J* = 8.4, 12H, phenyl-C*H*), 7.07 (d, *J* = 8.4, 12H, phenyl-C*H*), 7.34 (dd, *J* = 7.2, 8.5, 6H, pyridine-C*H*), 10.18 (s, 6H, N*H*). ^{13}C NMR (125.76 MHz, CD_3CN, 25 °C) δ = 56.03 (N(*C*H$_2$)$_3$), 111.07 (pyridine-*C*H), 116.36 (pyridine-*C*H), 123.98 (*o*-phenyl-*C*H), 124.96 (q, *J* = 271.0, *C*F$_3$), 126.81 (q, *J* = 32.4, *p*-phenyl-*C*), 126.56 (q, *J* = 3.7, *m*-phenyl-*C*H), 142.54, 143.09, 153.27 (pyridine-*C*), 158.19 (pyridine-*C*). ^{19}F NMR (376.84 MHz, CD_3CN, 25 °C) δ = -62.97 (phenyl-C*F*$_3$), -79.37 (OTf).

Synthesis of $(L^H)Zn(N_3)_2$. A 20 mL scintillation vial was charged with zinc perchlorate hexahydrate (0.012 g, 0.032 mmol). A separate vial containing L^H (0.019 g, 0.033 mmol) in 4 mL acetone was added to the zinc containing vial and stirred. After 30 min, sodium azide (0.014 g, 0.215 mmol) was added. After 2 hr, volatiles were removed in vacuo. The resulting solid was extracted into 6 mL CH_2Cl_2, filtered, dried, and washed with 15 mL diethyl ether to afford an off-white powder assigned as $(L^H)Zn(N_3)_2$ (0.011 g, 0.015 mmol, 48%). ^{1}H NMR (500 MHz, CD_2Cl_2, 25 °C) δ = 4.11 (s, 6H, N(C*H*$_2$)$_3$), 6.48 (d, *J* = 7.0, 3H, pyridine-C*H*), 6.78 (d, *J* = 8.0, 3H, pyridine-C*H*), 6.96 (d, *J* = 7.5, 6H, phenyl-C*H*), 7.04 (t, *J* = 7.5, 3H, phenyl-C*H*), 7.20 (t, *J* = 7.5, 6H, phenyl-C*H*), 7.35 (t, *J* = 8.0, 3H, pyridine-C*H*), 9.31 (s, 3H, N*H*). ^{13}C NMR (125.76 MHz, CD_2Cl_2, 25 °C) δ = 61.42 (N(*C*H$_2$)$_3$), 108.01 (pyridine-*C*H), 113.16 (pyridine-*C*H), 122.34 (phenyl-*C*H), 124.55 (phenyl-*C*H), 129.80 (phenyl-*C*H), 139.46 (pyridine-*C*H), 140.05 (phenyl-*C*), 152.55 (pyridine-*C*), 157.12 (pyridine-*C*).

Synthesis of $(L^{OMe})Zn(N_3)_2$. A 20 mL scintillation vial was charged with zinc perchlorate hexahydrate (0.010 g, 0.027 mmol). A separate vial containing L^{OMe} (0.018 g, 0.028 mmol) in 4 mL acetone was added to the zinc containing vial and stirred. After 30 min, sodium azide (0.011 g, 0.169 mmol) was added. After 3 hr, volatiles were removed in vacuo. The resulting solid was extracted into 6 mL CH_2Cl_2, filtered, dried, and washed with 10 mL diethyl ether to afford an off-white powder assigned as $(L^{OMe})Zn(N_3)_2$ (0.021 g, 0.026 mmol, 98%). Single, X-ray quality crystals were obtained by slow diffusion of diethyl ether into an acetonitrile solution at room temperature. ^{1}H NMR (500 MHz, CD_2Cl_2, 25 °C) δ = 3.78 (s, 9H, OC*H*$_3$), 4.09 (s, 6H, N(C*H*$_2$)$_3$), 6.50 (d, *J* = 7.2, 3H, pyridine-C*H*), 6.57 (d, *J* = 8.8, 3H, pyridine-C*H*), 6.81 (d, *J* = 8.8, 6H, phenyl-C*H*), 6.96 (d, *J* = 8.8, 6H, phenyl-C*H*), 7.36 (t, *J* = 8.0, 3H, pyridine-C*H*), 8.99 (s, 3H, N*H*). ^{13}C NMR (125.76 MHz, CD_2Cl_2, 25 °C) δ = 55.87 (O*C*H$_3$), 60.30 (N(*C*H$_2$)$_3$), 107.96 (pyridine-*C*H), 112.71 (pyridine-*C*H), 115.15 (phenyl-*C*H), 125.87 (phenyl-*C*H), 131.68 (pyridine-*C*H), 140.49 (phenyl-*C*), 152.22 (pyridine-*C*), 157.82 (phenyl-*C*), 158.58 (pyridine-*C*).

Synthesis of (L^{NMe2})$Zn(N_3)_2$. A 20 mL scintillation vial was charged with zinc perchlorate hexahydrate (0.011 g, 0.030 mmol). The contents of a separate vial containing L^{NMe2} (0.021 g, 0.030 mmol) in 4 mL acetone were added to the zinc containing vial and stirred. After 30 min, sodium azide (0.012 g, 0.185 mmol) was added. After 3 hr, volatiles were removed in vacuo. The resulting solid was extracted into 10 mL CH_2Cl_2, filtered, dried, and washed with diethyl ether (10 mL), benzene (10 mL), and finally *n*-pentane (10 mL) to afford a yellow powder assigned as (L^{NMe2})$Zn(N_3)_2$ (0.018 g, 0.021 mmol, 72%). Single, X-ray quality crystals were obtained by slow diffusion of diethyl ether into an acetonitrile solution at room temperature. ^{1}H NMR (500 MHz, CD_2Cl_2, 25 °C) δ = 2.93 (s, 18H, N(CH_3)$_2$), 4.05 (s, 6H, N(CH_2)$_3$), 6.50 (d, *J* = 6.8, 3H, pyridine-C*H*), 6.57 (d, *J* = 8.4, 3H, pyridine-C*H*), 6.66 (d, *J* = 8.8, 6H, phenyl-C*H*), 6.98 (d, *J* = 8.8, 6H, phenyl-C*H*), 7.37 (t, *J* = 8.0, 3H, pyridine-C*H*), 8.90 (s, 3H, N*H*). ^{13}C NMR (125.76 MHz, CD_2Cl_2, 25 °C) δ = 40.90 (N(*C*H_3)$_2$), 53.43 (N(*C*H_2)$_3$), 108.25 (pyridine-*C*H), 112.25 (pyridine-*C*H), 113.58 (phenyl-*C*H), 126.45 (phenyl-C*H*), 127.51 (pyridine-*C*H), 140.48 (phenyl-*C*), 149.47 (phenyl-*C*), 152.00 (pyridine-*C*), 159.56 (pyridine-*C*).

Synthesis of (L^{CF3})$Zn(N_3)_2$. A 20 mL scintillation vial was charged with zinc perchlorate hexahydrate (0.013 g, 0.035 mmol). The contents of a separate vial containing L^{H} (0.027 g, 0.035 mmol) in 4 mL acetone were added to the zinc containing vial and stirred. After 30 min, sodium azide (0.014 g, 0.215 mmol) was added. After 3 hr, volatiles were removed in vacuo. The resulting solid was extracted into 6 mL CH_2Cl_2, filtered, dried, and washed with 10 mL diethyl ether to afford an off-white powder assigned as (L^{CF3})$Zn(N_3)_2$ (0.029 g, 0.032 mmol, 91%). ^{1}H NMR (500 MHz, CD_2Cl_2, 25 °C) δ = 4.16 (s, 6H, N(CH_2)$_3$), 6.63 (d, *J* = 6.8, 3H, pyridine-C*H*), 6.87 (d, *J* = 8.4, 3H, pyridine-C*H*), 6.92 (d, *J* = 8.0, 6H, phenyl-C*H*), 7.35 (d, *J* = 8.4, 6H, phenyl-C*H*), 7.45 (t, *J* = 7.6, 3H, pyridine-C*H*), 9.36 (s, 3H, N*H*). ^{13}C NMR (125.76 MHz, CD_2Cl_2, 25 °C) δ = 61.31 (N(*C*H_2)$_3$), 109.32 (pyridine-*C*H), 115.03 (pyridine-*C*H), 119.70 (phenyl-*C*H), 124.48 (q, *J* = 271, *C*F_3), 125.29 (q, *J* = 32.5, phenyl-*C*), 127.00 (q, *J* = 2.5, phenyl-*C*H), 140.86 (phenyl-*C*), 142.87 (pyridine-*C*H), 152.94 (pyridine-*C*), 155.44 (pyridine-*C*). ^{19}F NMR (375.91 MHz, CD_2Cl_2, 25 °C) δ = -62.56.

Synthesis of [(TPA)$Zn(N_3)$][ClO_4]. A 20 mL scintillation vial was charged with zinc perchlorate hexahydrate (0.013 g, 0.035 mmol). The contents of a separate vial containing tris(2-pyridylmethyl)amine (0.010 g, 0.034 mmol) in 6 mL acetone were added to the zinc containing vial and stirred. After 30 min, sodium azide (0.014 g, 0.215 mmol) was added. After 3 hr, volatiles were removed in vacuo. The resulting solid was extracted into 6 mL CH_2Cl_2, filtered, dried, and washed with 6 mL THF to afford a white powder assigned as [(TPA)$Zn(N_3)$][ClO_4] (0.008 g, 0.016 mmol, 46%). Single, X-ray quality crystals were obtained by slow diffusion of diethyl ether into a methanol solution at room temperature. ^{1}H NMR (500 MHz, CD_2Cl_2, 25 °C) δ = 4.31 (s, 6H, N(CH_2)$_3$), 7.60-7.65 (m, 6H, pyridine-C*H*), 8.05 (t, *J* = 7.5, 3H, pyridine-C*H*), 8.89 (d, *J* = 5.0, 3H, pyridine-C*H*). ^{13}C NMR (125.76 MHz, CD_2Cl_2, 25 °C) δ = 57.14 (N(*C*H_2)$_3$), 125.42 (pyridine-*C*H), 125.91 (pyridine-*C*H), 142.06 (pyridine-*C*H), 149.46 (pyridine-*C*H), 155.11 (pyridine-*C*).

Synthesis of (TPA)$Zn(N_3)_2$. A 20 mL scintillation vial was charged with zinc nitrate hexahydrate (0.059 g, 0.198 mmol), tris(2-pyridylmethyl)amine (0.058 g, 0.200 mmol), and 6 mL methanol and stirred for 15 min. Sodium azide (0.027 g, 0.415 mmol) was added, stirred for 3 hr, and volatiles were removed in vacuo. The resulting solid was extracted into 12 mL CH_2Cl_2, filtered, dried, and washed with 2 x 10 mL diethyl ether to afford a white powder assigned as (TPA)$Zn(N_3)_2$ (0.078 g, 0.178 mmol, 89%). Single, X-ray quality crystals were obtained by layering a MeOH/EtOAc (4:1) solution with diethyl ether at room temperature. ^{1}H NMR (500 MHz, CD_2Cl_2, 25 °C) δ = 4.32 (s, 6H, N(CH_2)$_3$), 7.36 (d, *J* = 8.0, 3H, pyridine-C*H*), 7.40 (t, *J* = 6.5, 3H, pyridine-C*H*), 7.81 (t, *J* = 7.5, 3H, pyridine-C*H*), 8.81 (d, *J* = 5.0, 3H, pyridine-C*H*). ^{13}C NMR (125.76 MHz, CD_2Cl_2, 25 °C) δ = 59.98 (N(*C*H_2)$_3$), 124.35 (pyridine-*C*H), 124.86 (pyridine-*C*H), 140.16 (pyridine-*C*H), 148.83 (pyridine-*C*H), 154.60 (pyridine-*C*).

Synthesis of $[L^HZnCl][X]$ from $[L^H{}_2Zn_2O_2][X]_2$ and $PhICl_2$ (X = OTf, ClO_4). Inside a glovebox, a 50 mL round bottom flask was charged with iodobenzene dichloride (0.018 g, 0.065 mmol). In a separate vial, $[L^H{}_2Zn_2O_2][OTf]_2$ (0.103 g, 0.065 mmol) was dissolved in 3 mL DCM and added in one portion to the round bottom flask. An aliquot of the solution was analyzed to ensure conversion. The solution was then diluted with an additional 3 mL DCM, filtered into a 20 mL scintillation vial, and layered with 15 mL Et_2O, resulting in precipitation of off-white solid overnight (0.080 g, 0.098 mmol, 76%) assigned as $[L^HZnCl][OTf]$. Characterization for X = OTf: ^{1}H NMR (400 MHz, CH_2Cl_2, 25 °C) δ = 4.11 (s, 6H, N(CH_2)$_3$), 6.79 (d, *J* = 7.6, 3H, pyridine-C*H*), 6.99 (d, *J* = 8.8, 3H, pyridine-C*H*), 7.20 (t, *J* = 7.2, 3H, aryl-C*H*), 7.23 (d, *J* = 7.6, 6H, phenyl-C*H*), 7.38 (t, *J* = 7.6, 6H, phenyl-C*H*), 7.60 (t, *J* = 7.6, 3H, aryl-C*H*), 9.62 (s, 3H, N*H*). ^{1}H NMR (400 MHz, CD_3CN, 25 °C) δ = 4.10 (s, 6H, N(CH_2)$_3$), 6.72 (d, *J* = 7.2, 3H, pyridine-C*H*), 6.96 (d, *J* = 8.4, 3H, pyridine-C*H*), 7.09-7.15 (m, 9H, o-phenyl-C*H* and aryl-C*H*), 7.31 (t, *J* = 8.0, 6H, *m*-phenyl-C*H*), 7.61 (t, *J* = 7.6, 3H, aryl-C*H*), 9.25 (s, 3H, N*H*). ^{13}C NMR (125.76 MHz, CD_3CN, 25 °C) δ = 58.62 (N(*C*H_2)$_3$), 110.05 (pyridine-*C*H), 114.94 (pyridine-*C*H), 122.95 (phenyl-*C*H), 125.80 (phenyl-*C*H), 130.67 (phenyl-*C*H), 139.59 (pyridine-*C*H), 142.31 (phenyl-*C*), 153.18 (pyridine-*C*), 158.57 (pyridine-*C*). The same procedure was employed to synthesize the analogous perchlorate species of which single, X-ray quality crystals were obtained by slow diffusing *n*-pentane into a dichloroethane solution at room temperature. Characterization for X = ClO_4: ^{1}H NMR (400 MHz, CD_2Cl_2, 25 °C) δ = 4.15 (s, 6H, N(CH_2)$_3$), 6.84 (d, *J* = 7.6, 3H, pyridine-C*H*), 7.01 (d, *J* = 8.8, 3H, pyridine-C*H*), 7.21 (t, *J* = 7.2, 3H, aryl-C*H*), 7.25 (d, *J* = 7.6, 6H, phenyl-C*H*), 7.39 (t, *J* = 7.6, 6H, phenyl-C*H*), 7.63 (t, *J* = 7.6, 3H, aryl-C*H*), 9.63 (s, 3H, N*H*). ^{1}H NMR (400 MHz, CD_3CN, 25 °C) δ = 4.10 (s, 6H, N(CH_2)$_3$), 6.72 (d, *J* = 7.2, 3H, pyridine-C*H*), 6.96 (d, *J* = 8.4, 3H, pyridine-C*H*), 7.09-7.15 (m, 9H, o-phenyl-C*H* and aryl-C*H*), 7.31 (t, *J* = 8.0, 6H, *m*-phenyl-C*H*), 7.61 (t, *J* = 7.6, 3H, aryl-C*H*), 9.25 (s, 3H, N*H*).

Synthesis of $[L^HZnCl][OTf]$ from $[L^H{}_2Zn_2O_2][OTf]_2$ and $[NH_4]_2[Ce(NO_3)_6]$. A 20 mL scintillation vial was charged with $[L^H{}_2Zn_2O_2][OTf]_2$ (0.044 g, 0.028 mmol) and 4 mL MeCN. While stirring $[Bu_4N][Cl]$ was added (0.150 mL, aqueous 0.7409 M stock solution, 0.111 mmol) followed by ceric ammonium nitrate (0.080 mL, aqueous 0.7004 M stock solution, 0.055 mmol) resulting in a rapid color change from colorless to brown. The solution was diluted with 6 mL DCM and 10 mL H_2O. The H_2O layer was discarded, and an additional 5 mL H_2O added. The organic phase was extracted with DCM (5 x 2 mL). The combined organics were dried, redissolved in minimal DCM and filtered. To the filtrate 15 mL diethyl ether was added resulting in precipitation of a tan solid. The solid was collected and dried to afford $[L^HZnCl][OTf]$ (0.018 g, 0.022 mmol, 40%).

Attempted synthesis of a dizinc peroxide with TPA^{OPh} ligand. A 20 mL scintillation vial was charged with $Zn(OTf)_2$ (0.0025 g, 0.007 mmol), TPA^{OPh} (0.0040 g, 0.007 mmol), and 1 mL of MeCN. Metalation was confirmed by NMR spectroscopy, then, while stirring, hydrogen peroxide (30% in H_2O; 1.44 µL, 0.014 mmol) and triethylamine (1.08 µL, 0.008 mmol) were added. An NMR of the crude mixture was immediately obtained, revealing demetalation.

Attempted synthesis of a dizinc peroxide with TPA ligand. Note: this reaction was performed on the benchtop with no attempts to exclude air or moisture. A 20 mL scintillation vial was charged with tris(2-methylpyridyl)amine (0.034 g, 0.117 mmol), $Zn(OTf)_2$ (0.043 g, 0.118 mmol), and 2 mL MeCN and stirred until fully dissolved. Hydrogen peroxide (30% in H_2O; 26 µL, 0.237 mmol) and diisopropylethylamine (41 µL, 0.235 mmol) were added sequentially and stirred for 4 min. To the solution was added 15 mL diethyl ether. Centrifugation afforded colorless viscous oil which was triturated with pentane to afford a colorless semi-solid. Infrared and NMR spectroscopies are consistent with formation of $[(TPA)_3Zn_3(CO_3)][OTf]_4$.[8]

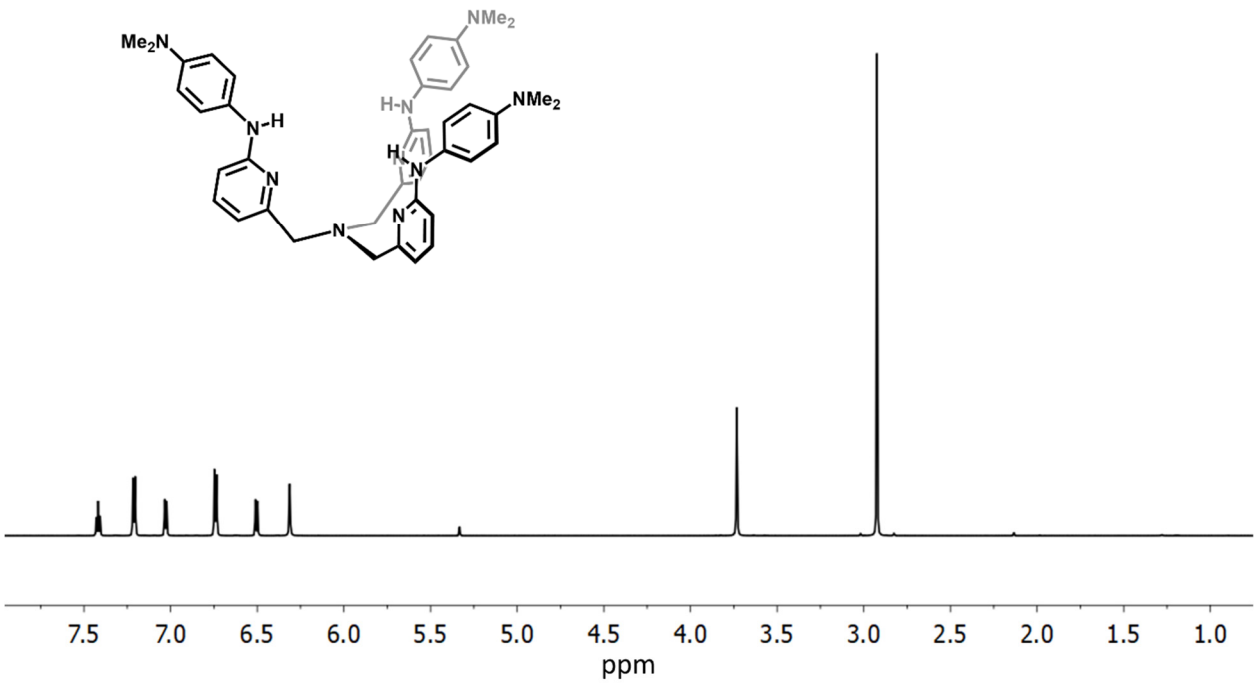

Figure S1 ^{1}H NMR spectrum (CD_2Cl_2, ambient temperature) of L^{NMe2}.

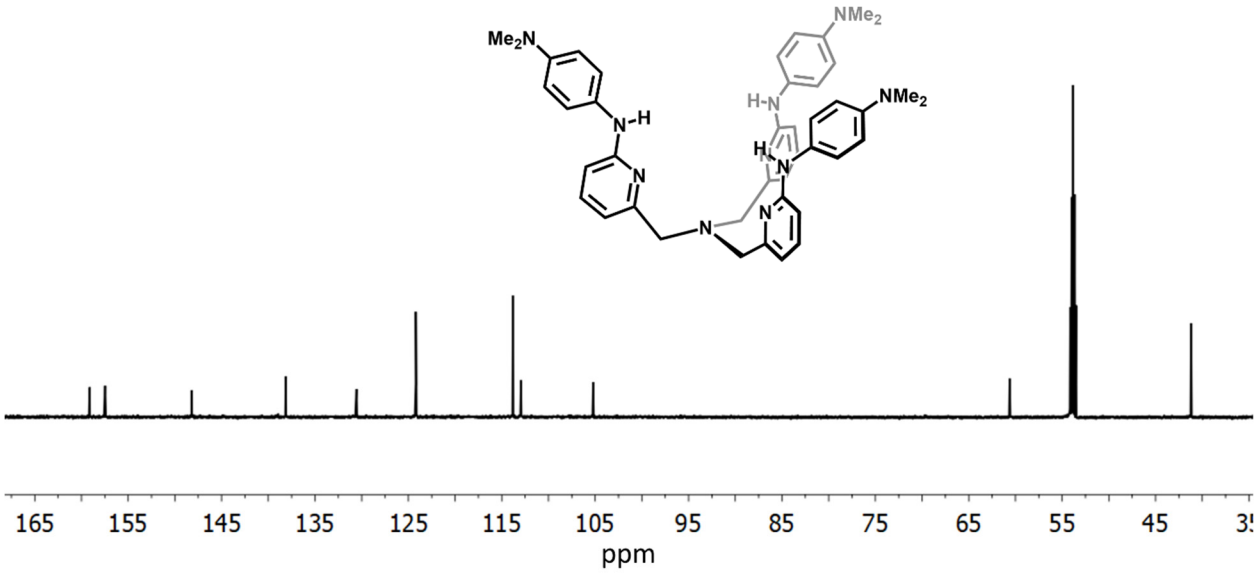

Figure S2 ^{13}C NMR spectrum (CD_2Cl_2, ambient temperature) of L^{NMe2}.

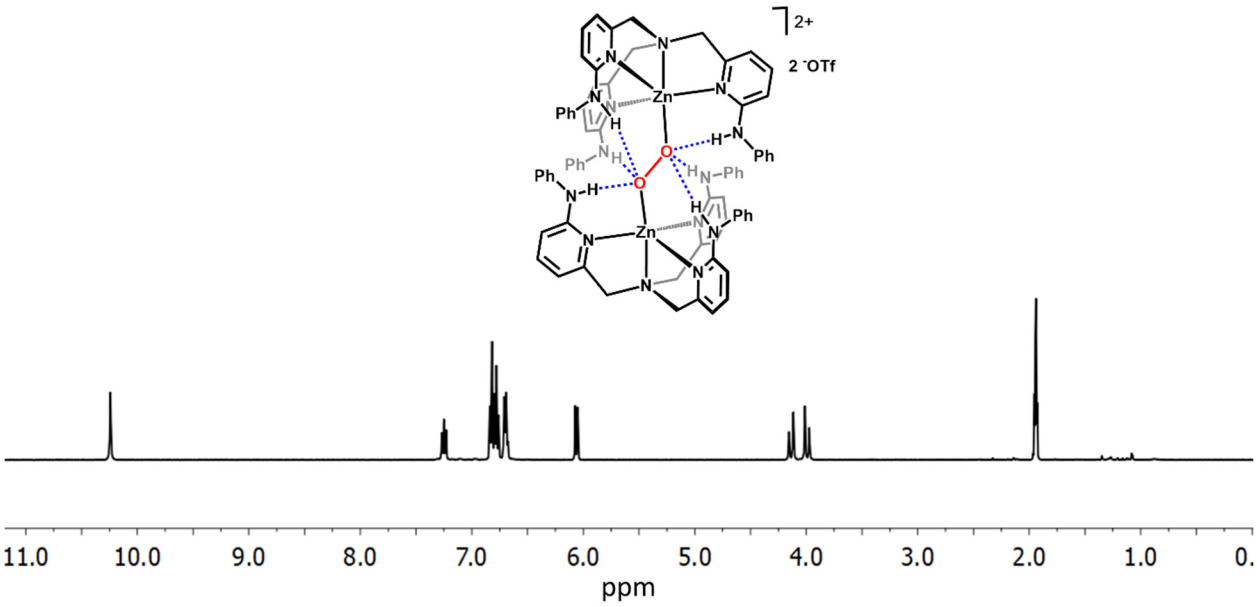

Figure S3 ^{1}H NMR spectrum (CD_3CN, ambient temperature) of $[L^{H}_2Zn_2O_2][OTf]_2$.

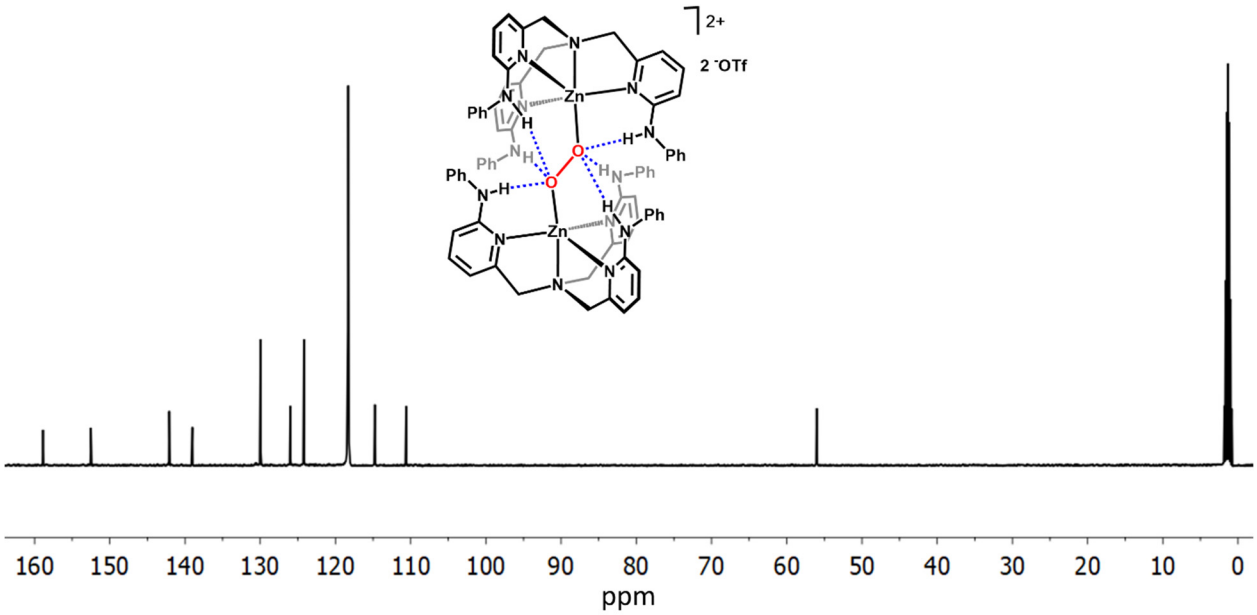

Figure S4 ^{13}C NMR spectrum (CD_3CN, ambient temperature) of $[L^{H}_2Zn_2O_2][OTf]_2$.

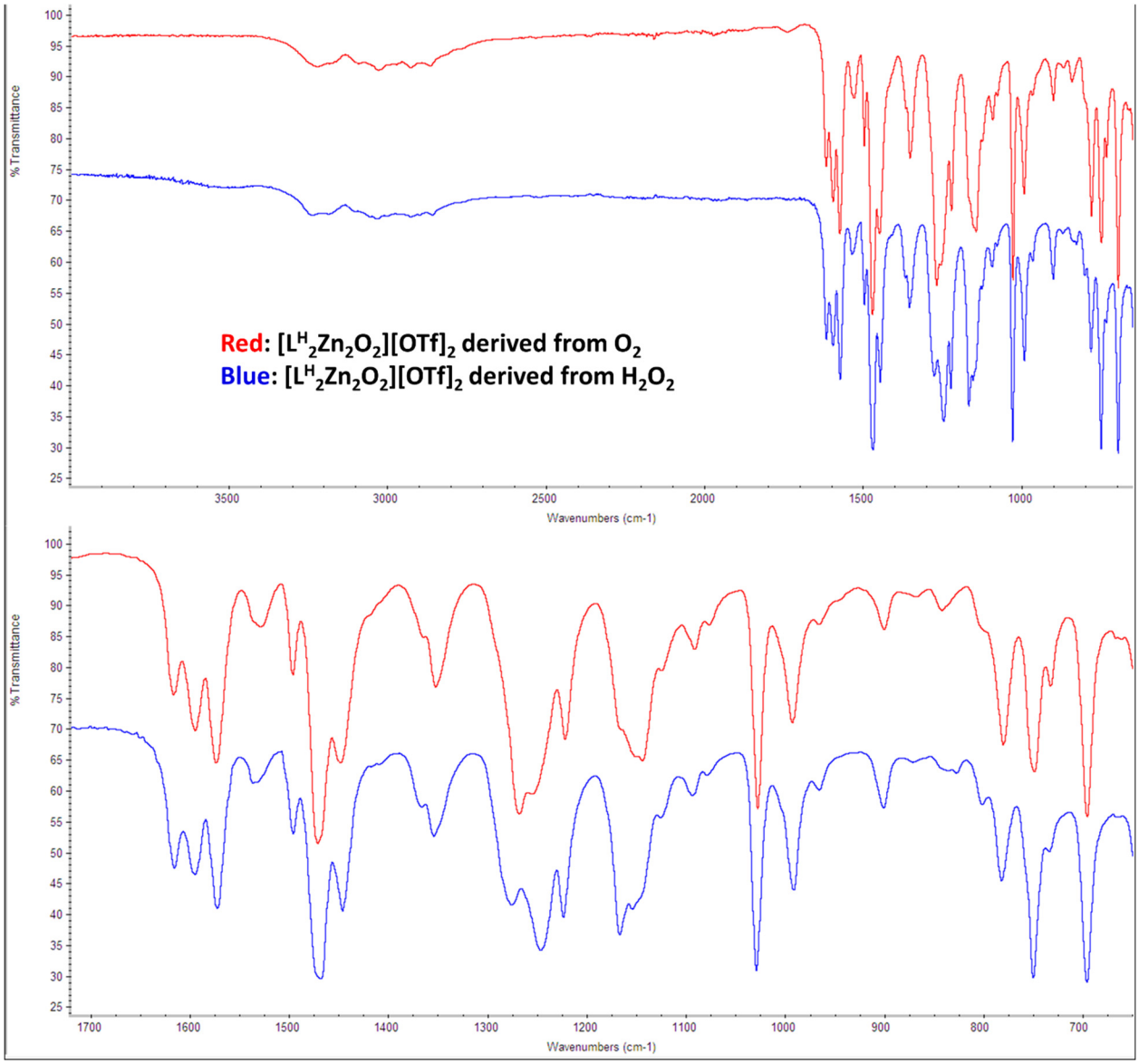

Figure S5 Comparison of infrared spectra for isolated samples of $[L^{H}{}_2Zn_2O_2][OTf]_2$ synthesized from O_2 (red) and from H_2O_2 (blue).

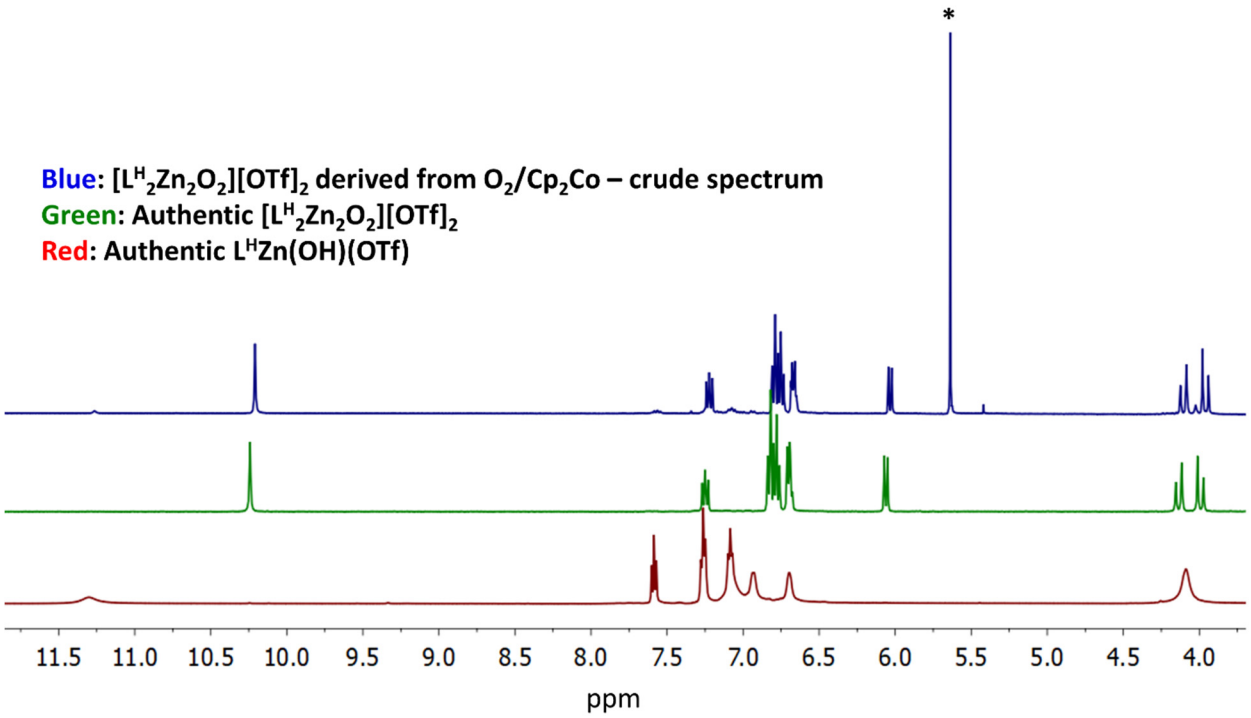

Figure S6 Top: crude ^{1}H NMR spectrum of $[L^{H}_{2}Zn_{2}O_{2}][OTf]_{2}$ derived from dioxygen and cobaltocene. The asterisk denotes $[Cp_{2}Co][OTf]$. Middle: Purified sample of $[L^{H}_{2}Zn_{2}O_{2}][OTf]_{2}$. Bottom: authentic sample of $L^{H}Zn(OH)(OTf)$. All spectra were recorded in MeCN at ambient temperature.

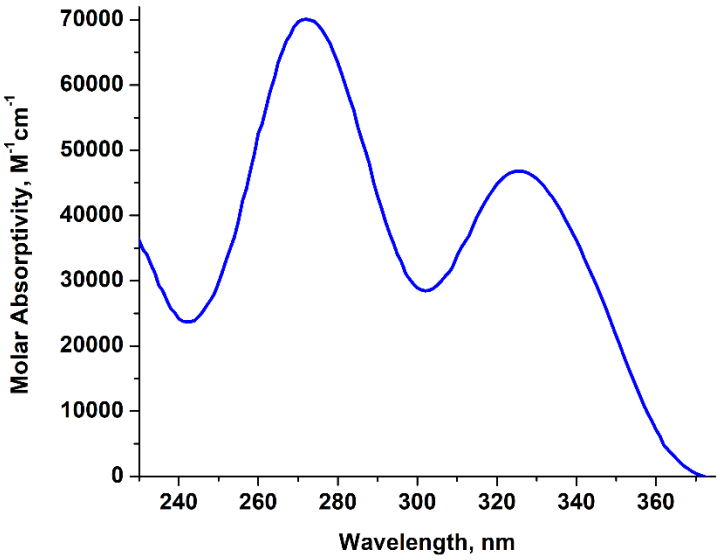

Figure S7 Electronic absorption spectrum of $[L^{H}_{2}Zn_{2}O_{2}][OTf]_{2}$ recorded in acetonitrile at ambient temperature.

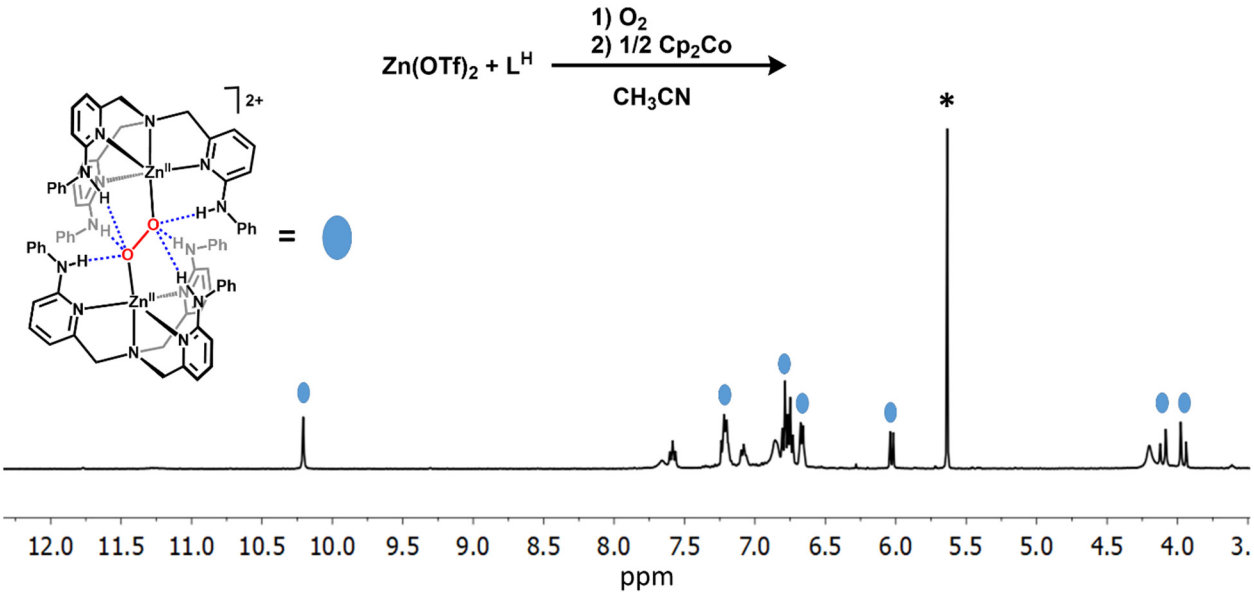

Figure S8 Crude ^{1}H NMR spectrum (CH_3CN, ambient temperature) of substoichiometric (0.5 equivalents) cobaltocene addition to a O_2 saturated MeCN solution of $Zn(OTf)_2$ and L^H. The asterisk denotes $[Cp_2Co][OTf]$. The blue ovals denote $[L^H_2Zn_2O_2][OTf]_2$. The remaining resonances are attributed to an adduct between $Zn(OTf)_2$ and L^H. The experimental set up was analogous to that described above for the stoichiometric cobaltocene reaction.

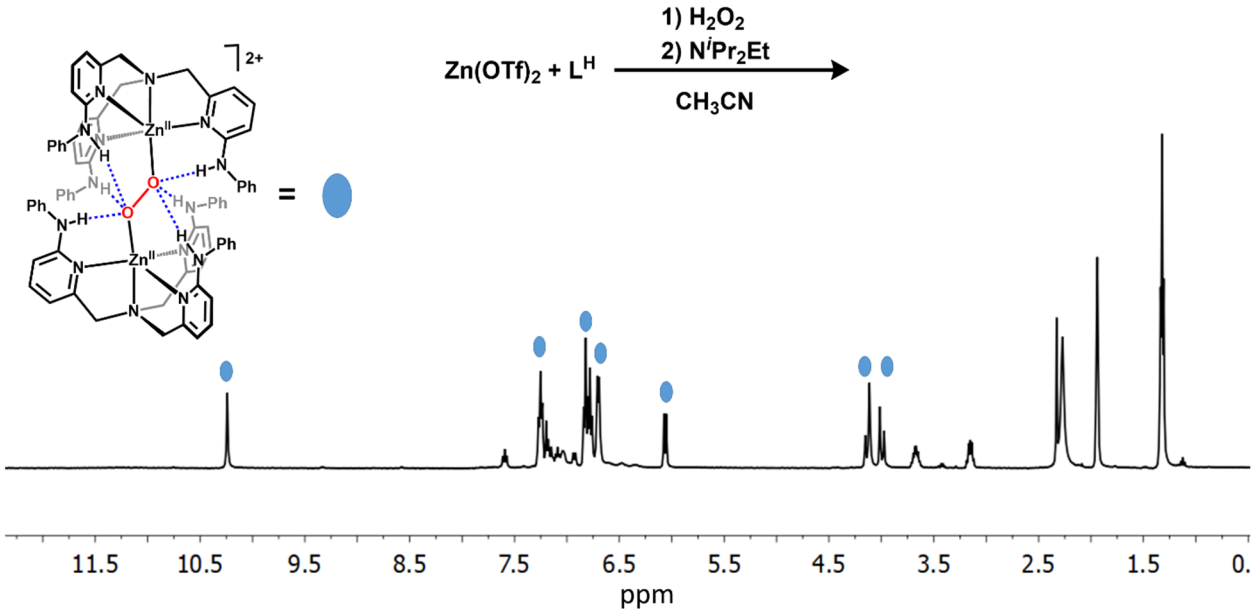

Figure S9 Crude ^{1}H NMR spectrum (CD_3CN, ambient temperature) of attempted formation of a zinc hydroperoxo species. The blue ovals denote $[L^H_2Zn_2O_2][OTf]_2$. The remaining resonances are attributed to an adduct between $Zn(OTf)_2$ and L^H.

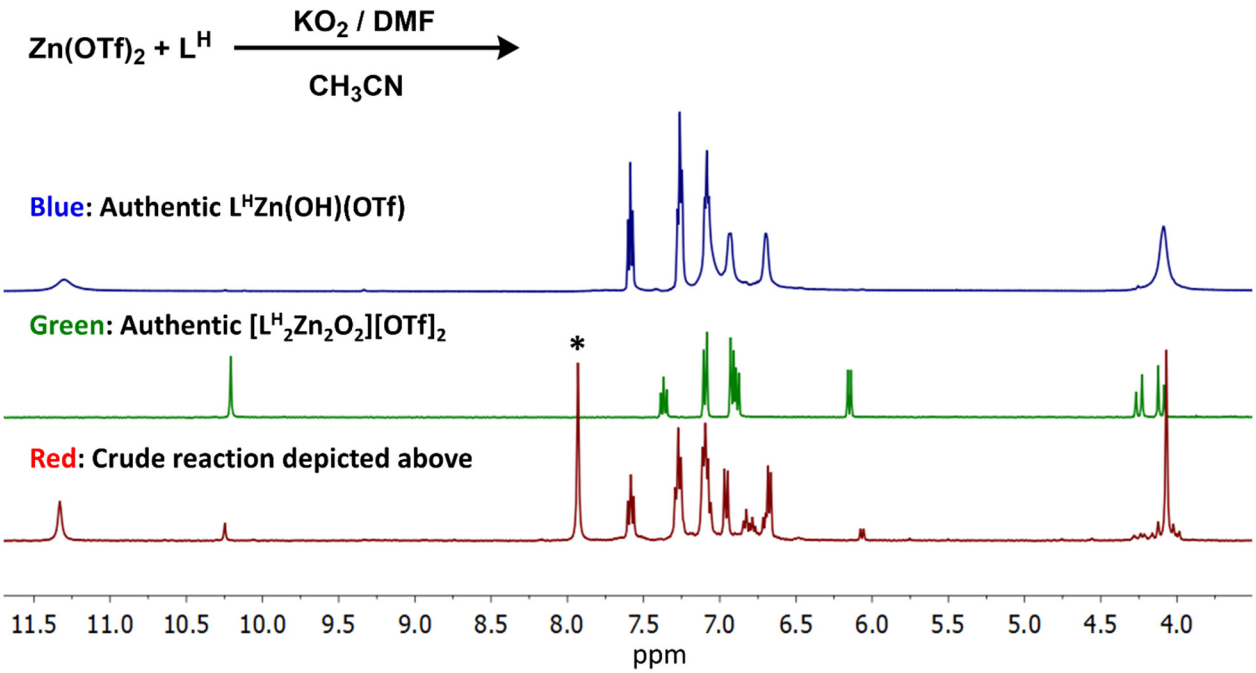

Figure S10 Bottom: crude ^{1}H NMR spectrum (CD_3CN, ambient temperature) of reaction between $Zn(OTf)_2$, L^H and KO_2 (DMF solution). The reaction produces predominantly $(L^H)Zn(OH)(OTf)$ with trace $[L^H{}_2Zn_2O_2][OTf]_2$. The asterisk denotes N,N-dimethylformamide. Authentic ^{1}H NMR spectra of $(L^H)Zn(OH)(OTf)$ (top, blue) and $[L^H{}_2Zn_2O_2][OTf]_2$ (middle, green) are included for reference.

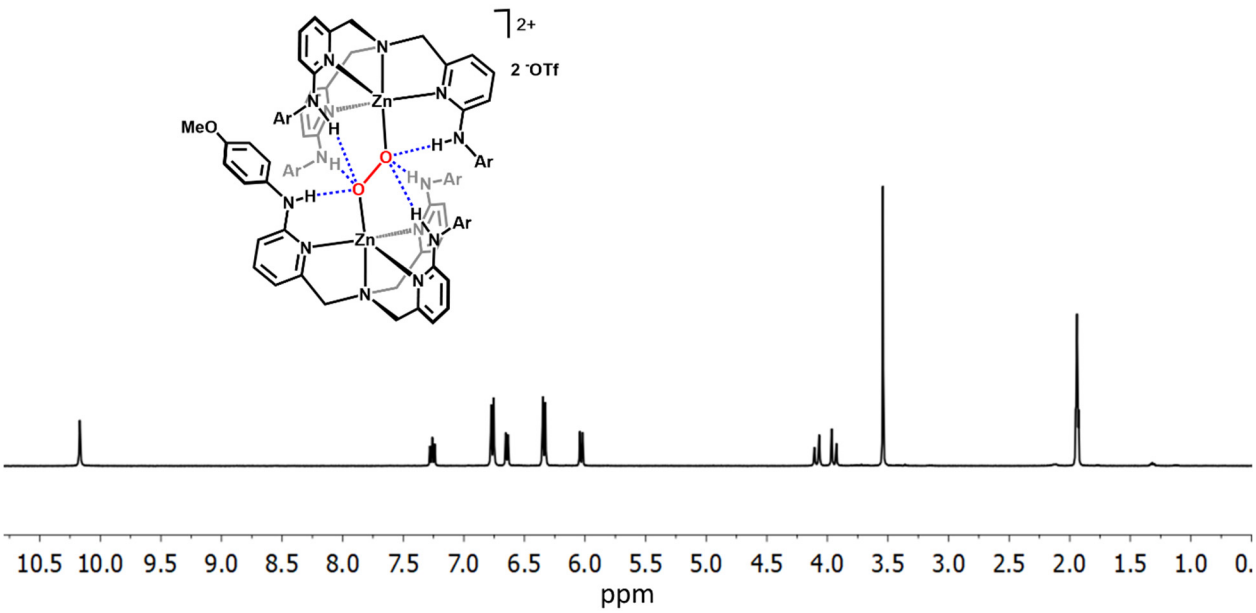

Figure S11 ^{1}H NMR spectrum (CD_3CN, ambient temperature) of $[L^{OMe}{}_2Zn_2O_2][OTf]_2$.

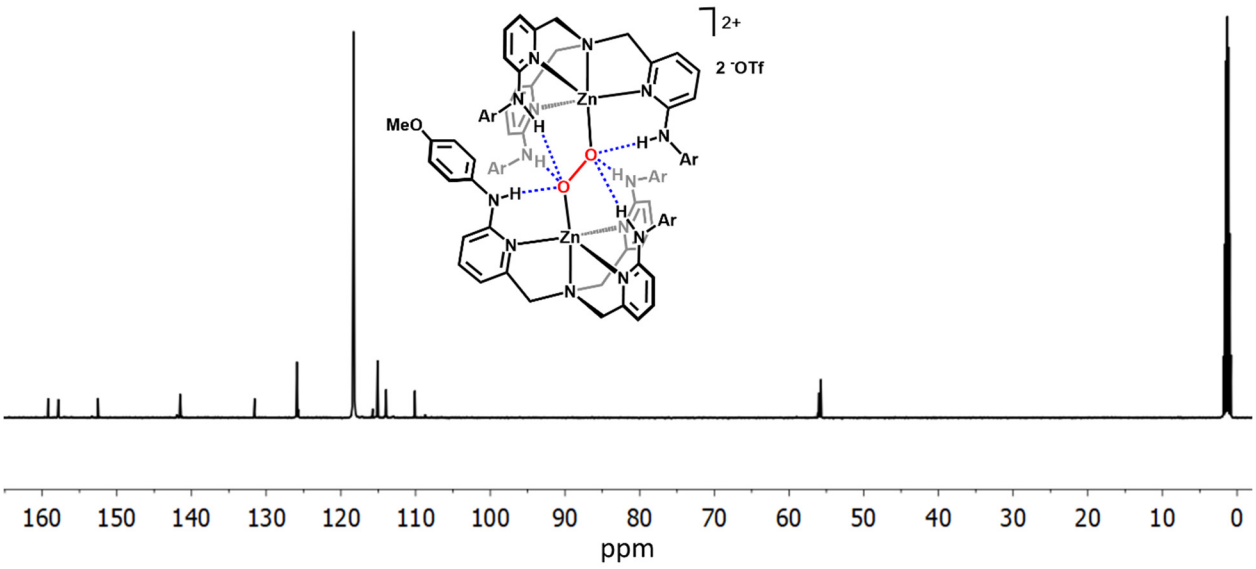

Figure S12 ^{13}C NMR spectrum (CD_3CN, ambient temperature) of $[L^{OMe}{}_2Zn_2O_2][OTf]_2$.

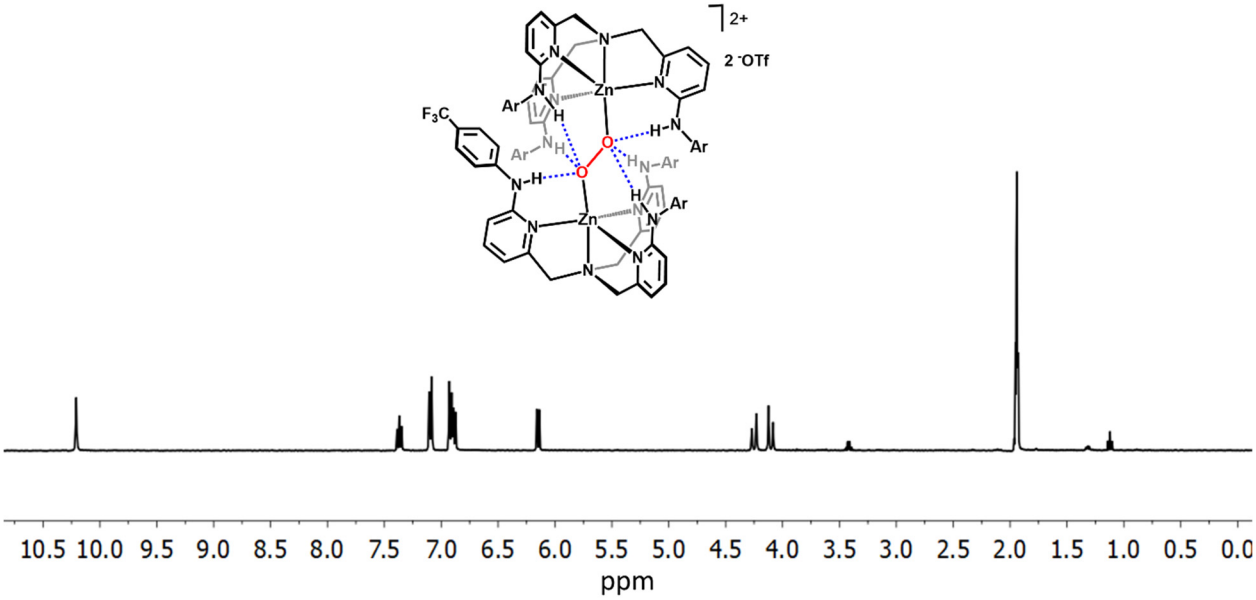

Figure S13 ^{1}H NMR spectrum (CD_3CN, ambient temperature) of $[L^{CF3}{}_2Zn_2O_2][OTf]_2$.

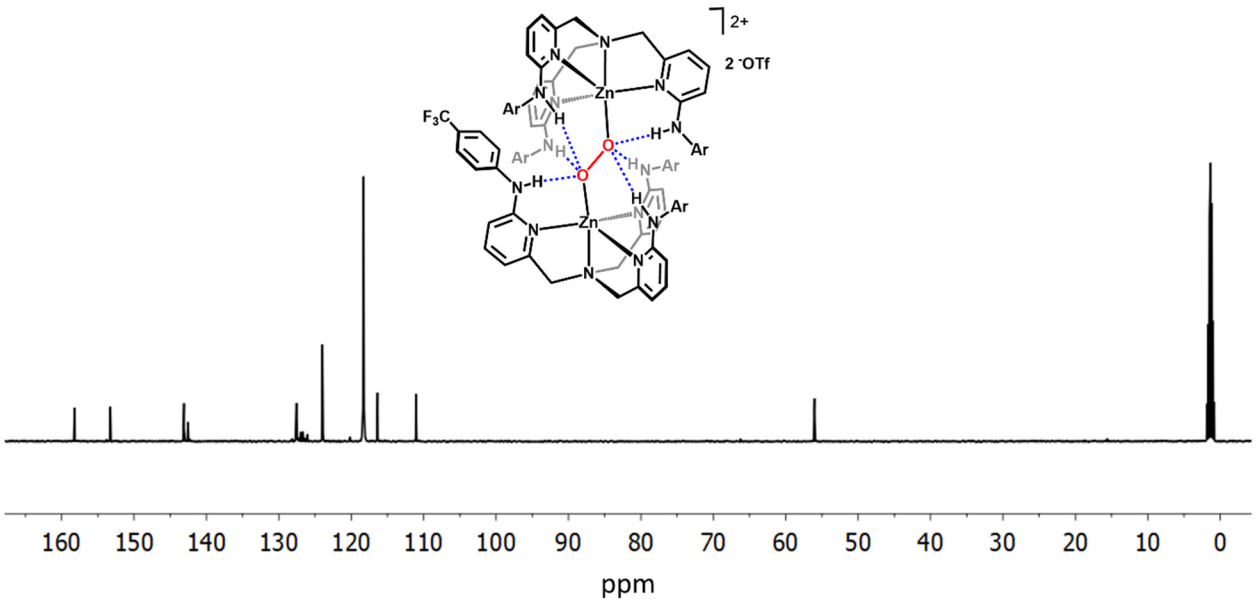

Figure S14 ^{13}C NMR spectrum (CD_3CN, ambient temperature) of $[L^{CF3}{}_2Zn_2O_2][OTf]_2$.

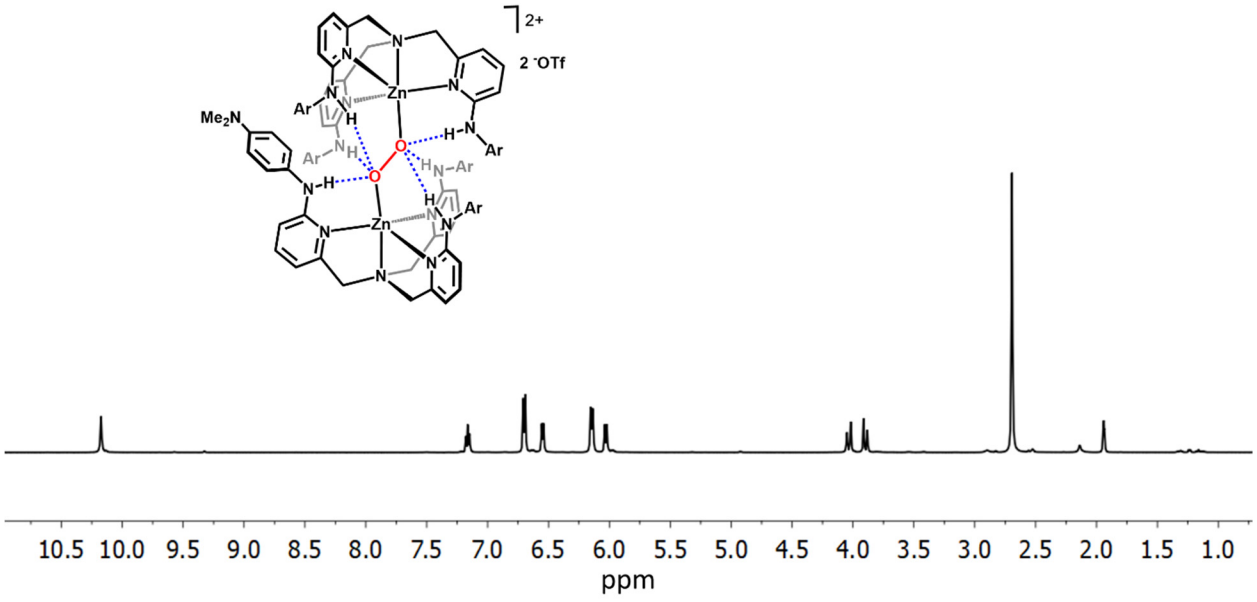

Figure S15 ^{1}H NMR spectrum (CD_3CN, ambient temperature) of $[L^{NMe2}{}_2Zn_2O_2][OTf]_2$.

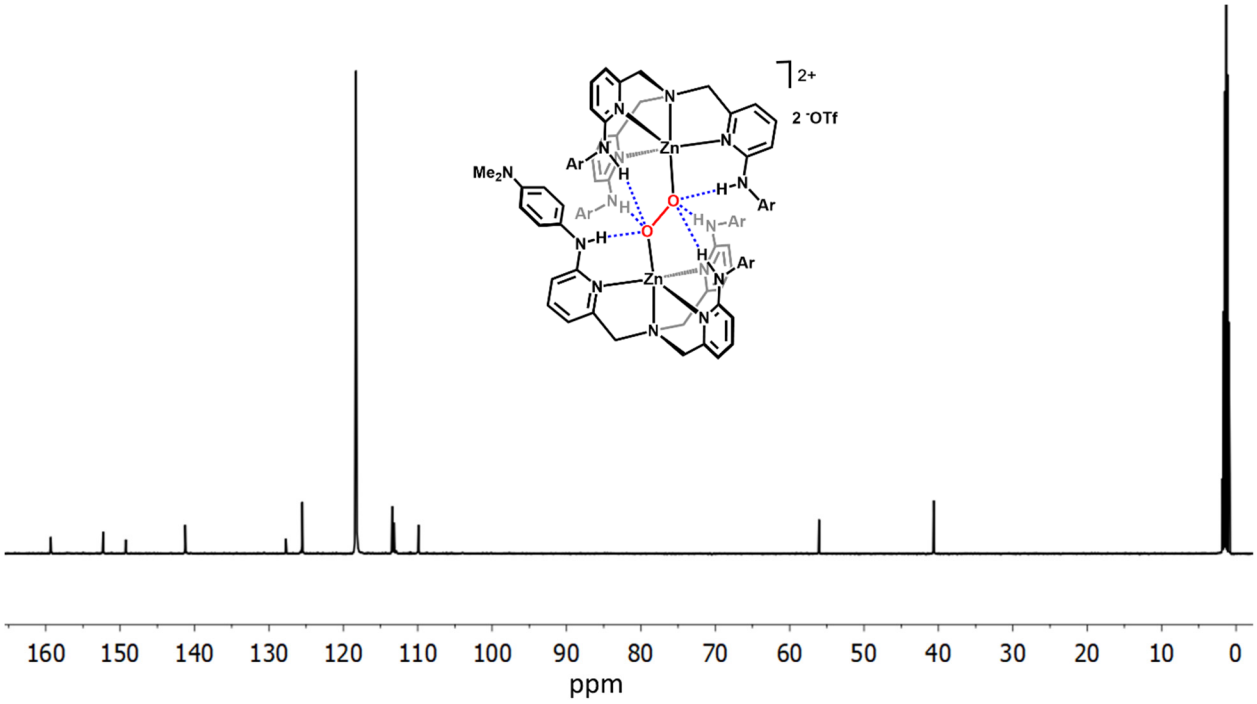

Figure S16 ^{13}C NMR spectrum (CD_3CN, ambient temperature) of $[L^{NMe2}{}_2Zn_2O_2][OTf]_2$.

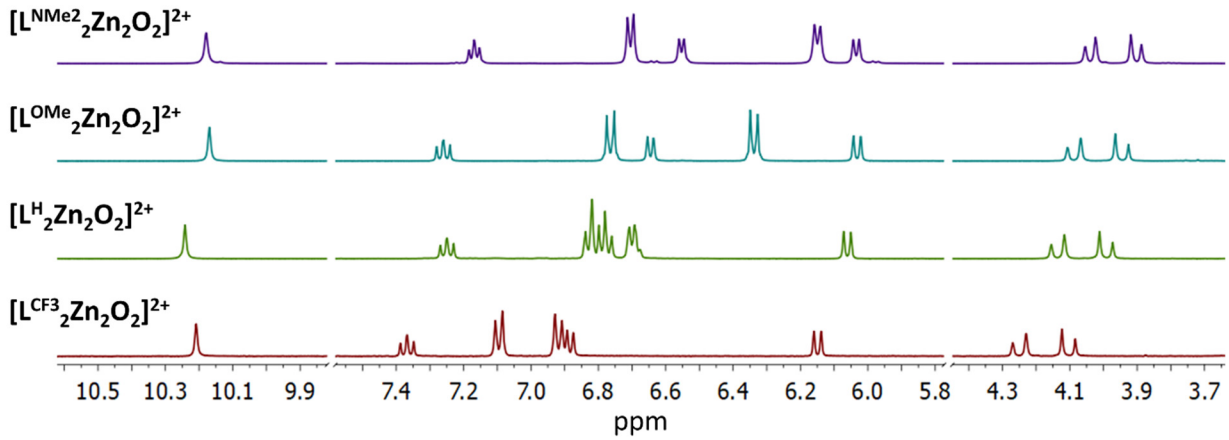

Figure S17 Overlay of ^{1}H NMR spectra (CD_3CN, ambient temperature) for $[L_2Zn_2O_2]^{2+}$ complexes.

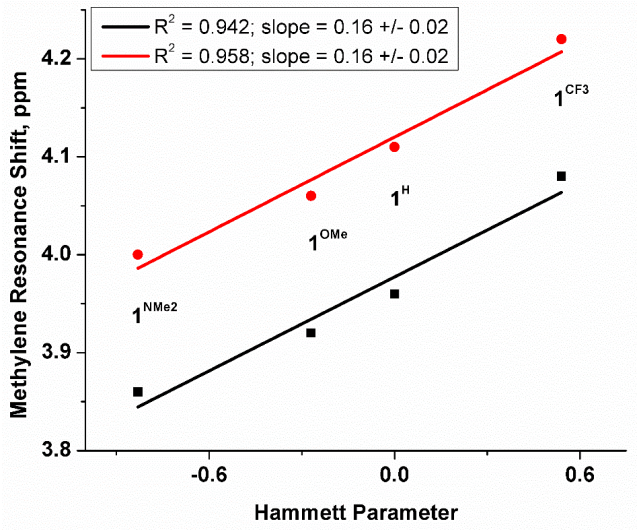

Figure S18 Correlation between Hammett parameter (σ) and shift of methylene resonances (ppm) for compounds $\mathbf{1}^{R}$.

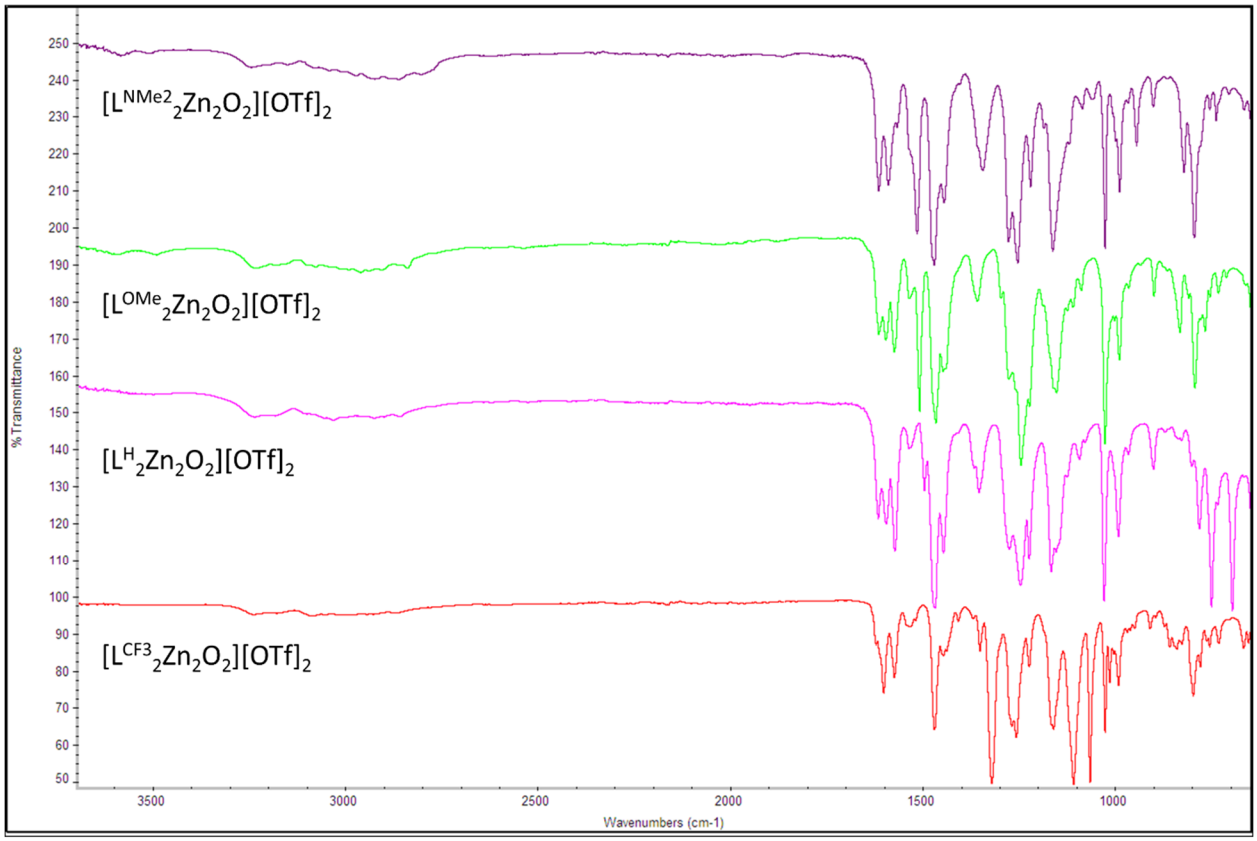

Figure S19 Overlay of infrared spectra (neat, ATR, ambient temperature) for $[L_2Zn_2O_2]^{2+}$ complexes.

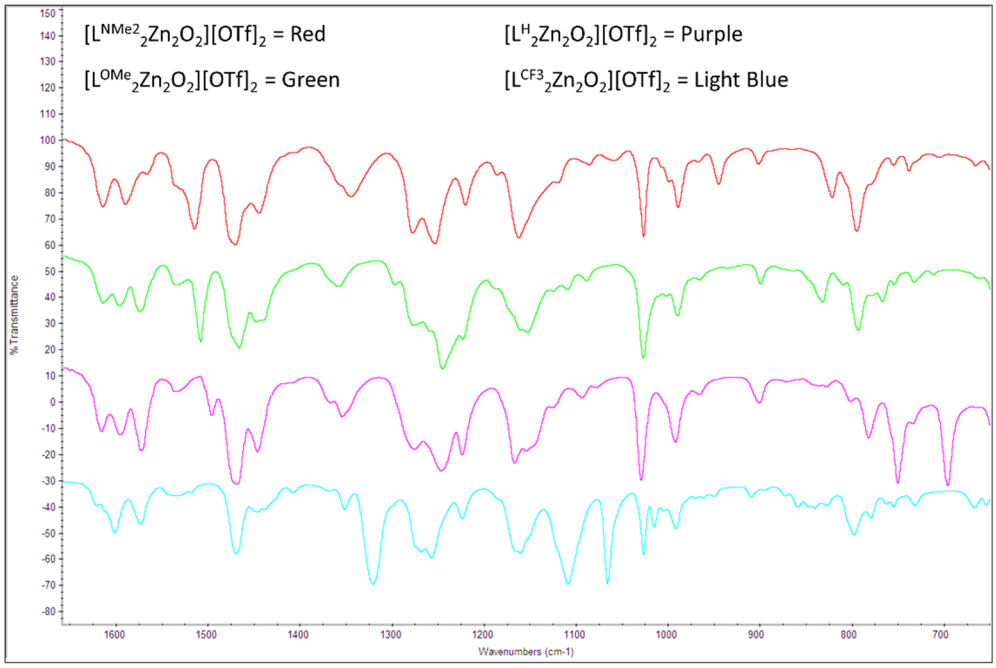

Figure S20 Overlay of infrared spectra (neat, ATR, ambient temperature) highlighting the fingerprint region for $[L_2Zn_2O_2]^{2+}$ complexes.

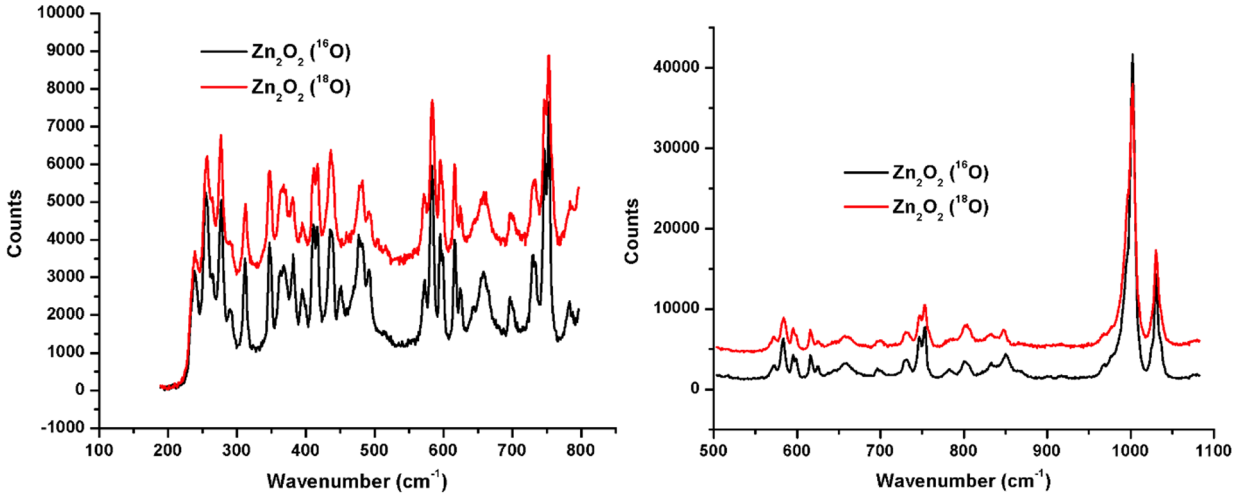

Figure S21 Overlay of Raman spectra for $[L^H_2Zn_2O_2][OTf]_2$ (black) and $[L^H_2Zn_2{}^{18}O_2][OTf]_2$ (red) complexes.

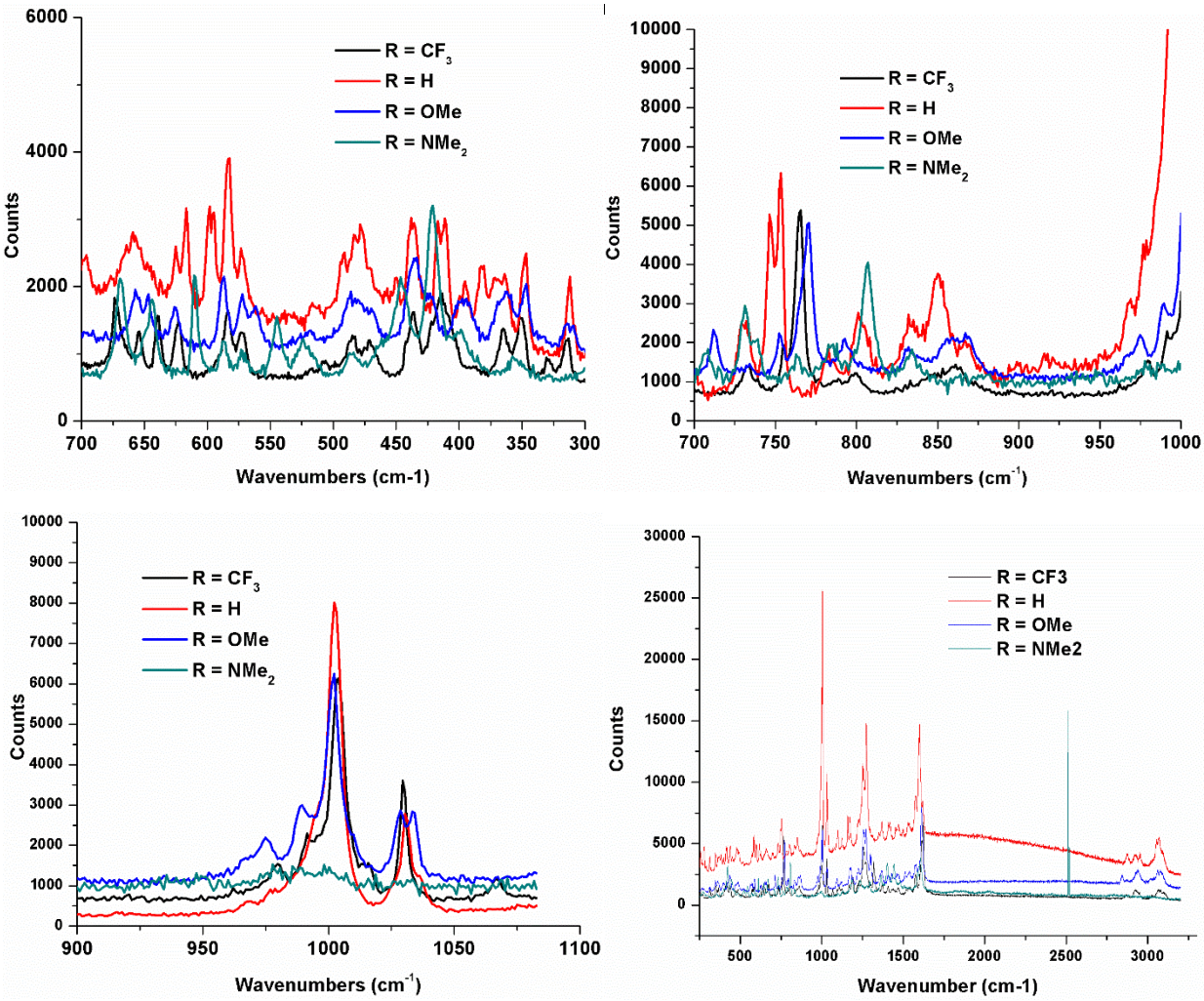

Figure S22 Overlay of Raman spectra for $[L^{R}{}_{2}Zn_{2}O_{2}][OTf]_{2}$ complexes.

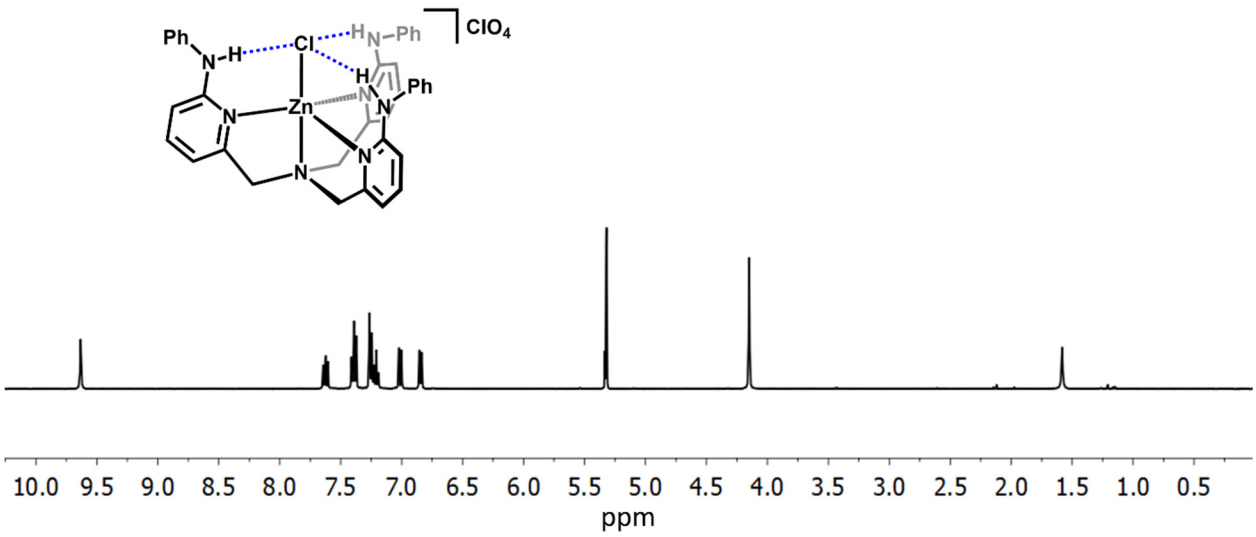

Figure S23 ^{1}H NMR spectrum (CD_2Cl_2, ambient temperature) of [(L^H)ZnCl][ClO_4].

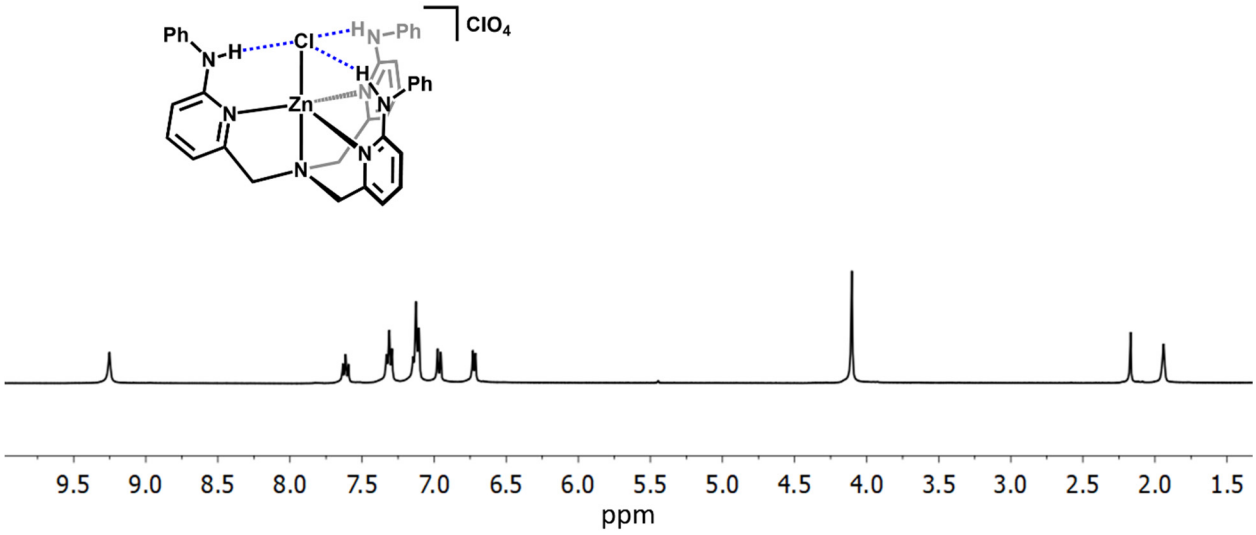

Figure S24 ^{1}H NMR spectrum (CD_3CN, ambient temperature) of [(L^H)ZnCl][ClO_4].

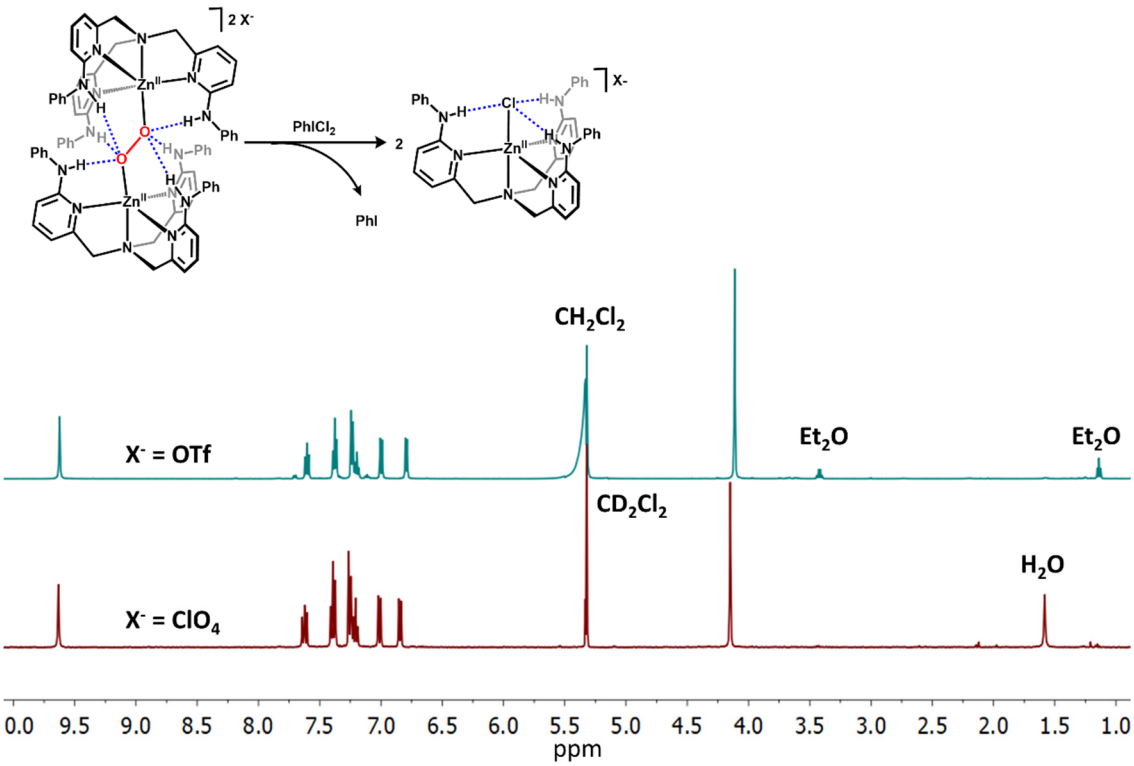

Figure S25 ^{1}H NMR spectra comparing [(L^{H})ZnCl][ClO$_4$] (bottom) and [(L^{H})ZnCl][OTf] (top).

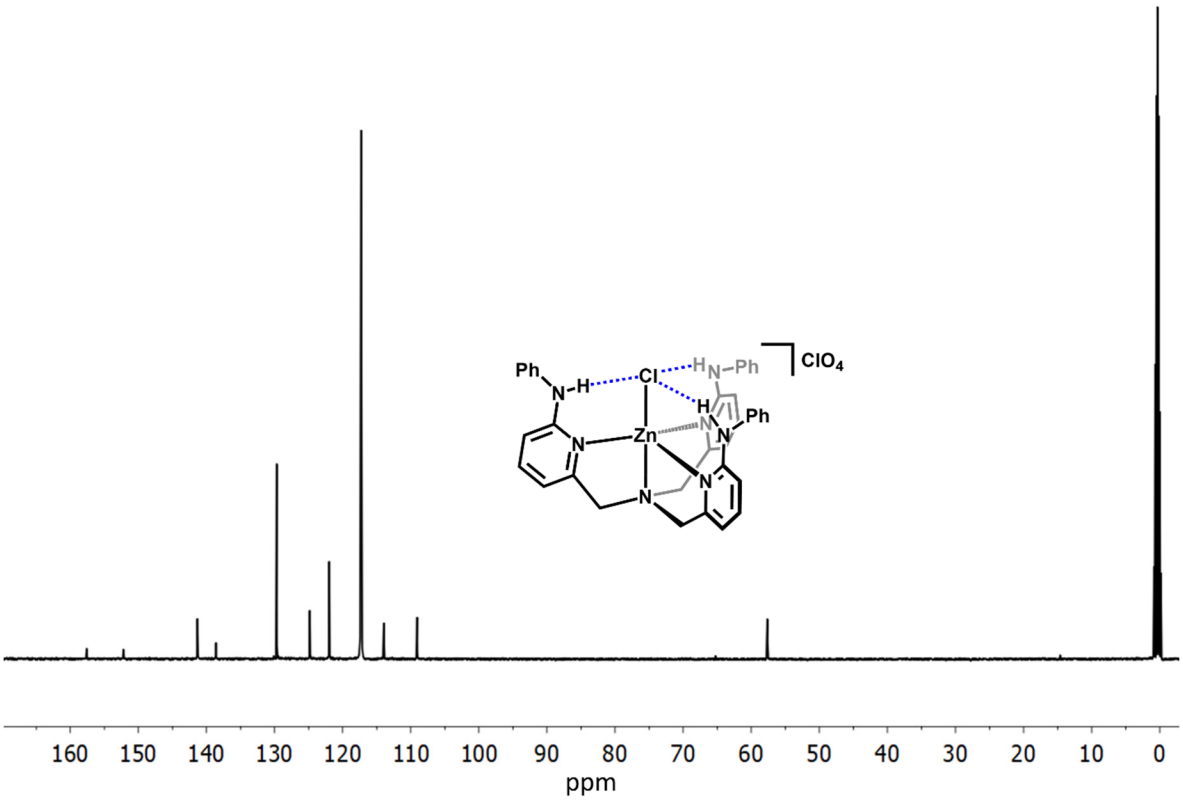

Figure S26 ^{13}C NMR spectrum (CD_3CN, ambient temperature) of [(L^{H})ZnCl][ClO$_4$].

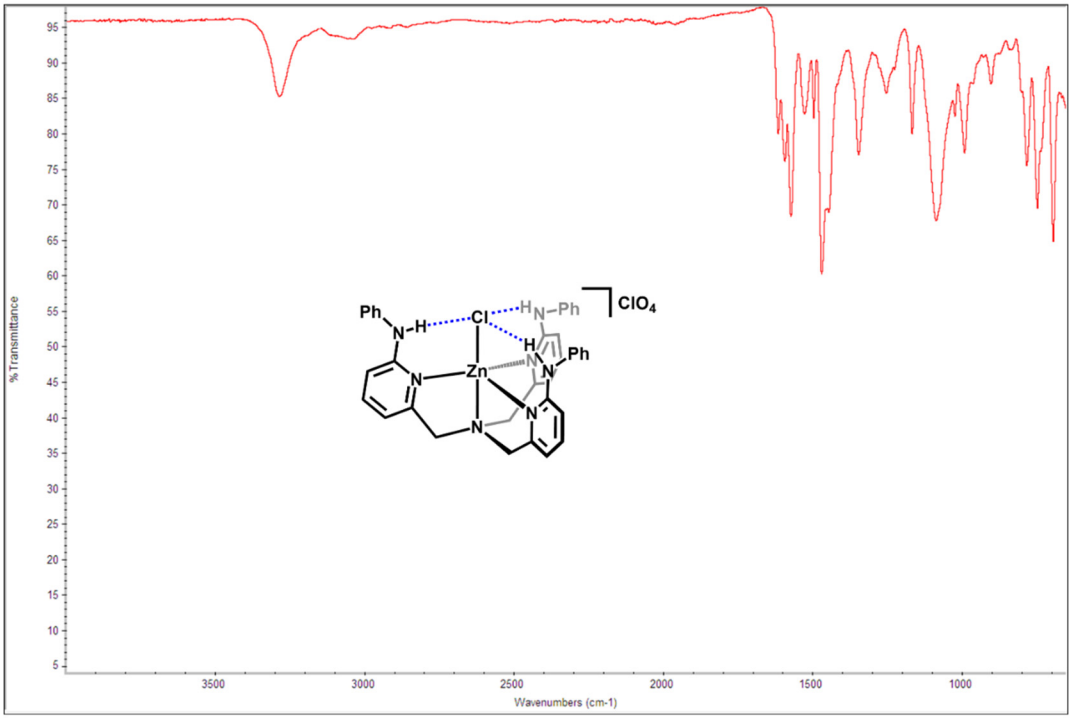

Figure S27 Infrared spectrum (neat, ATR, ambient temperature) of $[(L^{H})ZnCl][ClO_4]$.

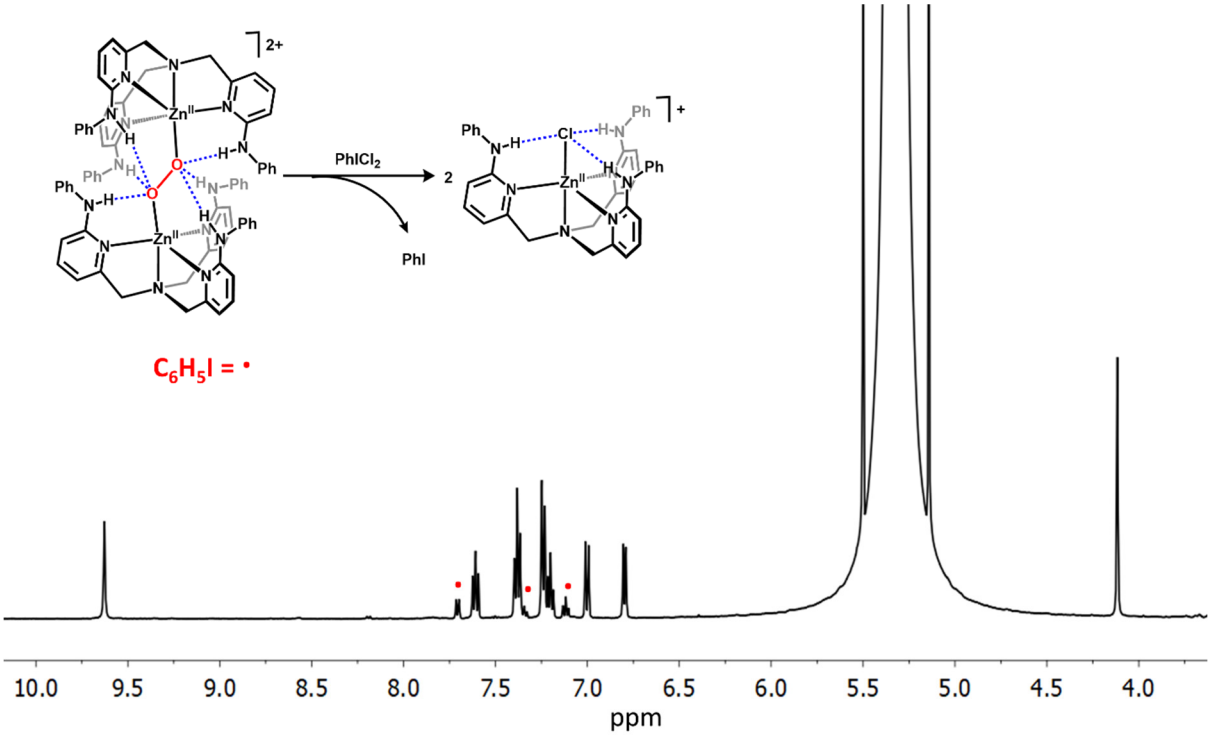

Figure S28 ^{1}H NMR spectrum (ambient temperature, CH_2Cl_2) of the crude mixture from reacting $[L^{H}{}_2Zn_2O_2][OTf]_2$ with $PhICl_2$.

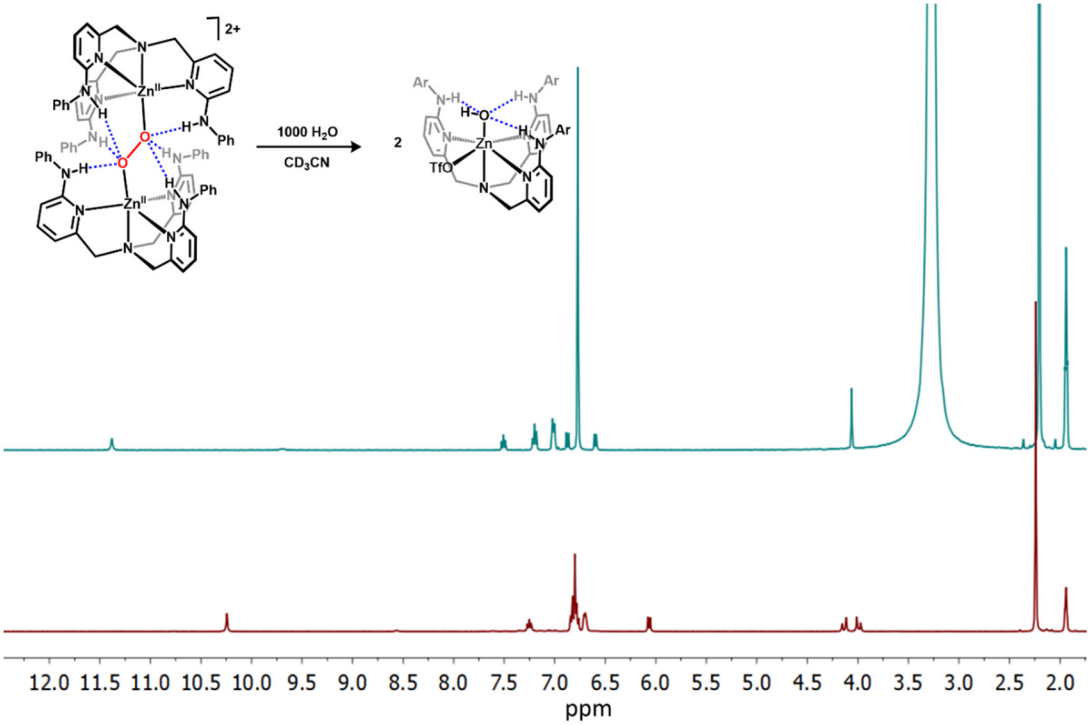

Figure S29 ^{1}H NMR spectra (ambient temperature, CD_3CN, mesitylene internal standard) prior to (bottom) and after addition of 1000 equivalents of H_2O to $[L^{H}{}_2Zn_2O_2][OTf]_2$.

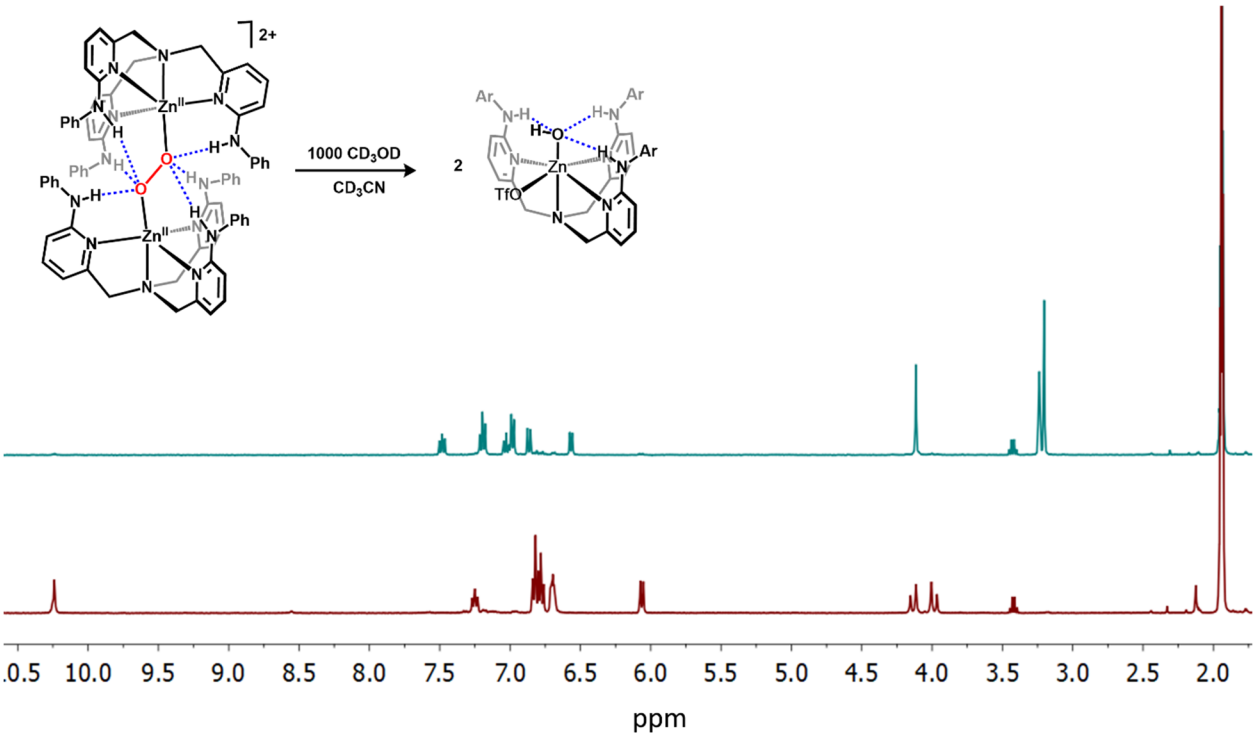

Figure S30 ^{1}H NMR spectra (ambient temperature, CD_3CN) prior to (bottom) and after addition of 1000 equivalents of CD_3OD to $[L^{H}{}_2Zn_2O_2][OTf]_2$.

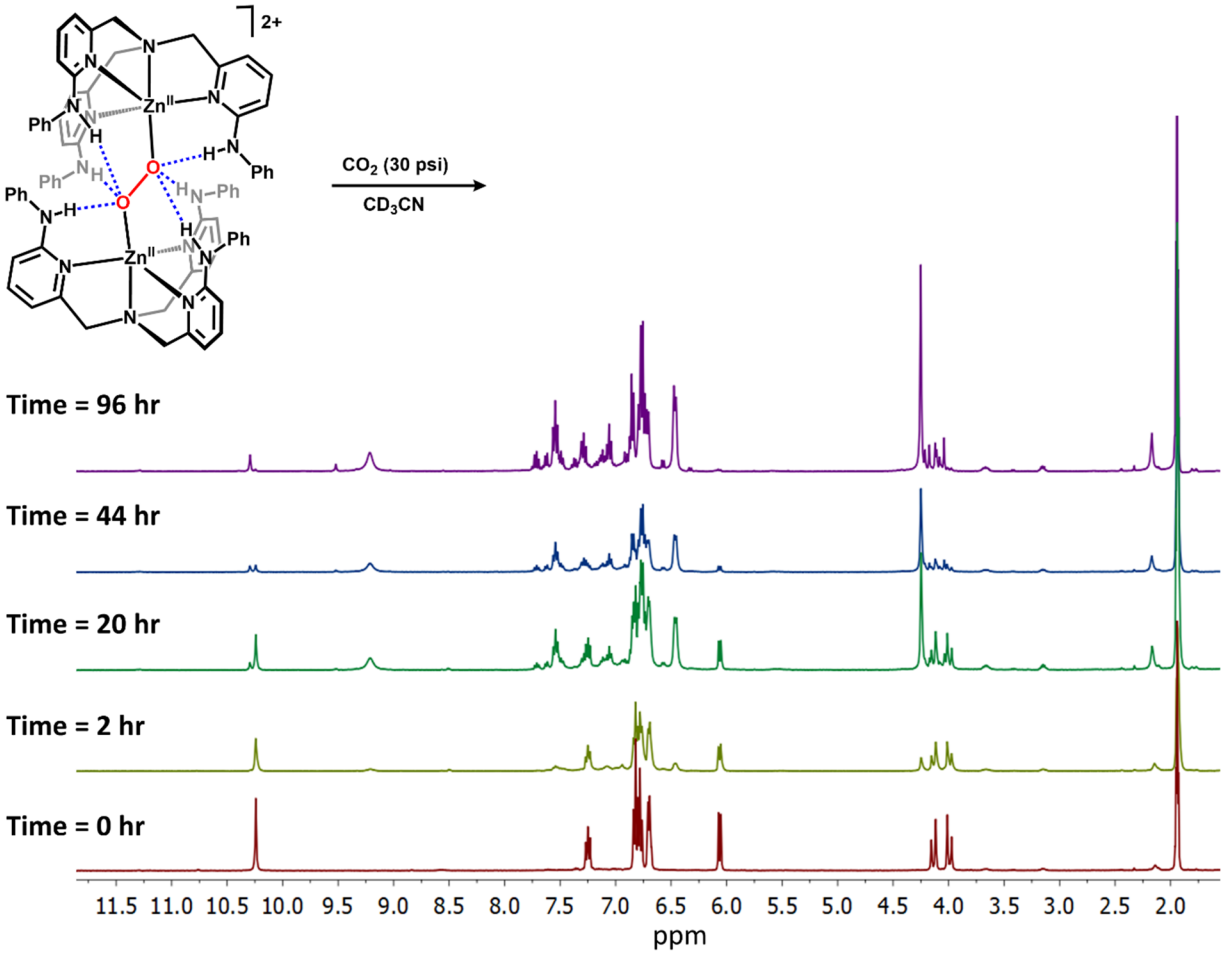

Figure S31 ^{1}H NMR spectra (ambient temperature, CD_3CN) illustrating decomposition of **1^{H}** under a pressurized CO_2 atmosphere.

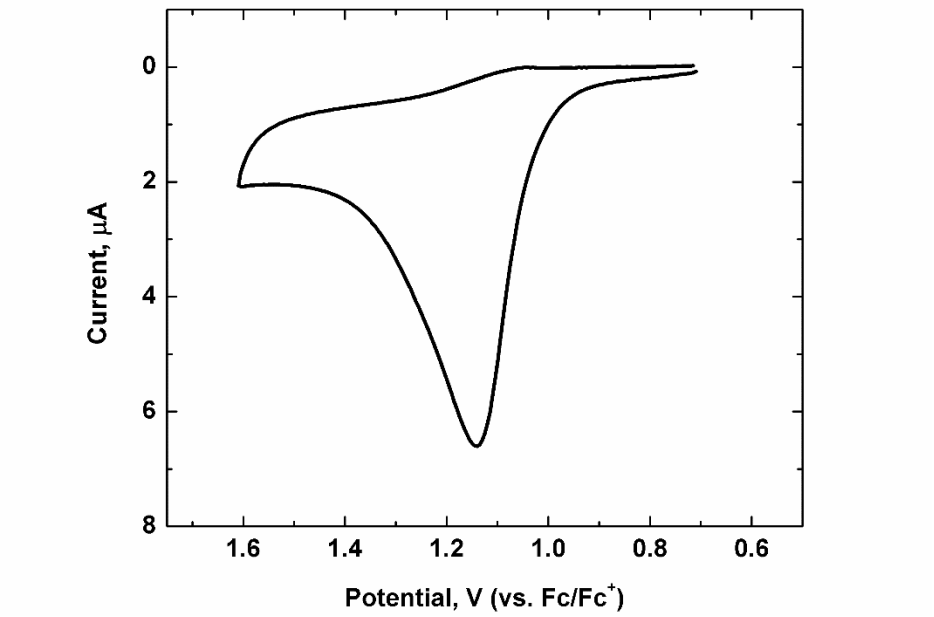

Figure S32 Cyclic voltammogram (Pt electrode, 100 mV/s scan rate, vs. internal Fc/Fc^{+}) of $[L^{H}{}_{2}Zn_{2}O_{2}][OTf]_{2}$ (2.6 mmol) recorded in $CH_{3}CN$ with 0.1 $[Bu_{4}N][ClO_{4}]$.

Oxidation of $[L^H_2Zn_2O_2][OTf]_2$: Detection and Quantification of Dioxygen

Dissolved O_2 was quantified using a Unisense Microsensor Monometer with an Ox-500 oxygen probe adapted from previous reports.[9,10]

Experiment #1: Addition of $[L^H_2Zn_2O_2][OTf]_2$ to aqueous solution of $[Bu_4N][Cl]$ and $[NH_4]_2[Ce(NO_3)_6]$

A 3-neck round bottom flask was filled with tetrabutylammonium chloride (0.034 mL, aqueous 0.7409 M stock solution, 0.025 mmol), ceric ammonium nitrate (0.018 mL, aqueous 0.7004 M stock solution, 0.0125 mmol), 0.500 mL MeCN and water to a total volume of 40.48 mL. The other two necks of the flasks were sealed with rubber septa (to allow sparging) such that no headspace existed in the flask. The Ox-500 probe was calibrated with a three-point calibration in the Ox-500 probe was calibrated with a three-point calibration in N_2-sparged (0% O_2, $[O_2]$ = 0 mM), air-saturated (20.8% O_2, O_2 = 0.27 mM), and O_2-saturated (100% O_2, 1.3 mM) solutions. The dissolved $[O_2]$ concentration was estimated based on the Henry's law constant for O_2 in water, k_H = 1.3 mol L^{-1} bar^{-1}. Note that the $[O_2]$ concentrations are approximate and do not take into account the effects of the dissolved salts or ~1 % v/v MeCN in solution. These data illustrate that O_2 evolution only occurs when the two requisite components, $[L^H_2Zn_2O_2][OTf]_2$ and ceric ammonium nitrate, are present.

The flask was reset analogous to description above, except the 0.500 mL MeCN was omitted. The solution was allowed to equilibrate. Upon equilibration, $[L^H_2Zn_2O_2][OTf]_2$ (0.010 g, 0.00629 mmol) was dissolved in 0.500 mL MeCN and injected into the flask resulting in a rapid increase of dioxygen. The dioxygen production was monitored until a plateau was observed. Subject to these experimental conditions, approximately 2.96 µmol of dioxygen were produced (corresponding to 47% of theoretical value of 6.29 µmol).

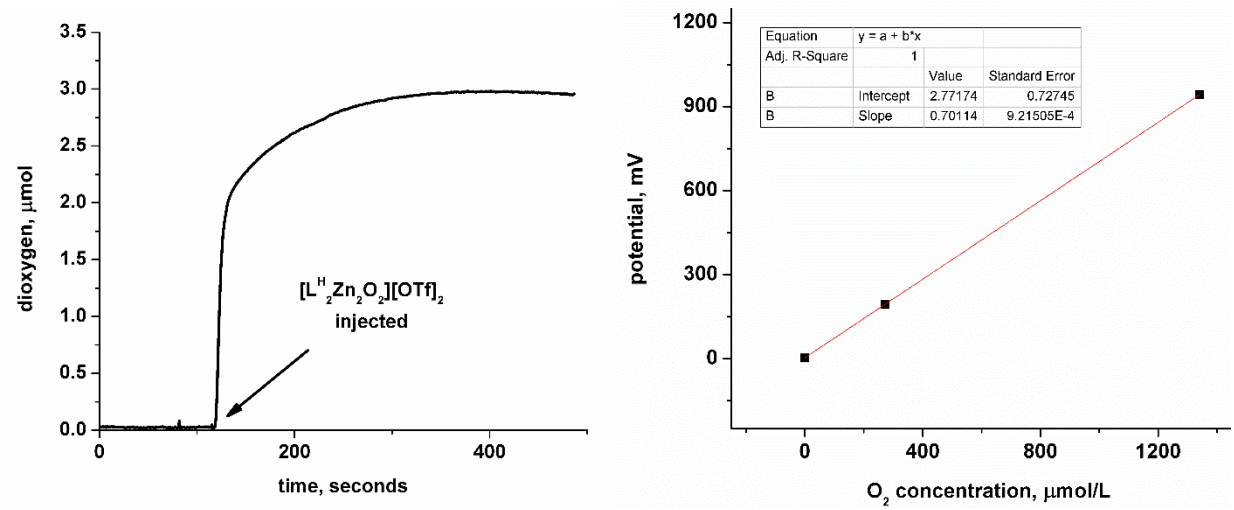

Figure S33 Left: Oxygen production as a result of oxidation of $[L^H_2Zn_2O_2][OTf]_2$ with ceric ammonium nitrate. Right: Calibration curve.

Experiment #2: Addition of $[NH_4]_2[Ce(NO_3)_6]$ to aqueous solution of $[Bu_4N][Cl]$ and $[L^H{}_2Zn_2O_2][OTf]_2$

A 3-neck round bottom flask was filled with tetrabutylammonium chloride (0.034 mL, aqueous 0.7409 M stock solution, 0.025 mmol), $[L^H{}_2Zn_2O_2][OTf]_2$ (0.010 g, 0.00629 mmol; dissolved in 0.500 mL MeCN), and water to a total volume of 40.98 mL. The other two necks of the flasks were sealed with rubber septa (to allow sparging) such that no headspace existed in the flask. The Ox-500 probe was calibrated with a three-point calibration in the Ox-500 probe was calibrated with a three-point calibration in N_2-sparged (0% O_2, $[O_2]$ = 0 mM), air-saturated (20.8% O_2, O_2 = 0.27 mM), and O_2-saturated (100% O_2, 1.3 mM) solutions. The dissolved $[O_2]$ concentration was estimated based on the Henry's law constant for O_2 in water, k_H = 1.3 mol L^{-1} bar^{-1}. Note that the $[O_2]$ concentrations are approximate and do not take into account the effects of the dissolved salts or ~1 % v/v MeCN in solution. These data illustrate that O_2 evolution only occurs when the two requisite components, $[L^H{}_2Zn_2O_2][OTf]_2$ and ceric ammonium nitrate, are present.

The flask was reset analogous to description above. The solution was allowed to equilibrate. Upon equilibration, $[NH_4]_2[Ce(NO_3)_6]$ (0.018 mL, aqueous 0.7004 M stock solution, 0.0125 mmol) was injected into the flask resulting in a rapid increase of dioxygen. The dioxygen production was monitored until a plateau was observed. Subject to these experimental conditions, approximately 2.76 µmol of dioxygen were produced (corresponding to 45% of theoretical value of 6.29 µmol).

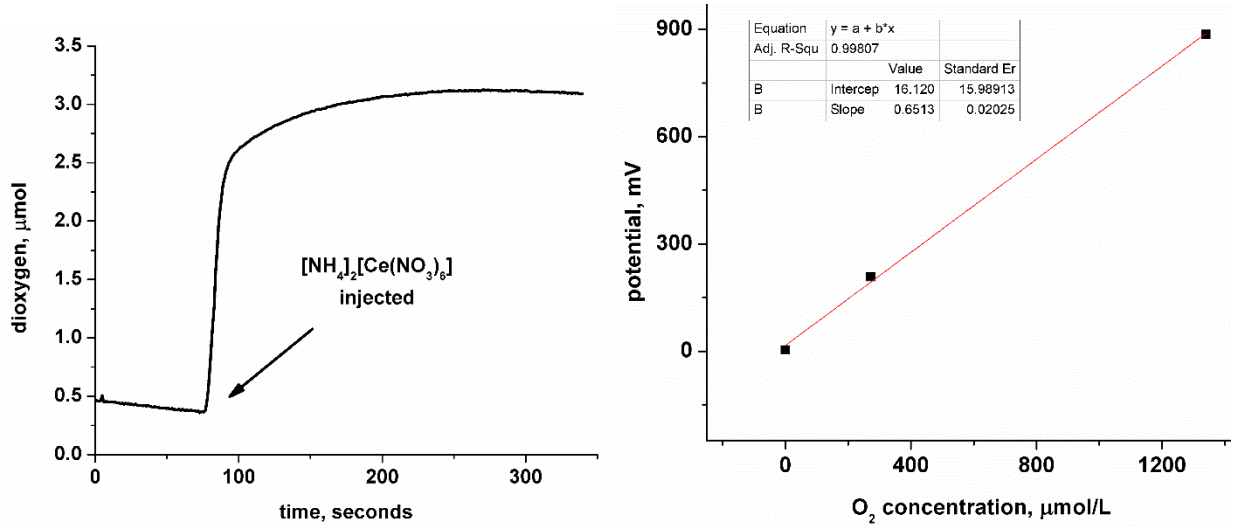

Figure S34 Left: Oxygen production as a result of oxidation of $[L^H{}_2Zn_2O_2][OTf]_2$ with ceric ammonium nitrate. Right: Calibration curve.

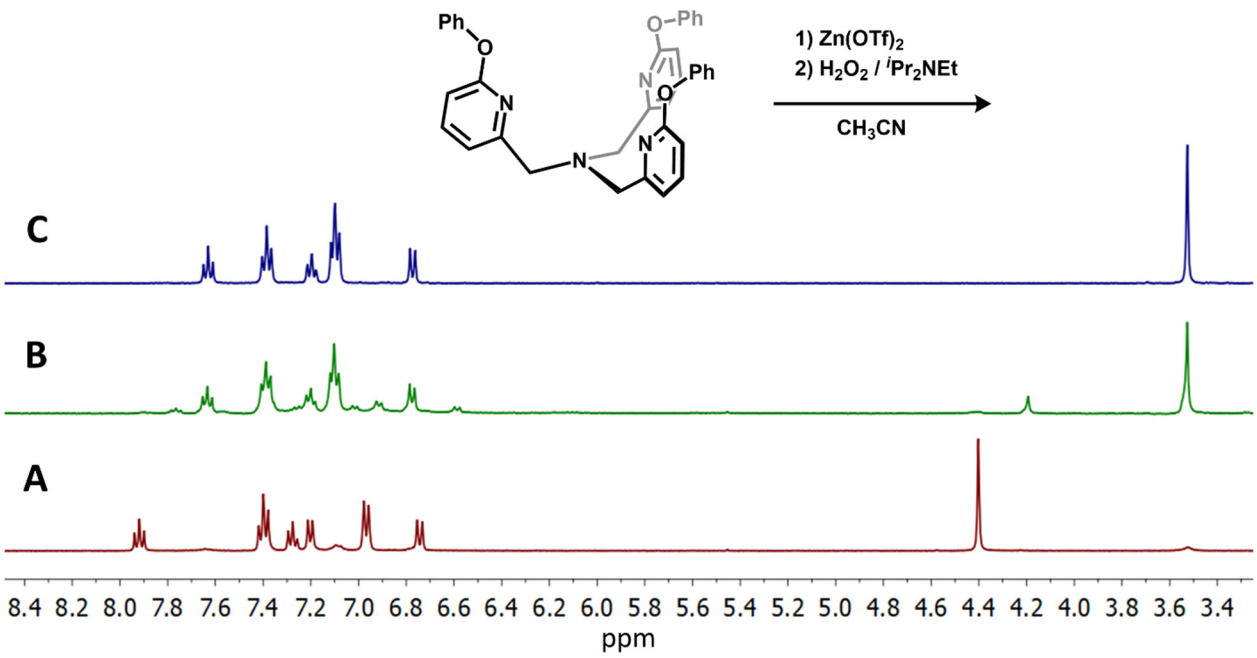

Figure S35 ^{1}H NMR spectra (ambient temperature, CH_3CN): A) after mixing TPA^{OPh} and $Zn(OTf)_2$, B) after addition of H_2O_2 (30% aqueous) and $^{i}Pr_2NEt$, and C) authentic sample of TPA^{OPh} for comparison.

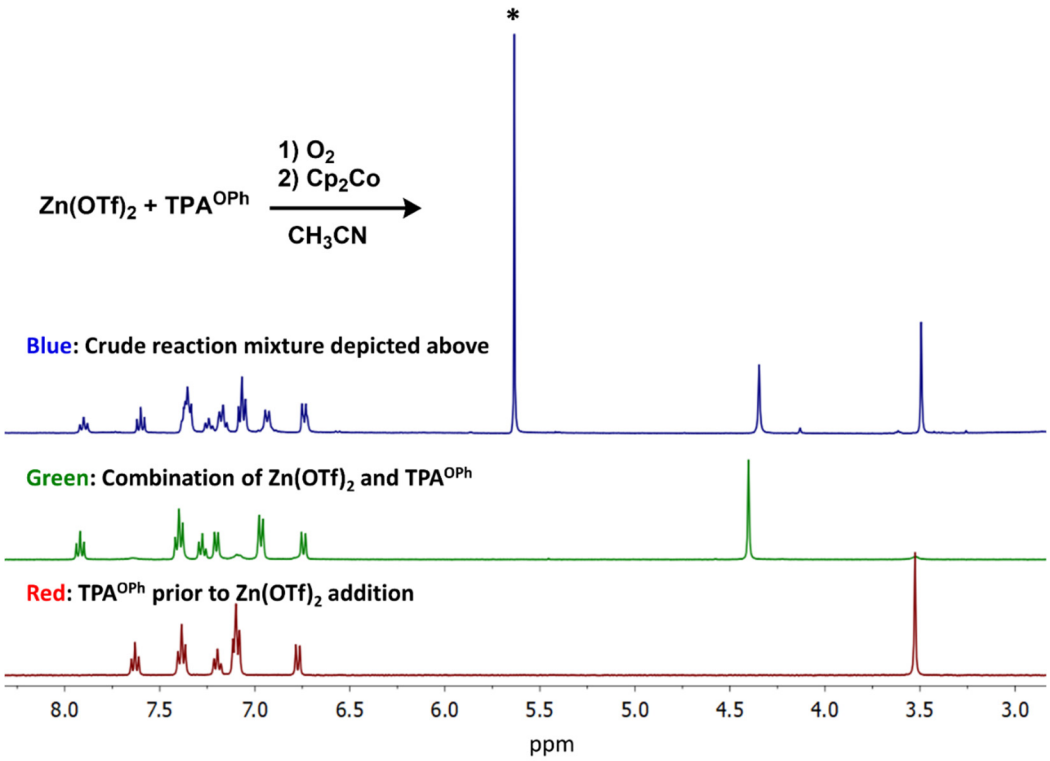

Figure S36 ^{1}H NMR spectra (ambient temperature, CH_3CN) of attempted formation of a dizinc peroxide complex with the TPA^{OPh} ligand. Bottom (red): free ligand prior to $Zn(OTf)_2$ addition. Middle (green): combination of $Zn(OTf)_2$ and TPA^{OPh}. Top (blue): crude spectrum after O_2 and cobaltocene addition. The experimental setup was analogous to that described for the synthesis of $\mathbf{1^H}$.

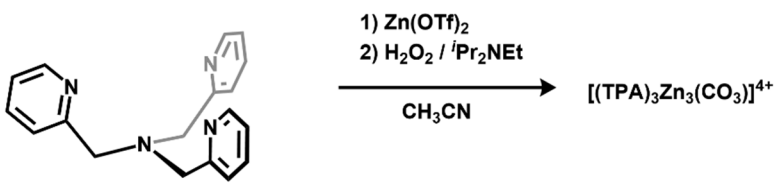

$[(TPA)_3Zn_3(CO_3)][ClO_4]_4$
***J. Chem. Soc. Chem. Commun.*, 1993, 1236**
Reported resonances (300 MHz, CD_3NO_2):
4.45, 7.19, 7.-2, 8.02, 8.89 ppm

$[(TPA)_3Zn_3(CO_3)][OTf]_4$
Crude reaction mixture, this work
Resonances (*) (400 MHz, CD_3NO_2):
4.43, 7.20, 7.54, 8.02, 8.92 ppm

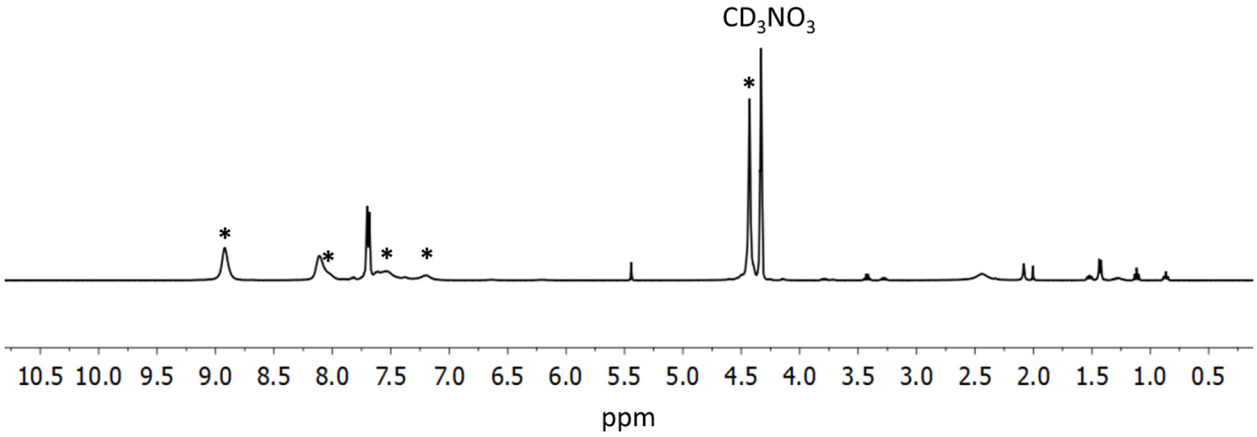

Figure S37 ^{1}H NMR spectrum (ambient temperature, CD_3NO_2) of attempted peroxide formation with TPA ligand.

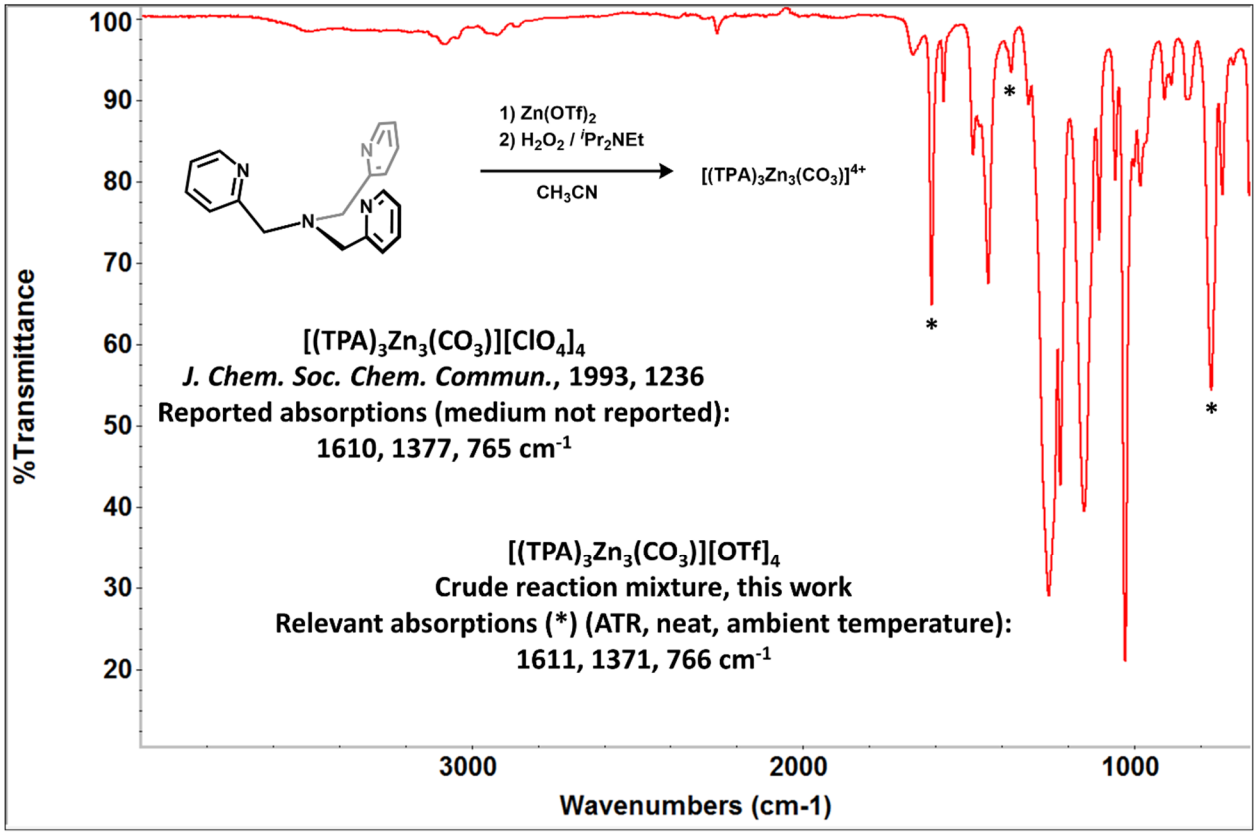

Figure S38 Infrared spectrum (ambient temperature, neat, ATR) of attempted peroxide formation with TPA ligand.

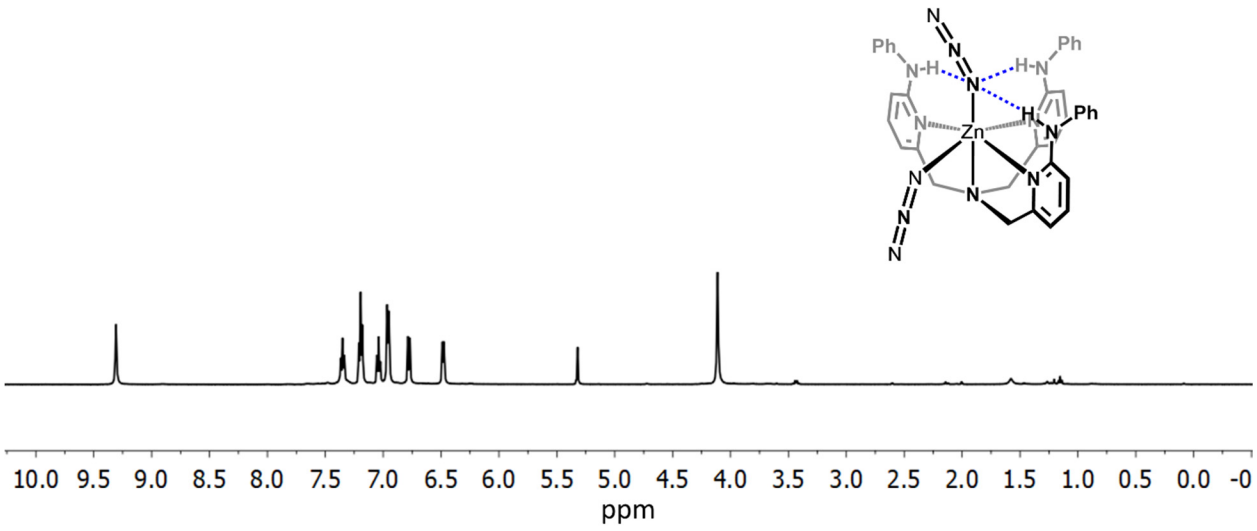

Figure S39 ^{1}H NMR spectrum (CD_2Cl_2, ambient temperature) of $(L^{H})Zn(N_3)_2$.

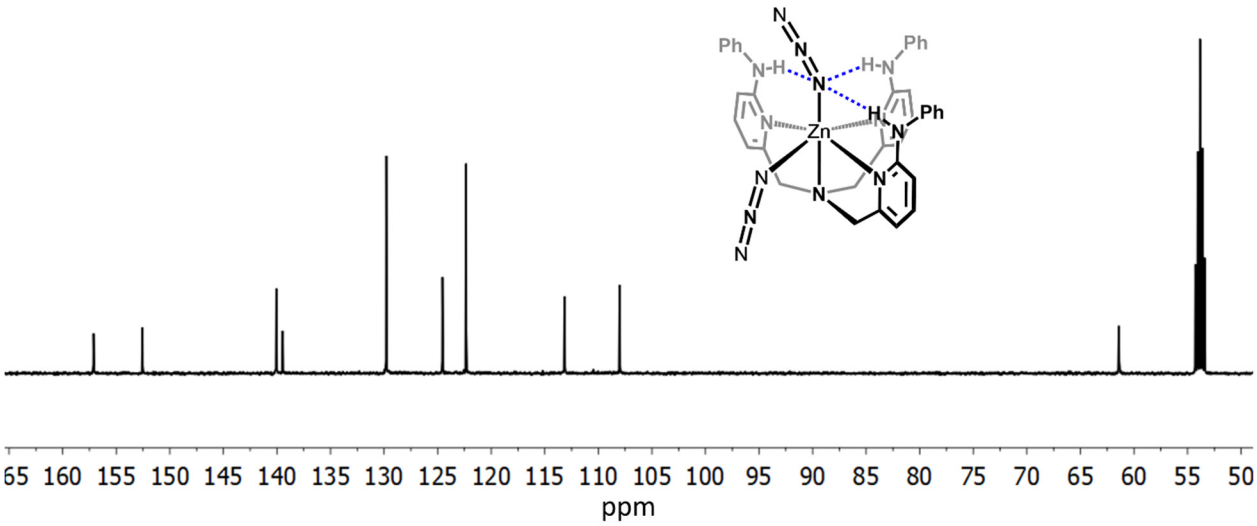

Figure S40 ^{13}C NMR spectrum (CD_2Cl_2, ambient temperature) of $(L^H)Zn(N_3)_2$.

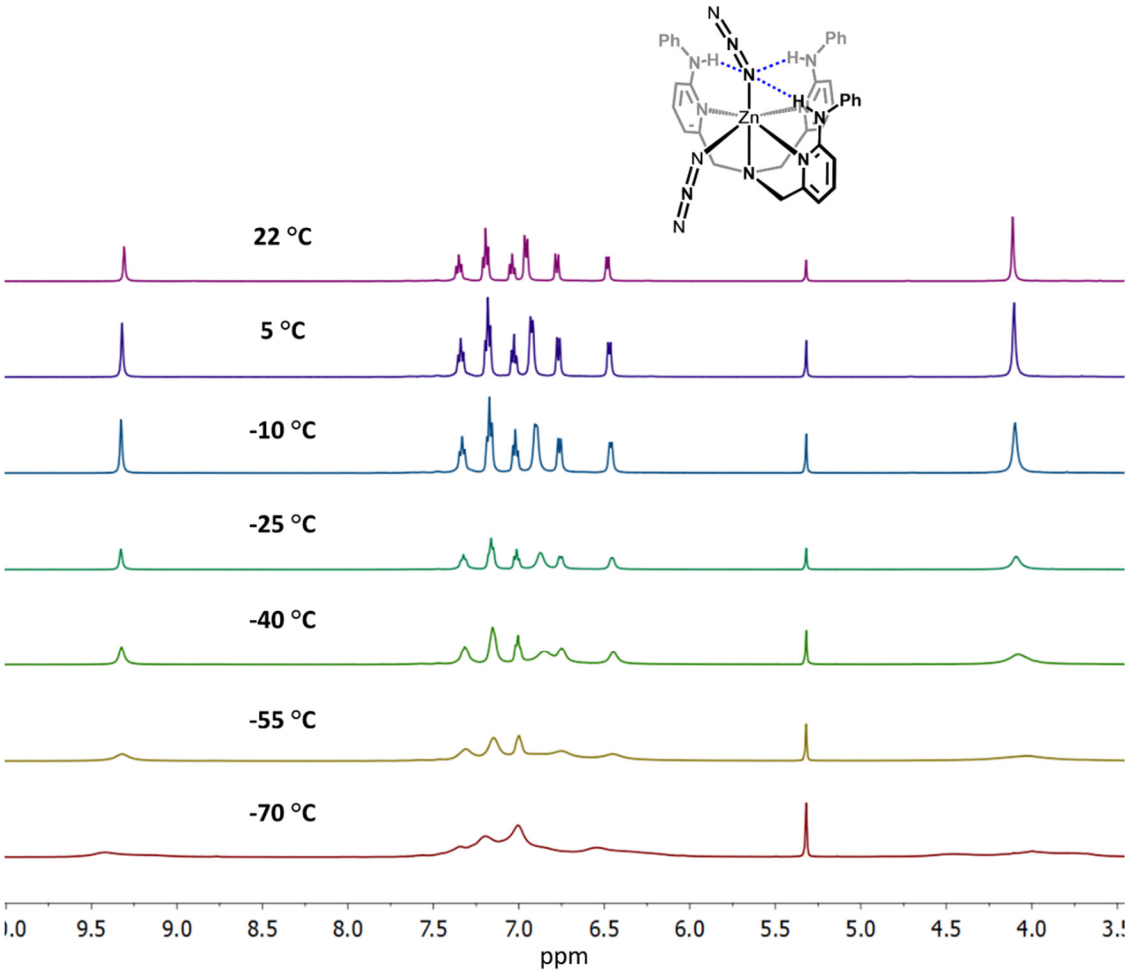

Figure S41 Variable temperature ^1H NMR spectra (CD_2Cl_2) of $(L^H)Zn(N_3)_2$.

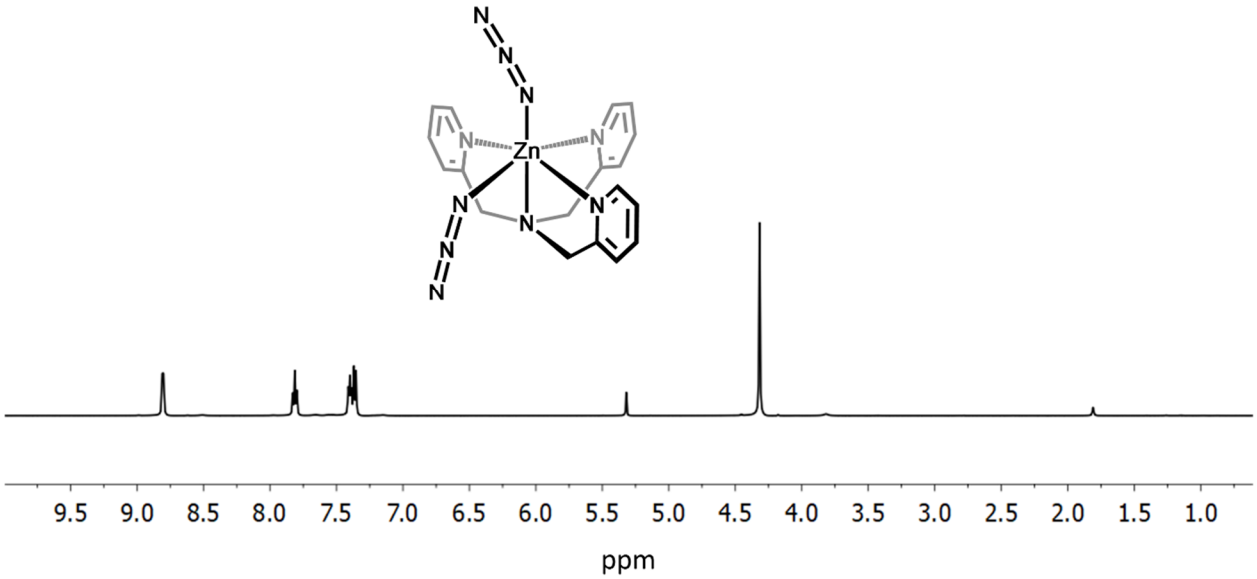

Figure S42 ^{1}H NMR spectrum (CD_2Cl_2, ambient temperature) of (TPA)Zn$(N_3)_2$.

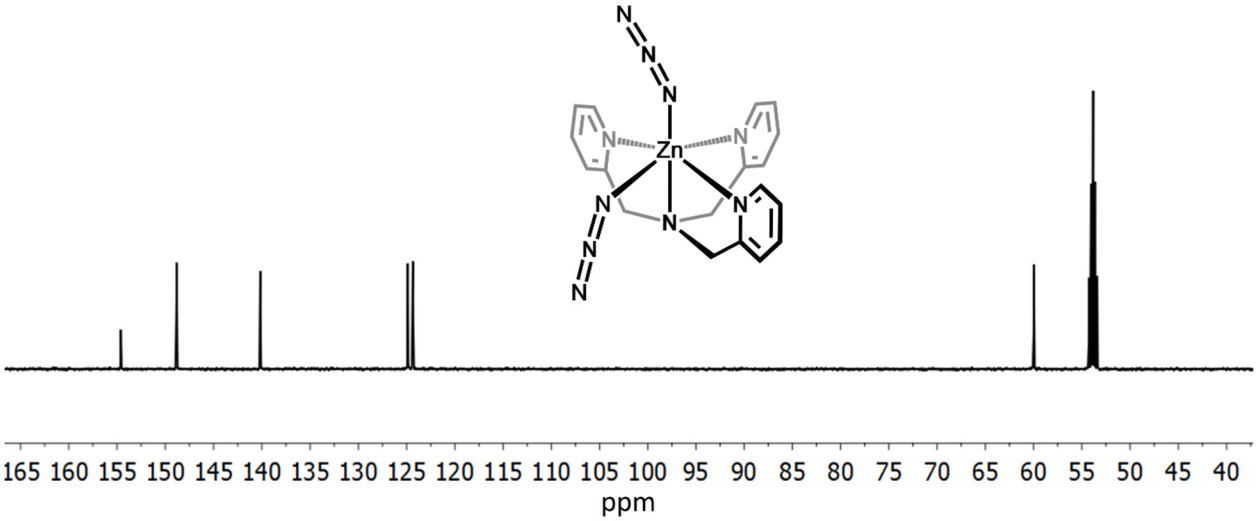

Figure S43 ^{13}C NMR spectrum (CD_2Cl_2, ambient temperature) of (TPA)Zn$(N_3)_2$.

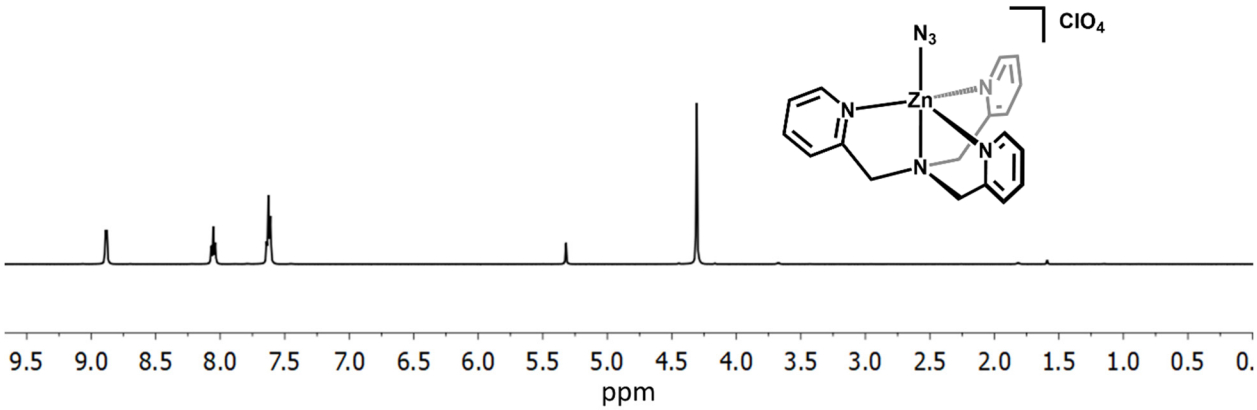

Figure S44 ^{1}H NMR spectrum (CD_2Cl_2, ambient temperature) of [(TPA)Zn(N_3)][ClO_4].

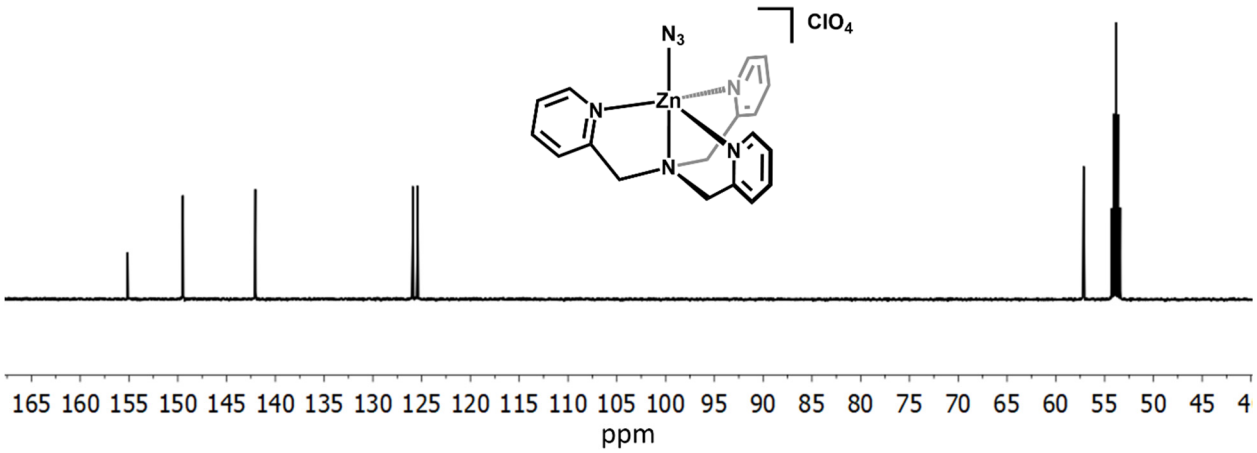

Figure S45 ^{13}C NMR spectrum (CD_2Cl_2, ambient temperature) of [(TPA)Zn(N_3)][ClO_4].

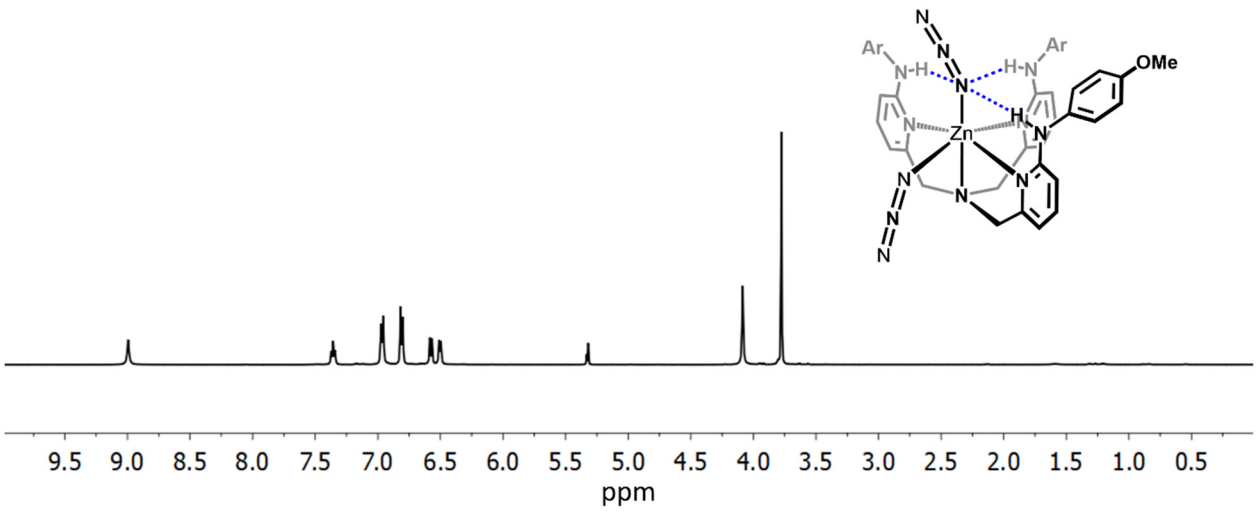

Figure S46 ^{1}H NMR spectrum (CD_2Cl_2, ambient temperature) of (L^{OMe})Zn(N_3)$_2$.

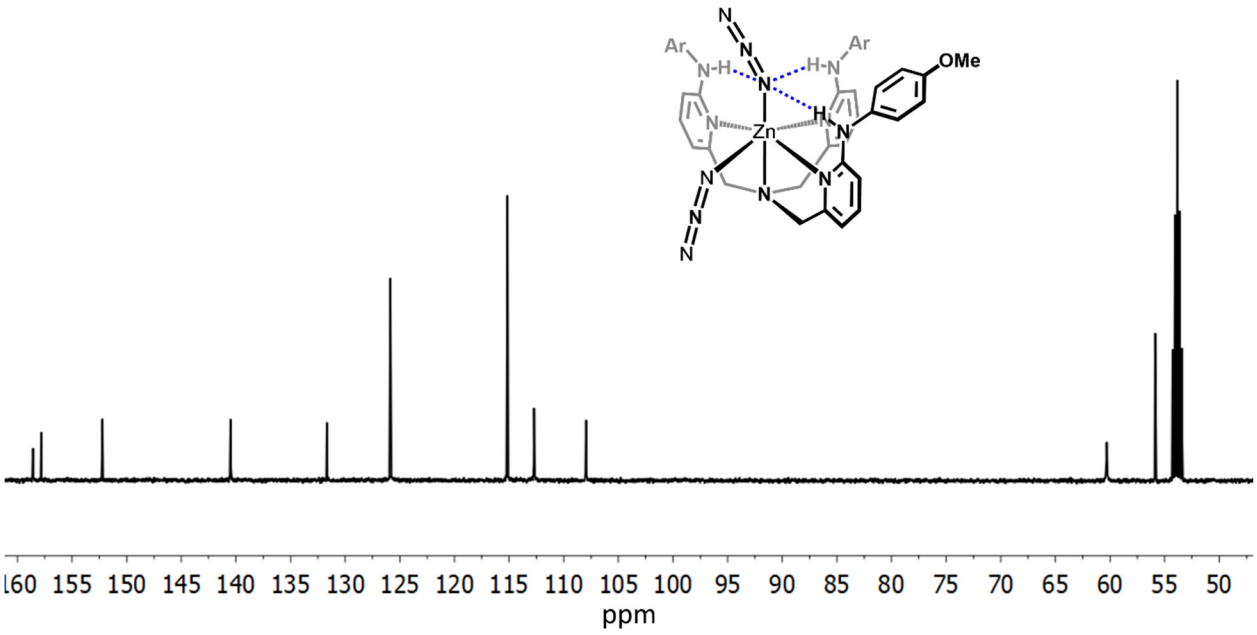

Figure S47 ^{13}C NMR spectrum (CD_2Cl_2, ambient temperature) of (L^{OMe})Zn(N_3)$_2$.

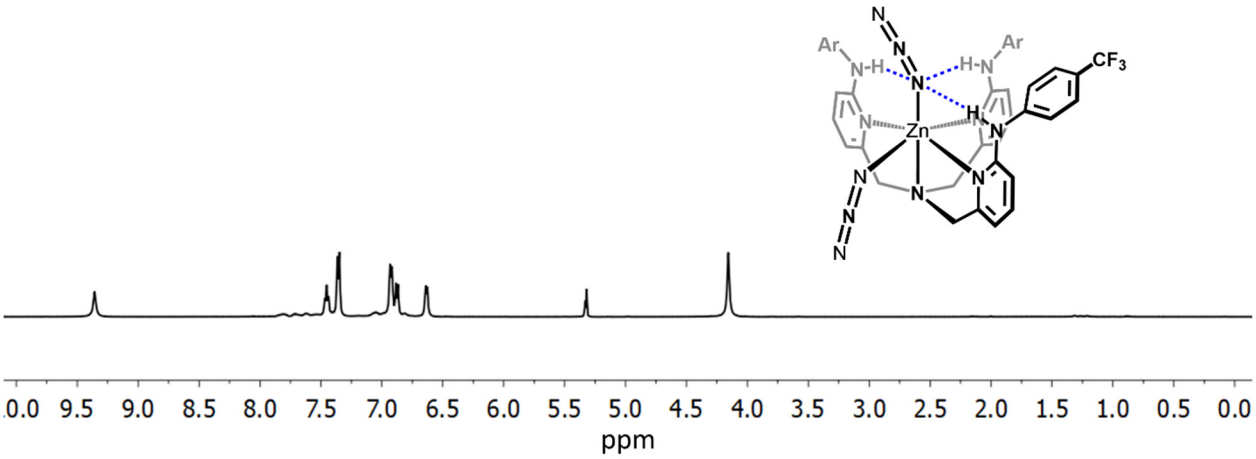

Figure S48 ^{1}H NMR spectrum (CD_2Cl_2, ambient temperature) of (L^{CF3})Zn(N_3)$_2$.

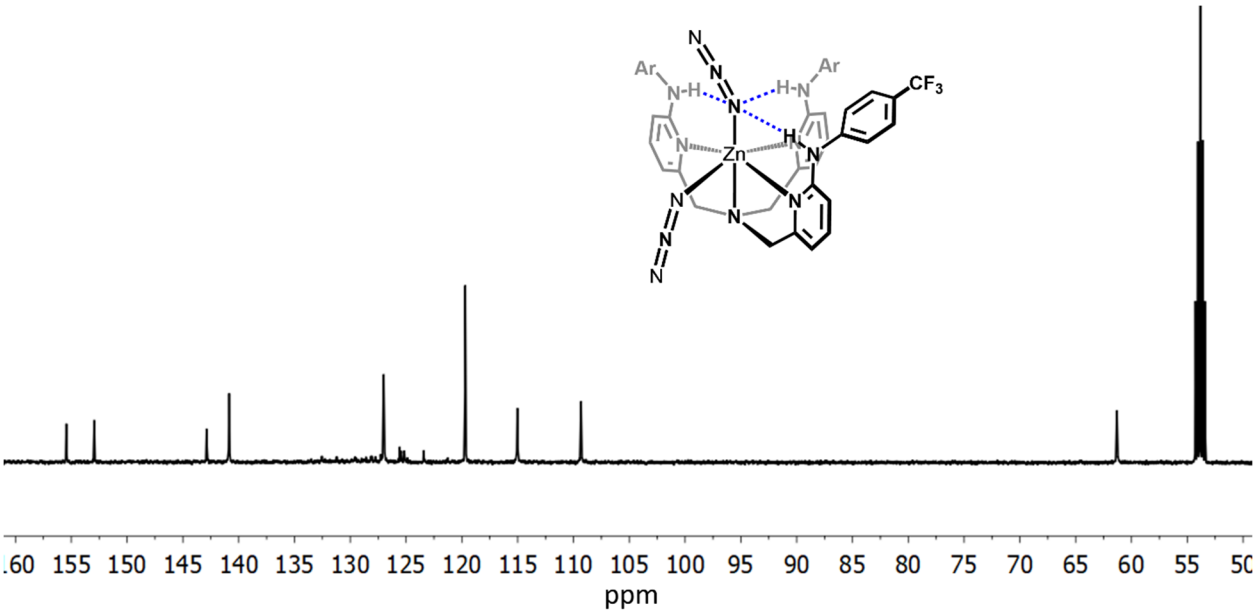

Figure S49 ^{13}C NMR spectrum (CD_2Cl_2, ambient temperature) of (L^{CF3})Zn(N_3)$_2$.

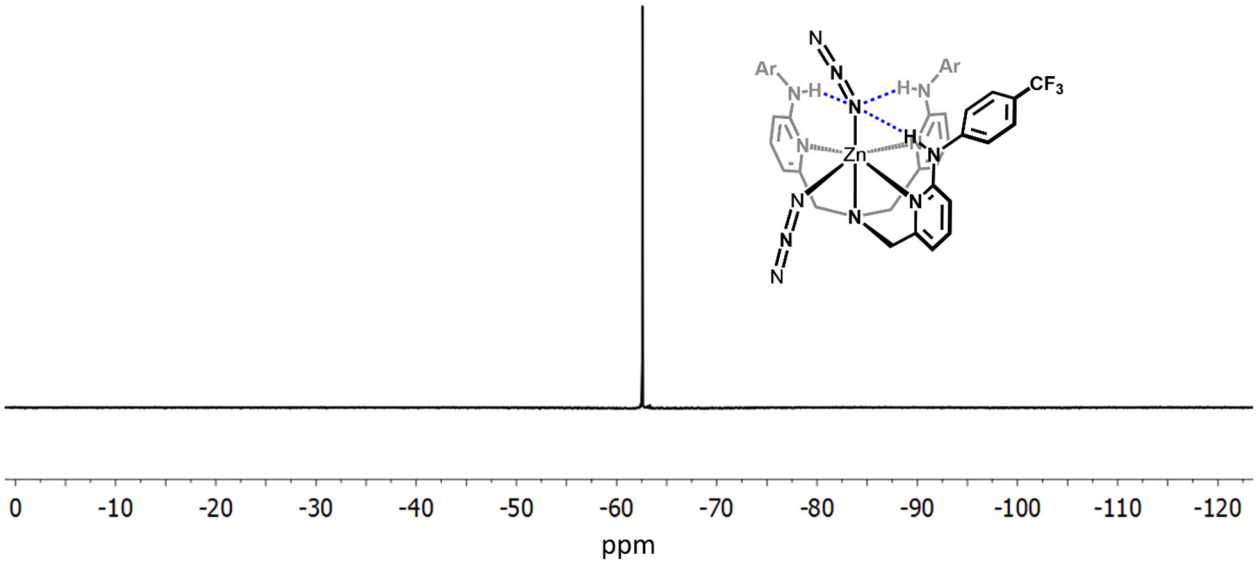

Figure S50 ^{19}F NMR spectrum (CD_2Cl_2, ambient temperature) of $(L^{CF3})Zn(N_3)_2$.

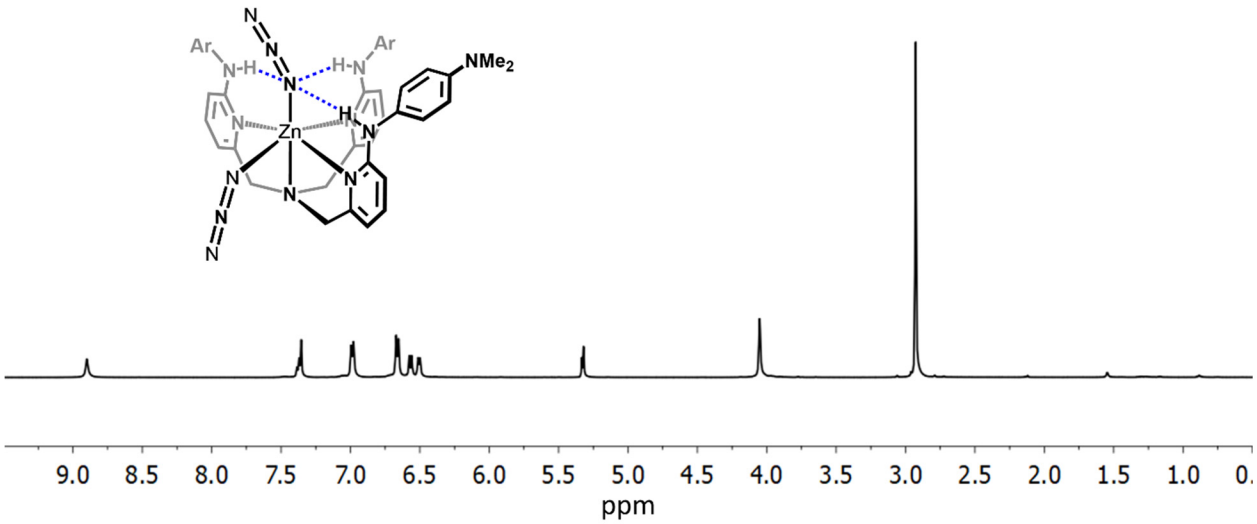

Figure S51 ^{1}H NMR spectrum (CD_2Cl_2, ambient temperature) of $(L^{NMe2})Zn(N_3)_2$.

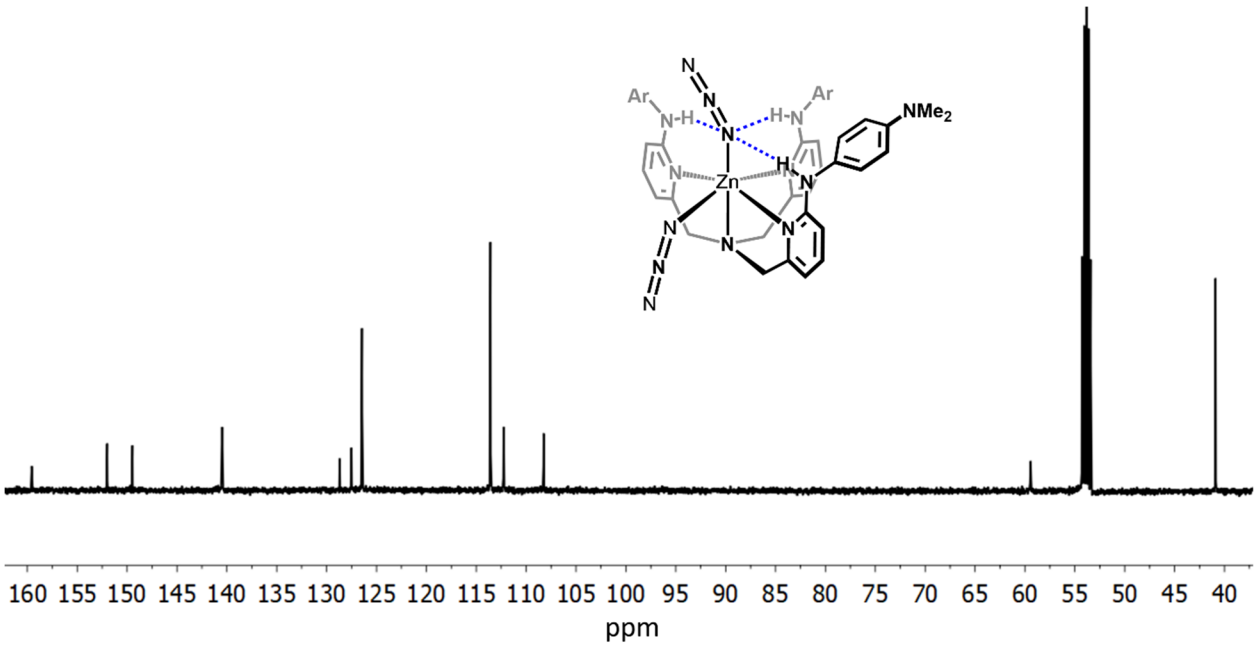

Figure S52 ^{13}C NMR spectrum (CD_2Cl_2, ambient temperature) of $(L^{NMe2})Zn(N_3)_2$.

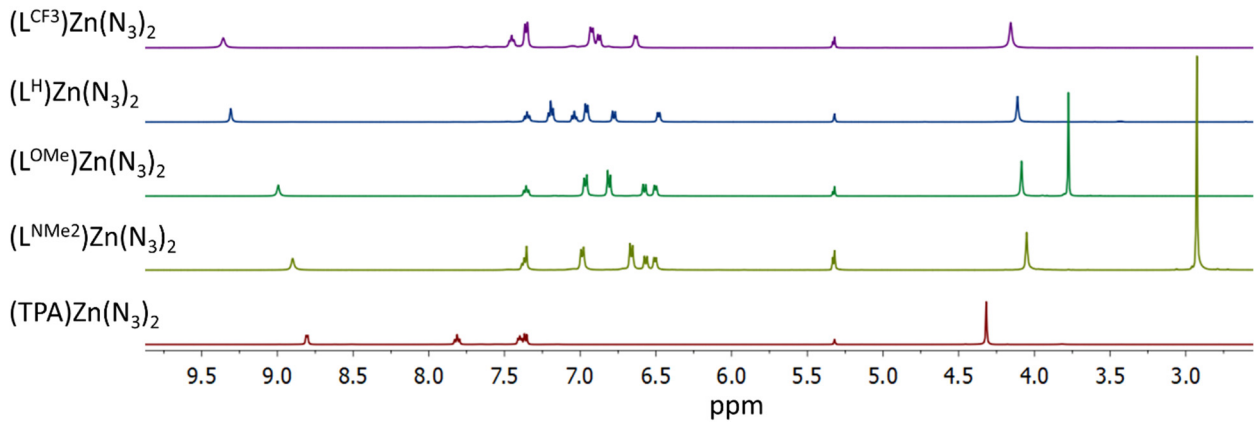

Figure S53 Overlay of ^{1}H NMR spectra (CD_2Cl_2, ambient temperature) for $Zn(N_3)_2$ complexes.

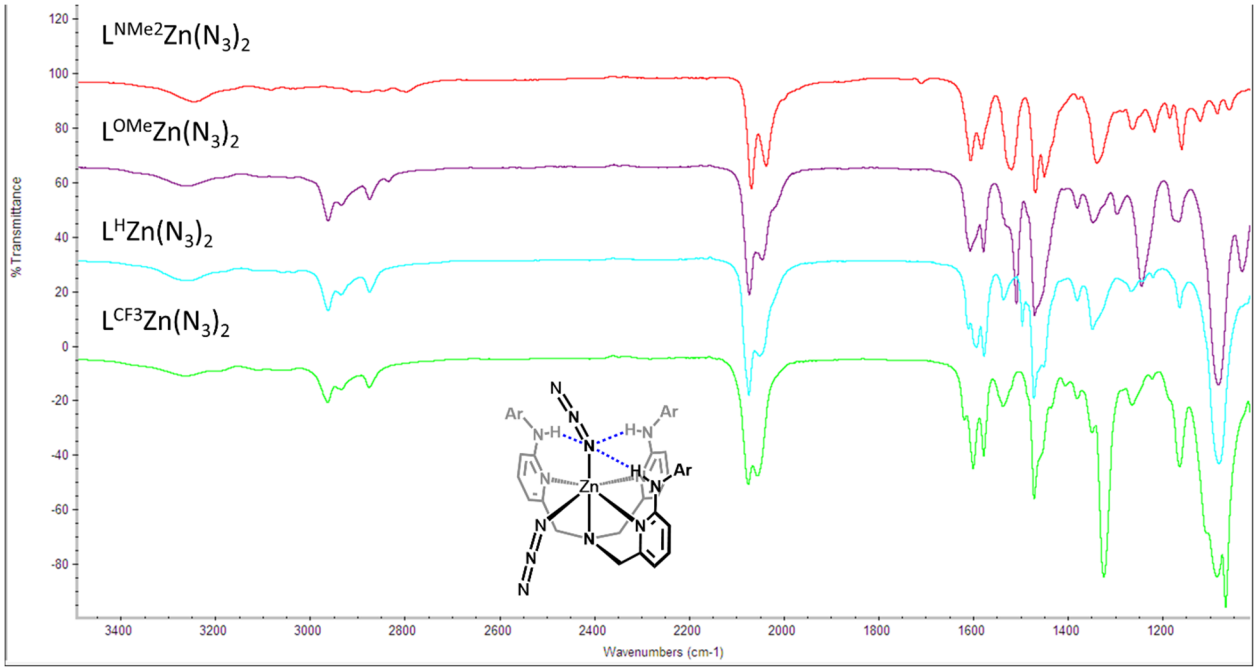

Figure S54 Overlay of infrared spectra (neat, ATR, ambient temperature) for $L^{R}Zn(N_3)_2$ complexes.

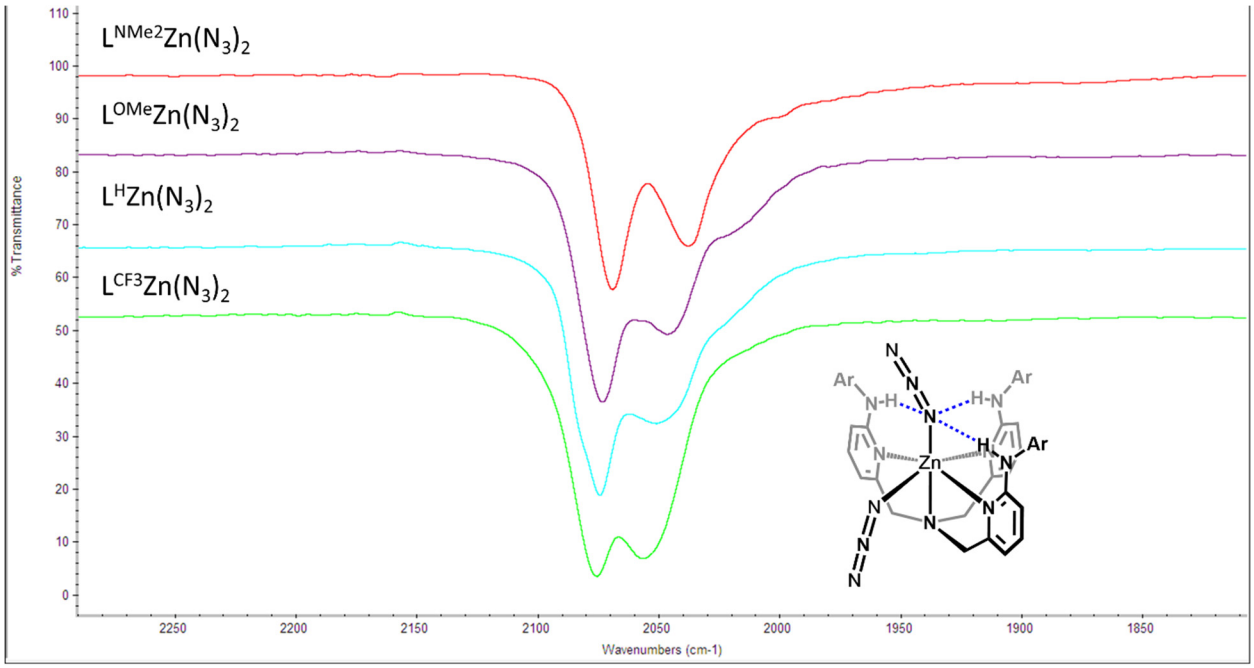

Figure S55 Overlay of infrared spectra (neat, ATR, ambient temperature) emphasizing the azide region for $L^{R}Zn(N_3)_2$ complexes.

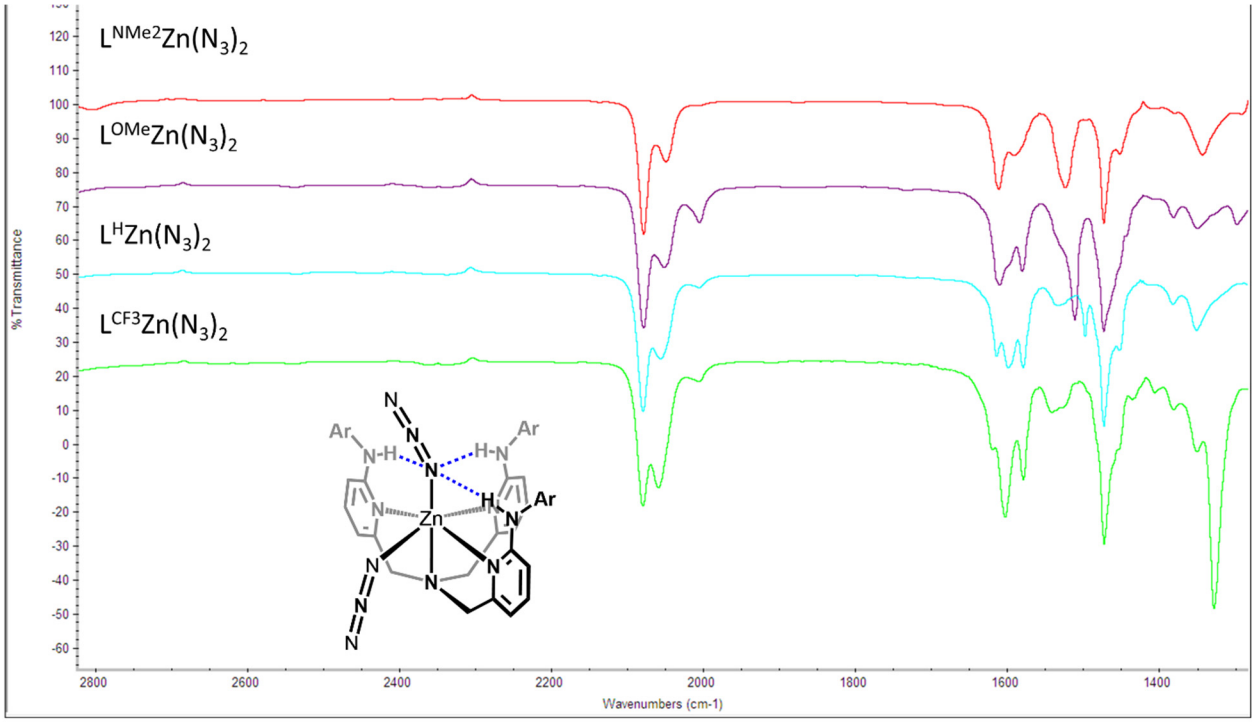

Figure S56 Overlay of infrared spectra (CH_2Cl_2 solution, ambient temperature) for $L^RZn(N_3)_2$ complexes.

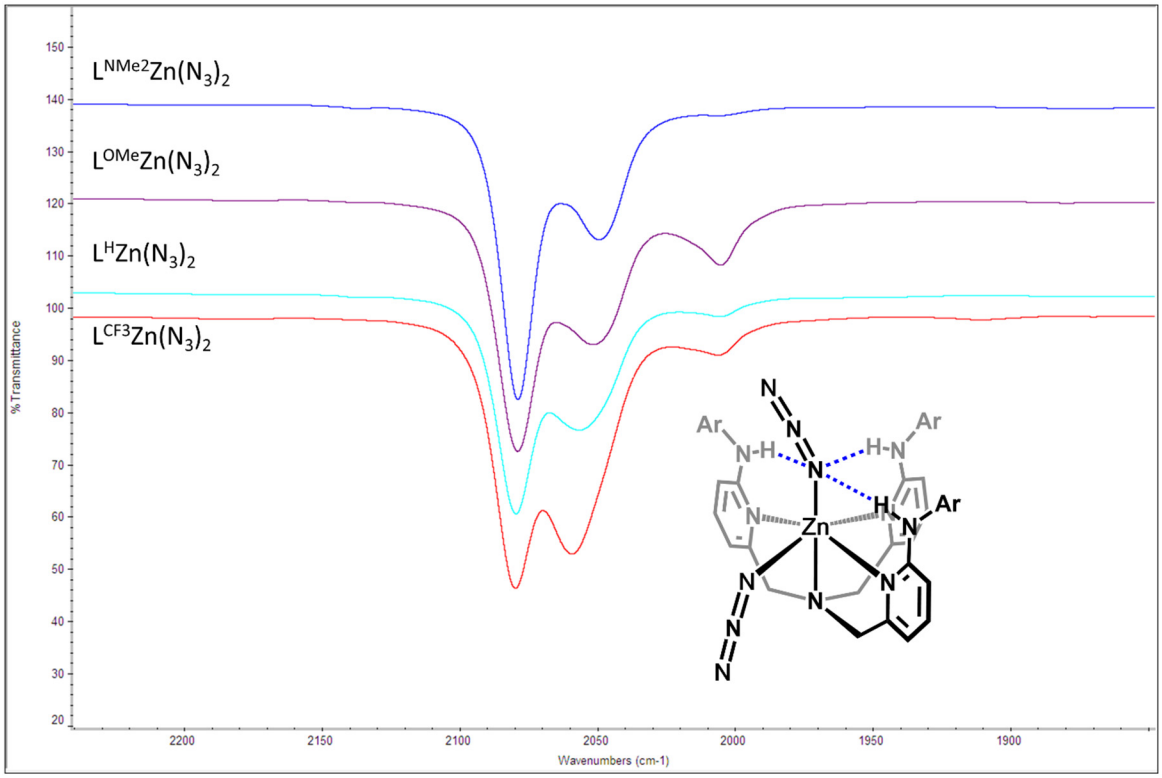

Figure S57 Overlay of infrared spectra (CH_2Cl_2 solution, ambient temperature) emphasizing the azide region for $L^RZn(N_3)_2$ complexes.

Table S1 Infrared spectral data for $\upsilon_{(N3)}$ (cm^{-1}) of $L^{R}Zn(N_3)_2$ compounds and $(TPA)Zn(N_3)_2$

	Solution (CH_2Cl_2)		Neat (ATR)	
Compound	Axial N_3 Ligand	Equatorial N_3 Ligand	Axial N_3 Ligand	Equatorial N_3 Ligand
$L^{NMe2}Zn(N_3)_2$	2079.0	2049.6	2069.2	2037.9
$L^{OMe}Zn(N_3)_2$	2079.1	2051.7	2073.4	2046.6
$L^{H}Zn(N_3)_2$	2079.7	2056.8	2074.5	2051.1
$L^{CF3}Zn(N_3)_2$	2079.9	2059.3	2075.7	2056.6
$(TPA)Zn(N_3)_2$	2069.2	2043.7	2057.7	2032.8

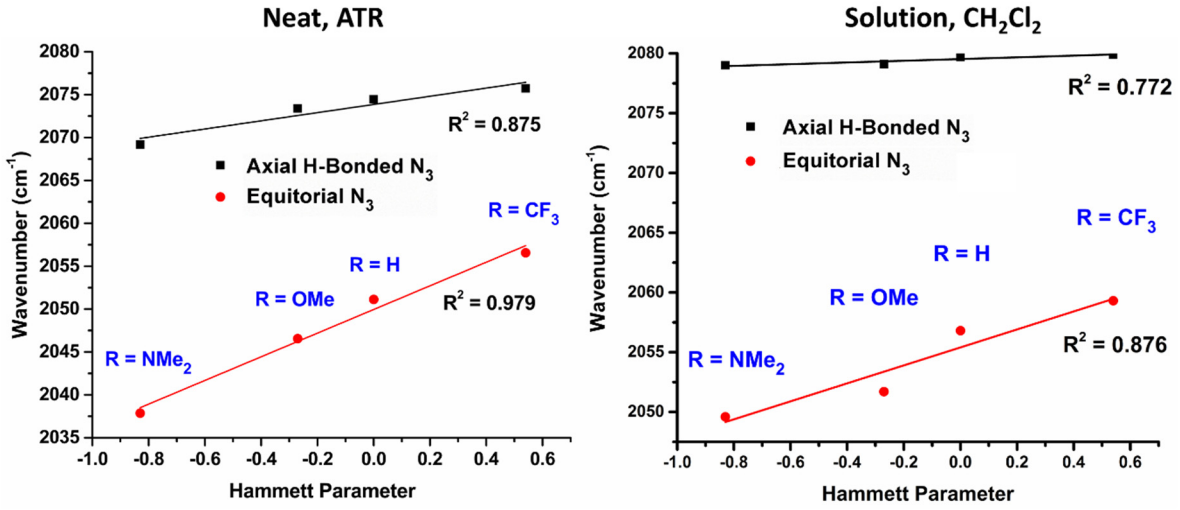

Figure S58 Plots of the $\upsilon_{(N3)}$of $L^{R}Zn(N_3)_2$ complexes versus Hammett parameters. Left: data obtained on solid samples. Right: data obtained in CH_2Cl_2 solution.

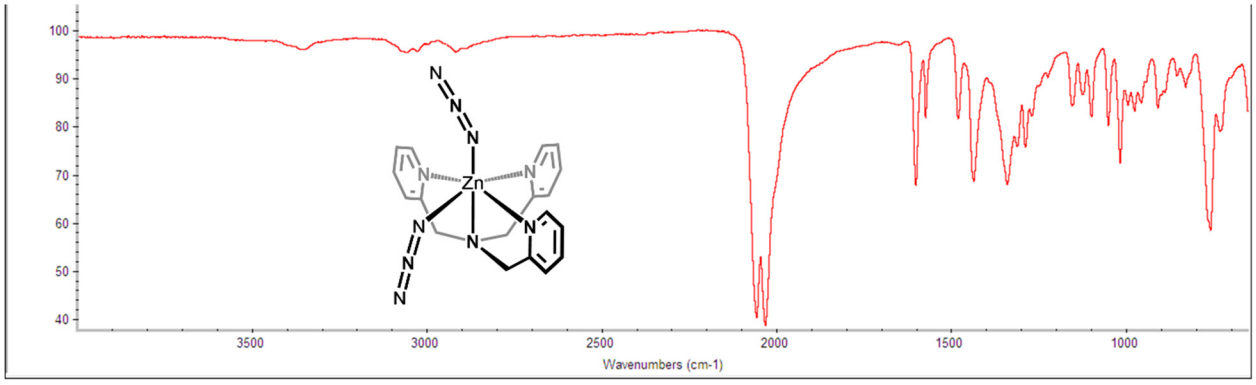

Figure S59 Infrared spectrum (neat, ATR, ambient temperature) of (TPA)Zn(N_3)$_2$.

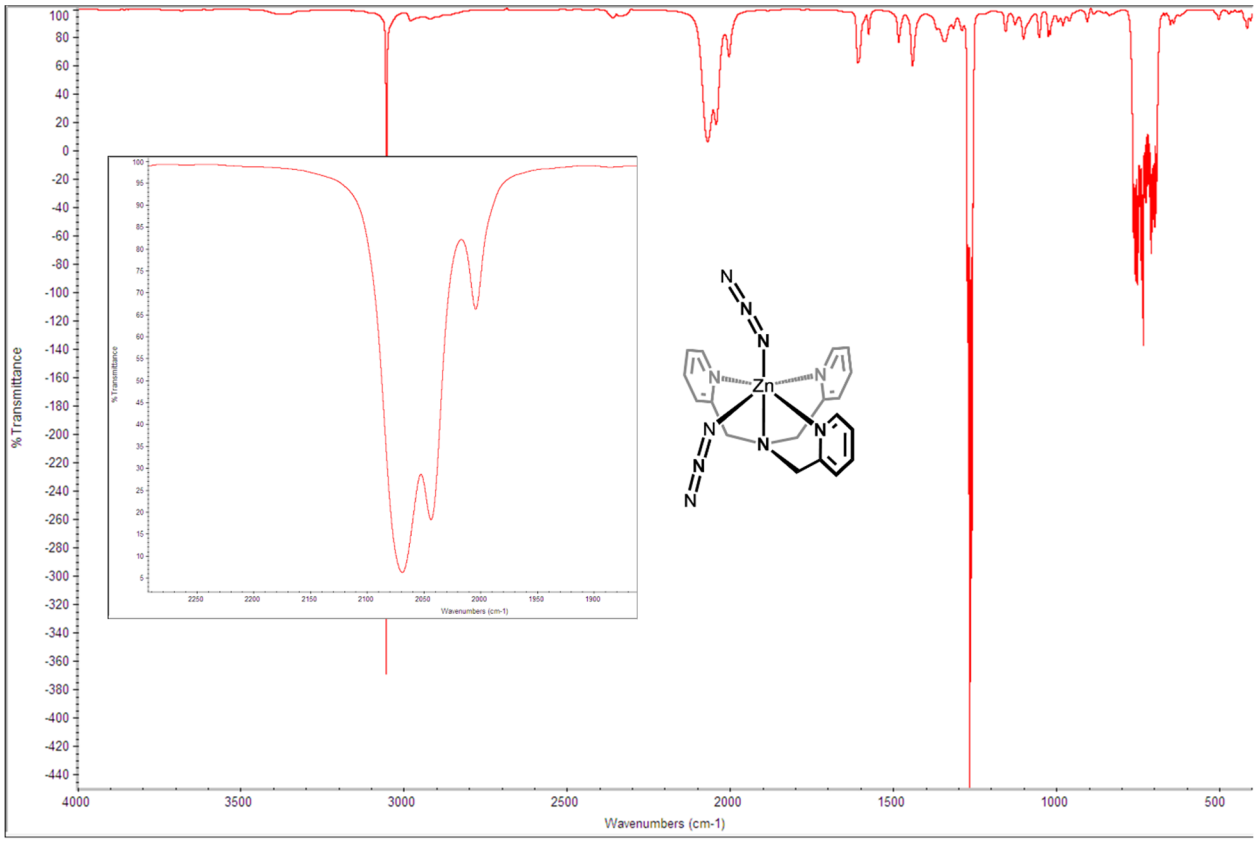

Figure S60 Infrared spectrum (CH_2Cl_2 solution, ambient temperature) of (TPA)Zn(N_3)$_2$. Inset emphasizes the azide region.

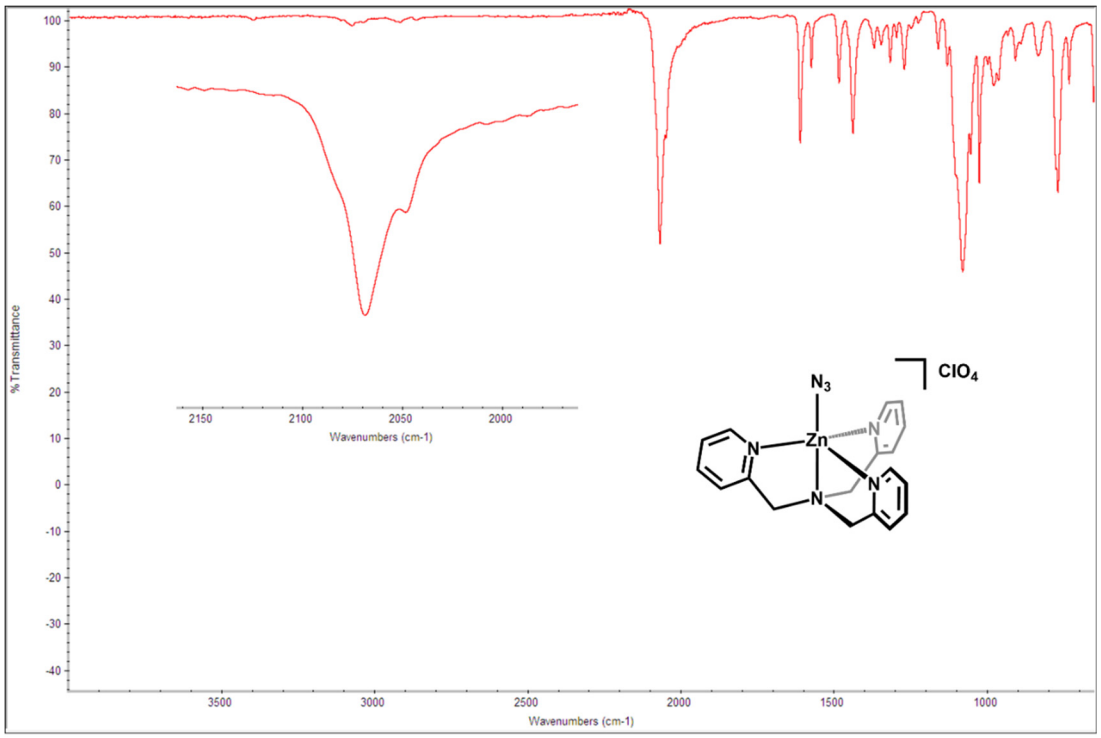

Figure S61 Infrared spectrum (neat, ATR, ambient temperature) of [(TPA)Zn(N_3)][ClO_4]. Inset emphasizes the azide region.

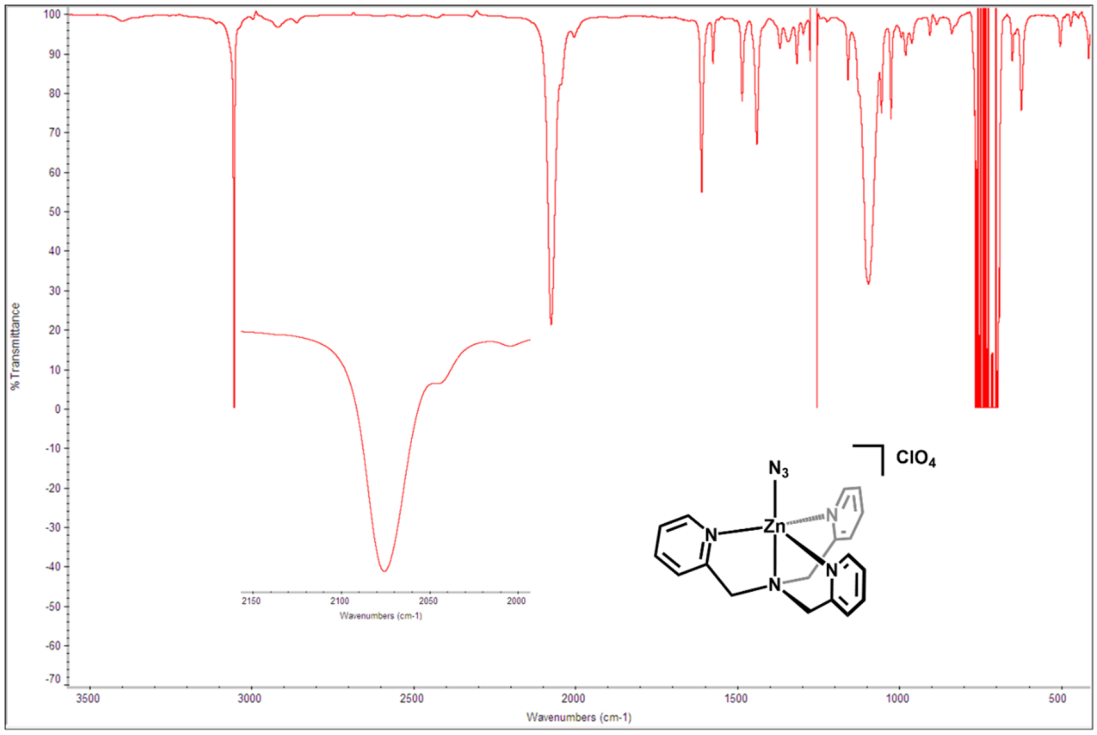

Figure S62 Infrared spectrum (CH_2Cl_2 solution, ambient temperature) of [(TPA)Zn(N_3)][ClO_4]. Inset emphasizes the azide region.

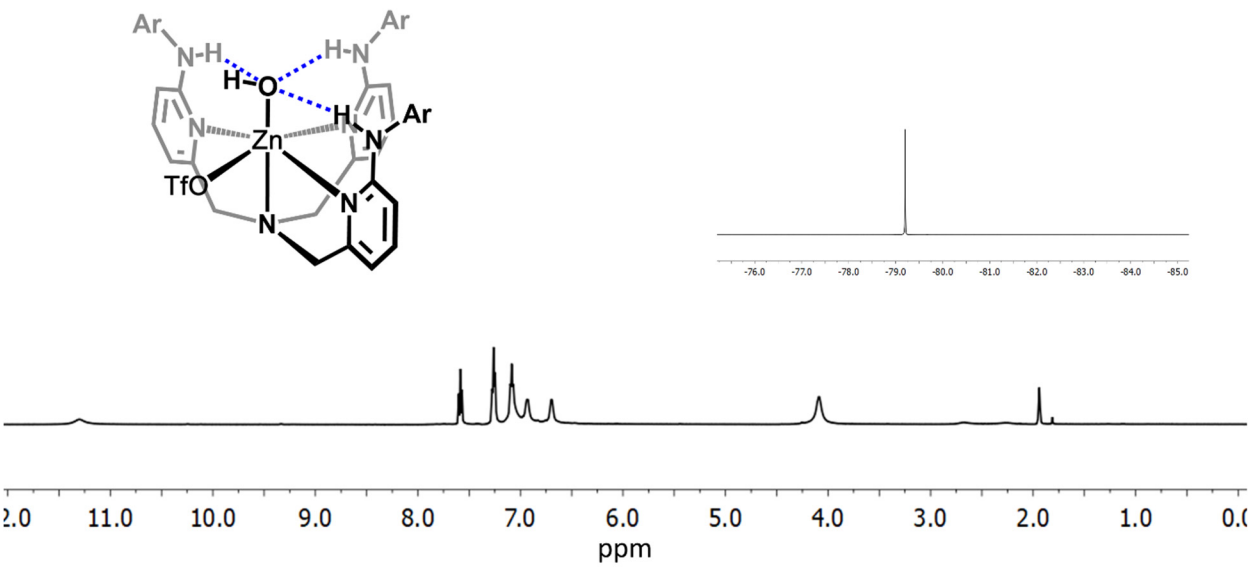

Figure S63 ^{1}H NMR spectrum (CD_3CN, 500 MHz, ambient temperature) of (L^H)Zn(OH)(OTf). Inset displays the ^{19}F spectrum.

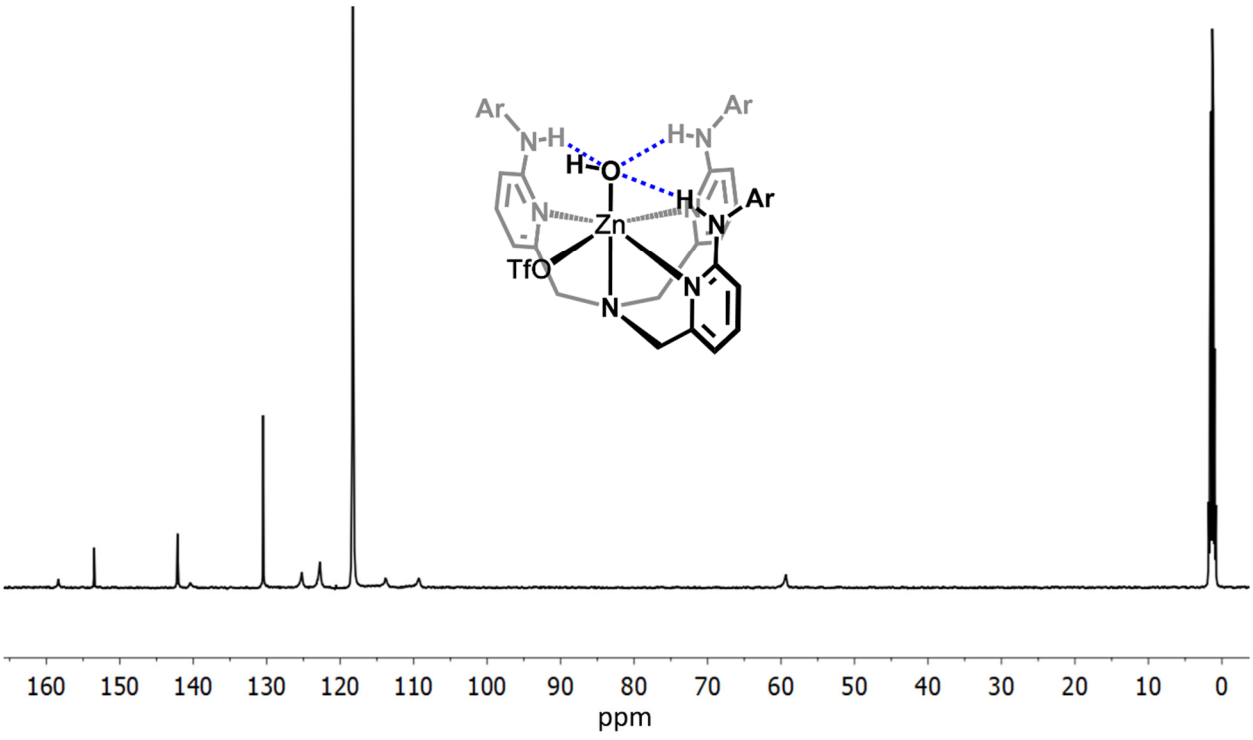

Figure S64 ^{13}C NMR spectrum (CD_3CN, ambient temperature) of (L^H)Zn(OH)(OTf).

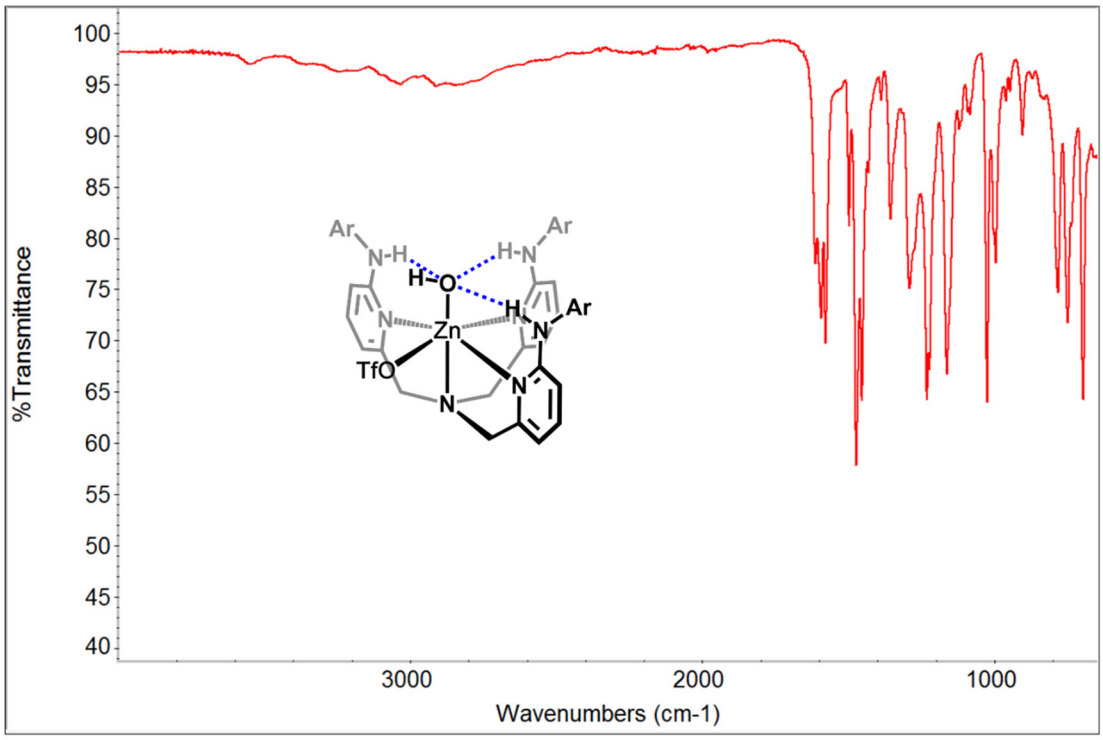

Figure S65 Infrared spectrum (neat, ATR, ambient temperature) of (L^H)Zn(OH)(OTf).

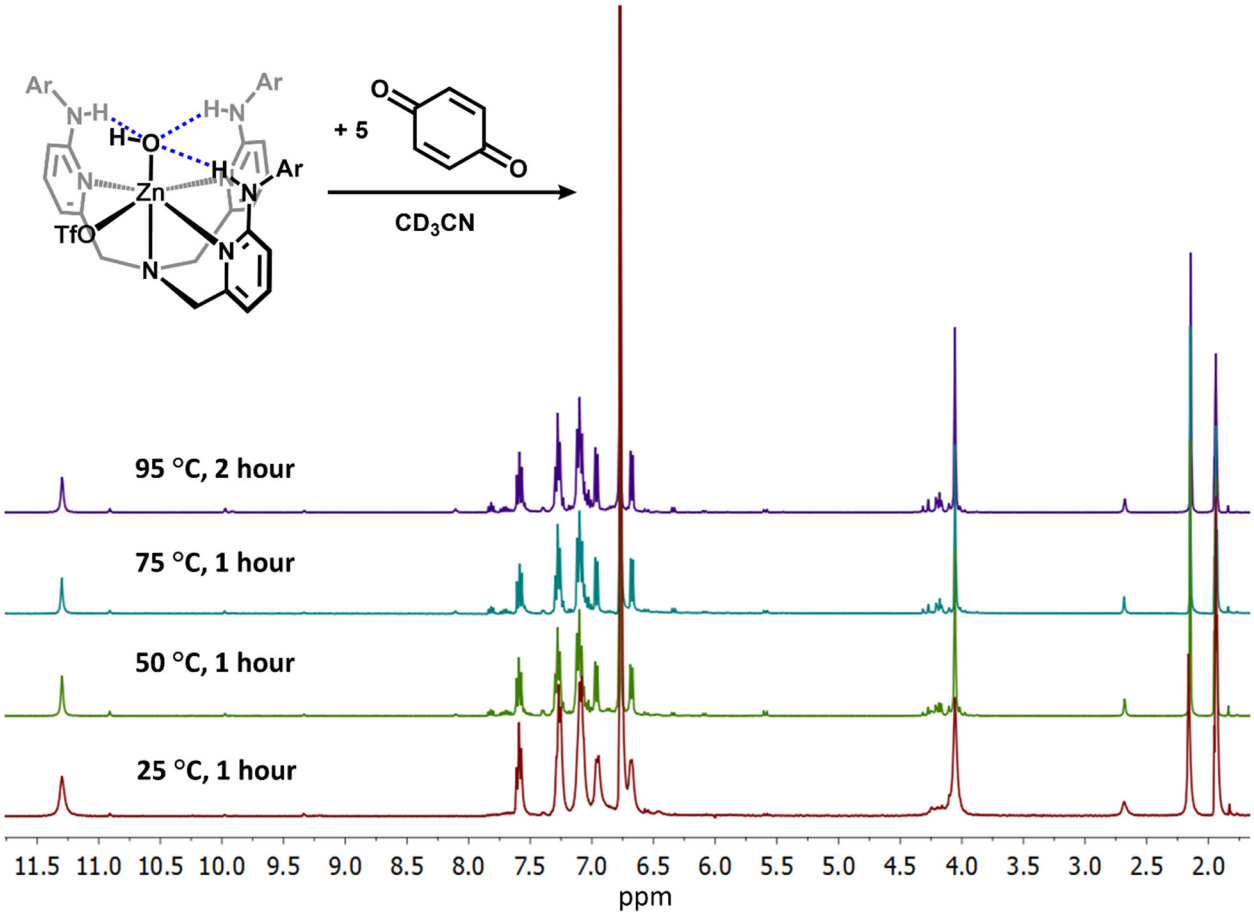

Figure S66 ^{1}H NMR spectra detailing attempt to oxidize (L^{H})Zn(OH)(OTf) with 1,4-benzoquinone to generate the peroxide species, $[L^{H}_{2}Zn_{2}O_{2}][OTf]_{2}$. Experimental setup: on a benchtop, open to air, (L^{H})Zn(OH)(OTf) and 1,4-benzoquinone (5 equivalents) were combined in $CD_{3}CN$ (dried over molecular sieves), transferred to an NMR tube, and monitored at various temperatures.

Compound: $[L^{H}{}_2Zn_2O_2][OTf]_2$

Local Name: jk3118

Table S2. Crystallographic parameters for $[L^{H}{}_2Zn_2O_2][OTf]_2$

Crystal data	
Chemical formula	$C_{72}H_{66}N_{14}O_2Zn_2{\cdot}2(CF_3O_3S){\cdot}2(C_2H_3N)$
M_r	1670.37
Crystal system, space group	Triclinic, $P\bar{1}$
Temperature (K)	150
a, *b*, *c* (Å)	11.8574 (6), 12.6382 (6), 14.5526 (6)
α, β, γ (°)	109.2223 (16), 102.1635 (17), 104.3283 (17)
V (Å^3)	1890.67 (15)
Z	1
Radiation type	Mo *K*α
μ (mm^{-1})	0.77
Crystal size (mm)	0.52 × 0.51 × 0.42
Data collection	
Diffractometer	Bruker AXS D8 Quest CMOS diffractometer
Absorption correction	Multi-scan *SADABS* 2016/2: Krause, L., Herbst-Irmer, R., Sheldrick G.M. & Stalke D., J. Appl. Cryst. 48 (2015) 3-10
T_{min}, T_{max}	0.677, 0.747
No. of measured, independent and observed [$I > 2s(I)$] reflections	139712, 14455, 12443
R_{int}	0.030
$(\sin\theta/\lambda)_{max}$ (Å^{-1})	0.771
Refinement	
$R[F^2 > 2\sigma(F^2)]$, $wR(F^2)$, *S*	0.032, 0.081, 1.04
No. of reflections	14455
No. of parameters	516
H-atom treatment	H atoms treated by a mixture of independent and constrained refinement
$\Delta\rho_{max}$, $\Delta\rho_{min}$ (e Å^{-3})	0.54, -0.53

Computer programs: Apex3 v2016.9-0 (Bruker, 2016), *SAINT* V8.37A (Bruker, 2016), *SHELXS97* (Sheldrick, 2008), *SHELXL2018*/1 (Sheldrick, 2015, 2018), SHELXLE Rev882 (Hübschle *et al.*, 2011).

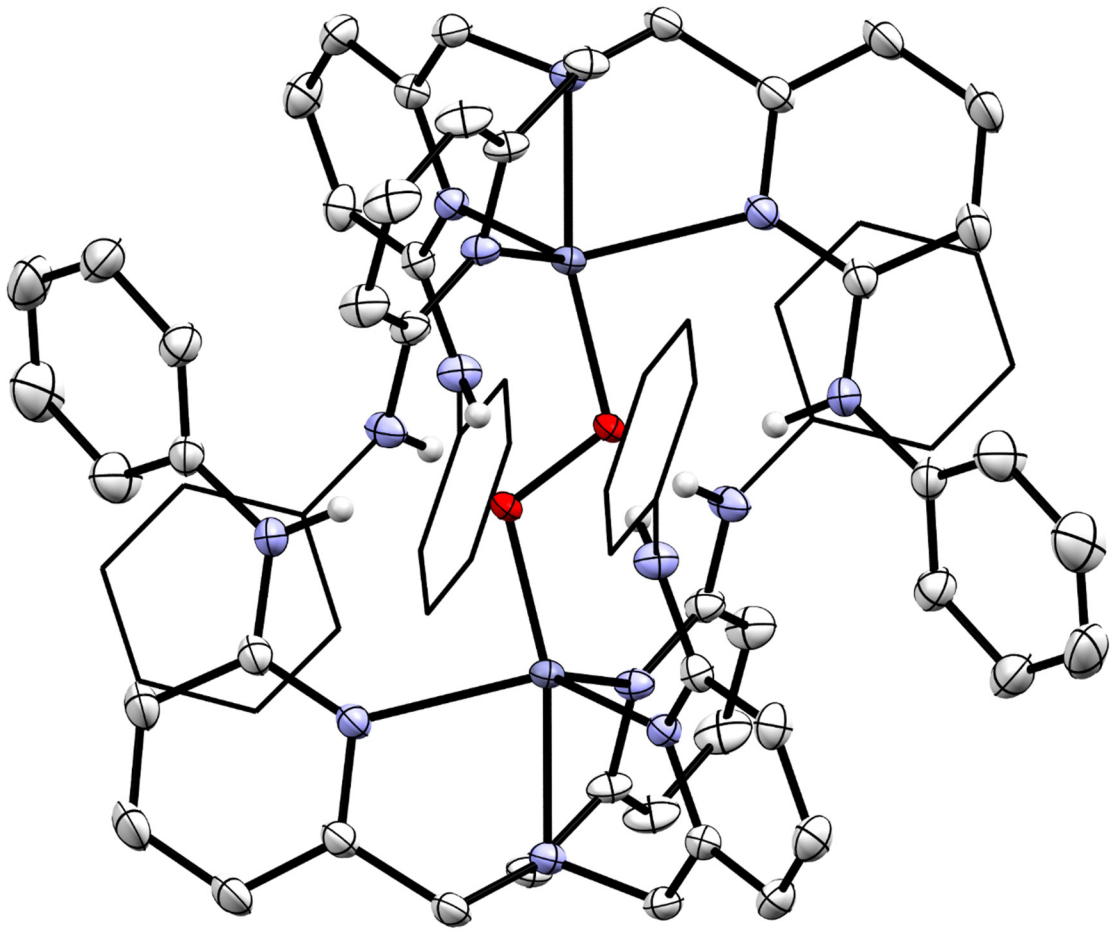

Figure S67 Molecular structure of the cationic portion of $[L^{H}{}_{2}Zn_{2}O_{2}][OTf]_{2}$ displayed with 50% probability ellipsoids. Select hydrogen atoms are omitted and select phenyl substituents are displayed in wireframe for clarity.

Compound: $[L^{OMe}{}_2Zn_2O_2][OTf]_2$

Local Name: ed430

Table S3. Crystallographic parameters for $[L^{OMe}{}_2Zn_2O_2][OTf]_2$

Crystal data	
Chemical formula	$C_{78}H_{78}N_{14}O_8Zn_2 \cdot 2(CF_3O_3S) \cdot 5(C_2H_3N)$
M_r	1973.69
Crystal system, space group	Triclinic, $P\overline{1}$
Temperature (K)	85
a, b, c (Å)	11.7511 (3), 12.9459 (3), 15.0500 (4)
α, β, γ (°)	90.065 (2), 96.490 (2), 97.362 (2)
V (Å^3)	2255.83 (10)
Z	1
Radiation type	Cu $K\alpha$
μ (mm^{-1})	1.83
Crystal size (mm)	0.18 × 0.18 × 0.12
Data collection	
Diffractometer	Dtrek-*CrysAlis PRO*-abstract goniometer imported rigaku-*D*TREK* images
Absorption correction	Multi-scan *CrysAlis PRO* 1.171.38.41 (Rigaku Oxford Diffraction, 2015) Empirical absorption correction using spherical harmonics, implemented in SCALE3 ABSPACK scaling algorithm.
T_{min}, T_{max}	0.788, 1.000
No. of measured, independent and observed [$I > 2s(I)$] reflections	33740, 8178, 7771
R_{int}	0.047
$(\sin \theta/\lambda)_{max}$ (Å^{-1})	0.608
Refinement	
$R[F^2 > 2\sigma(F^2)]$, $wR(F^2)$, S	0.050, 0.136, 1.06
No. of reflections	8178
No. of parameters	782
No. of restraints	442
H-atom treatment	H atoms treated by a mixture of independent and constrained refinement
$\Delta\rho_{max}$, $\Delta\rho_{min}$ (e Å^{-3})	0.69, -0.68

Computer programs: *CrysAlis PRO* 1.171.38.41 (Rigaku OD, 2015), *SHELXS97* (Sheldrick, 2008), *SHELXL2018*/1 (Sheldrick, 2015, 2018), SHELXLE Rev882 (Hübschle *et al.*, 2011).

Refinement details:

Two acetonitrile solvate molecules are each disordered over two positions. The U^{ij} components of the ADPs for each were restrained to be similar if closer than 2.0 Å. Subject to these conditions, the occupancy rates of the major and minor moieties for each acetonitrile refined to 0.906(3) and 0.094(3), and 0.521(3) and 0.479(3).

The OTf anion was modeled as disordered over two positions and the geometries were restrained to be similar (SAME). The U^{ij} components of ADPs for all atoms were restrained to be similar if closer than 2.0 Å. Subject to these conditions the occupancy rates of the major and minor moieties refined to 0.917(2) to 0.083(3).

A -OMe moiety was modeled as equally disordered over two positions due to close contact with a half-occupied acetonitrile and their geometries were restrained to be similar (SADI).

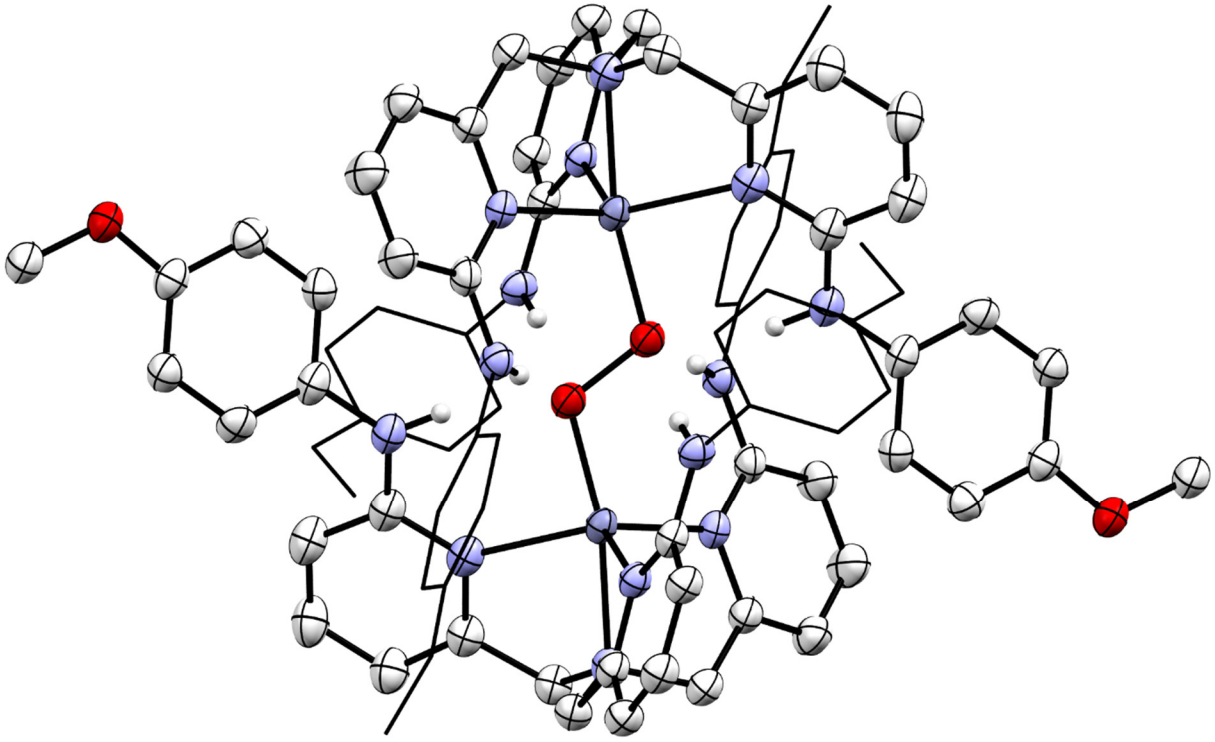

Figure S68 Molecular structure of the cationic portion of $[L^{OMe}{}_2Zn_2O_2][OTf]_2$ displayed with 50% probability ellipsoids. Select hydrogen atoms are omitted and select phenyl substituents are displayed in wireframe for clarity.

Compound: $[L^{CF3}{}_2Zn_2O_2][OTf]_2$

Local Name: ed429

Table S4. Crystallographic parameters for $[L^{CF3}{}_2Zn_2O_2][OTf]_2$

Crystal data	
Chemical formula	$C_{78}H_{60}F_{18}N_{14}O_2Zn_2 \cdot 2(CF_3O_3S) \cdot 0.648(C_4H_{10}O) \cdot 0.704(2 \times C_2H_3N)$
M_r	2073.21
Crystal system, space group	Monoclinic, $P2_1/n$
Temperature (K)	85
a, b, c (Å)	14.15647 (15), 14.20118 (16), 20.7331 (3)
β (°)	97.8476 (11)
V (Å^3)	4129.12 (9)
Z	2
Radiation type	Cu $K\alpha$
μ (mm^{-1})	2.29
Crystal size (mm)	0.14 × 0.06 × 0.03
Data collection	
Diffractometer	Dtrek-*CrysAlis PRO*-abstract goniometer imported rigaku-*D*TREK* images
Absorption correction	Multi-scan *CrysAlis PRO* 1.171.38.41 (Rigaku Oxford Diffraction, 2015) Empirical absorption correction using spherical harmonics, implemented in SCALE3 ABSPACK scaling algorithm.
T_{min}, T_{max}	0.738, 1.000
No. of measured, independent and observed [$I > 2s(I)$] reflections	62095, 7631, 7437
R_{int}	0.081
$(\sin \theta/\lambda)_{max}$ (Å^{-1})	0.608
Refinement	
$R[F^2 > 2\sigma(F^2)]$, $wR(F^2)$, S	0.046, 0.123, 1.03
No. of reflections	7631
No. of parameters	675
No. of restraints	92
H-atom treatment	H atoms treated by a mixture of independent and constrained refinement
$\Delta\rho_{max}$, $\Delta\rho_{min}$ (e Å^{-3})	0.58, -1.02

Computer programs: *CrysAlis PRO* 1.171.38.41 (Rigaku OD, 2015), *SHELXS97* (Sheldrick, 2008), *SHELXL2018*/1 (Sheldrick, 2015, 2018), SHELXLE Rev882 (Hübschle *et al.*, 2011).

Refinement details:

A solvent void displays partial occupancy by two half-diethyl ether molecules and two partial (not half) acetonitriles which were modeled as disordered. The bond distances and angles of both solvates were restrained to expected values. The U^{ij} components of ADPs of both solvates were restrained to be similar if closer than 2.0 Å. Subject to these conditions the occupancy rates of the major and minor moieties refined to 0.648(8) (ether) to 0.352(8) (2 x MeCN).

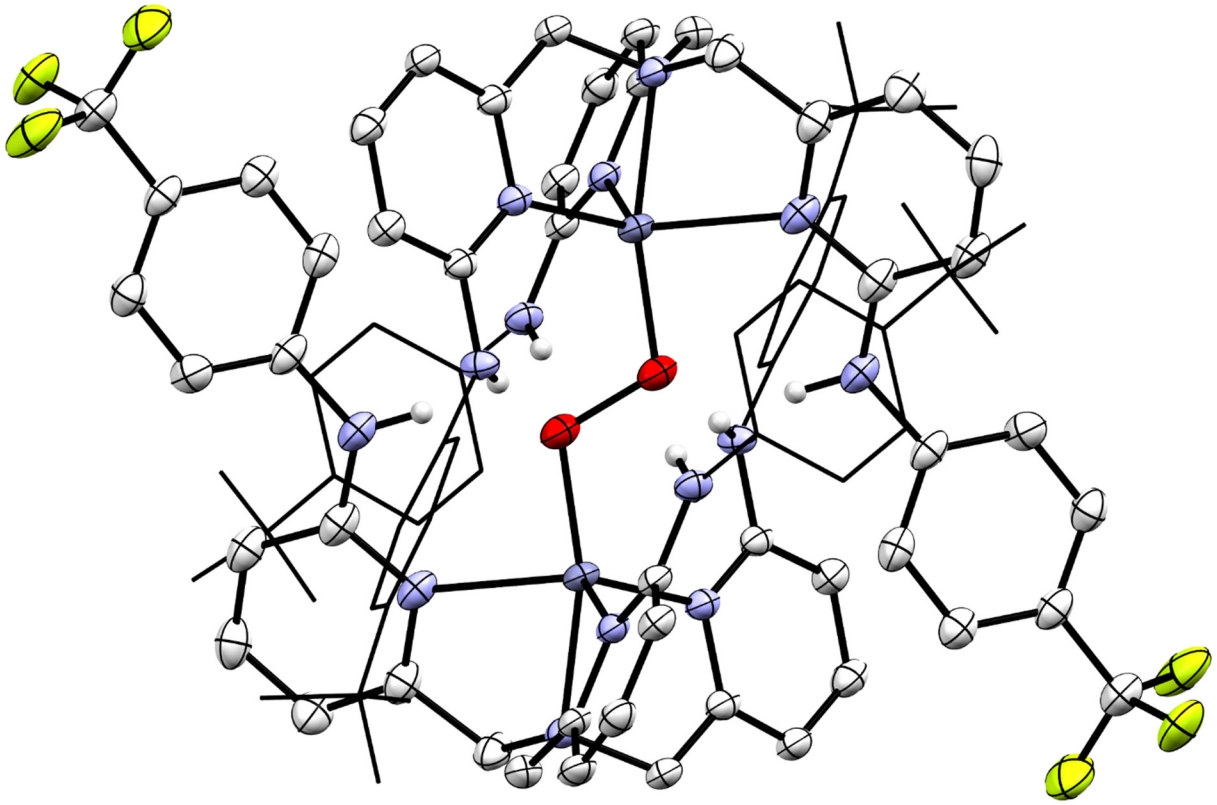

Figure S69 Molecular structure of the cationic portion of $[L^{CF3}{}_2Zn_2O_2][OTf]_2$ displayed with 50% probability ellipsoids. Select hydrogen atoms are omitted and select phenyl substituents are displayed in wireframe for clarity.

Compound: $[L^{NMe2}{}_2Zn_2O_2][OTf]_2$

Local Name: jk4100

Table S5. Crystallographic parameters for $[L^{NMe2}{}_2Zn_2O_2][OTf]_2$

Crystal data	
Chemical formula	$C_{84}H_{96}N_{20}O_2Zn_2{\cdot}2(CF_3O_3S){\cdot}1.504(C_5H_{12}){\cdot}6.5(C_2H_4Cl_2)$
M_r	2598.65
Crystal system, space group	Monoclinic, $P2_1/c$
Temperature (K)	90
a, b, c (Å)	17.2874 (15), 18.3243 (11), 19.0436 (17)
β (°)	100.0908 (19)
V (Å^3)	5939.3 (8)
Z	2
Radiation type	Mo $K\alpha$
μ (mm^{-1})	0.80
Crystal size (mm)	0.43 × 0.21 × 0.10
Data collection	
Diffractometer	Bruker AXS D8 Quest CMOS diffractometer
Absorption correction	Multi-scan *SADABS* 2016/2: Krause, L., Herbst-Irmer, R., Sheldrick G.M. & Stalke D., J. Appl. Cryst. 48 (2015) 3-10
T_{min}, T_{max}	0.255, 0.337
No. of measured, independent and observed [$I > 2s(I)$] reflections	100870, 18151, 11332
R_{int}	0.062
$(\sin q/l)_{max}$ (Å^{-1})	0.715
Refinement	
$R[F^2 > 2\sigma(F^2)]$, $wR(F^2)$, S	0.075, 0.248, 1.04
No. of reflections	18151
No. of parameters	1258
No. of restraints	2013
H-atom treatment	H atoms treated by a mixture of independent and constrained refinement
$\Delta\rho_{max}$, $\Delta\rho_{min}$ (e Å^{-3})	1.21, -0.71

Computer programs: Apex3 v2017.3-0 (Bruker, 2016), *SAINT* V8.38A (Bruker, 2016), *SHELXS97* (Sheldrick, 2008), *SHELXL2018*/3 (Sheldrick, 2015, 2018), SHELXLE Rev924 (Hübschle *et al.*, 2011).

Refinement details:

Substantial radiation damage and loss of intensity was observed during data collection, despite a low data collection temperature of 90 K. The data were corrected in Sadabs for radiation damage using a linear B-factor fit, resulting in the following statistics:

Run	B(start)	B(mid)	B(end)	Rad. Damage	factors
1	0.000	0.386	0.773	0.604 -	1.381
2	-0.811	-0.842	-0.874	0.432 -	1.414
3	-0.197	0.031	0.260	0.467 -	2.319

(please note that Run 1 was collected nine times faster but to a lower resolution than Runs 2 and 3 (0.795 for Run 1, 0.700 for Runs 2 and 3). Subsequent runs (4 and up) were affected to an increasing degree, substantially affecting data quality even after correction for radiation damage, and were not used.

The bridging peroxide ligand in the binding pocket is disordered over two alternative orientations. Both peroxide units are exactly inversion symmetric. The ADPs of the two oxygen atoms were constrained to be identical.

Amine H atom positions were refined and N-H distances were restrained to 0.88(2) Å, respectively.

Substantial disorder is observed for the solvate molecules and the triflate anions. The triflate anion was refined as disordered over two major and one minor orientation. The three disordered moieties were restrained to have similar geometries. U^{ij} components of ADPs for disordered atoms closer to each other than 2.0 Å were restrained to be similar. Subject to these conditions the occupancy rates refined to 0.501(2), 0.428(2) and 0.0711(18).

The triflate anions are surrounded by four sets of disordered solvate molecules. All solvate molecule positions were refined as disordered between 1,2-dichloroethane and pentane and were fitted to the experimental electron density using three or four differently oriented molecules of either 1,2-dichloroethane or pentane. All 1,2-dichloroethane molecules were restrained to have similar geometries, as were all pentane molecules. For the pivot pentane molecule (C52 to C56) C-C bond distances and angles were restrained to target values (C-C to 1.54(2) Å, 1,3 C...C distances to 2.50(2) Å). U^{ij} components of ADPs for disordered atoms of each solvent cluster closer to each other than 2.0 Å were restrained to be similar. A weak anti-bumping restraint (BUMP) was applied to keep disordered moiety H atoms from approaching other atoms too closely. Occupancies for individual moieties refined to values between 0.781(2) (for the 1,2-dichloroethane of Cl1 and Cl2), and 0.104(3) for the pentane of C67 to C71. See the atom list for exact values. Some apparent, but insufficiently resolved, additional disorder was omitted from the refinement model.

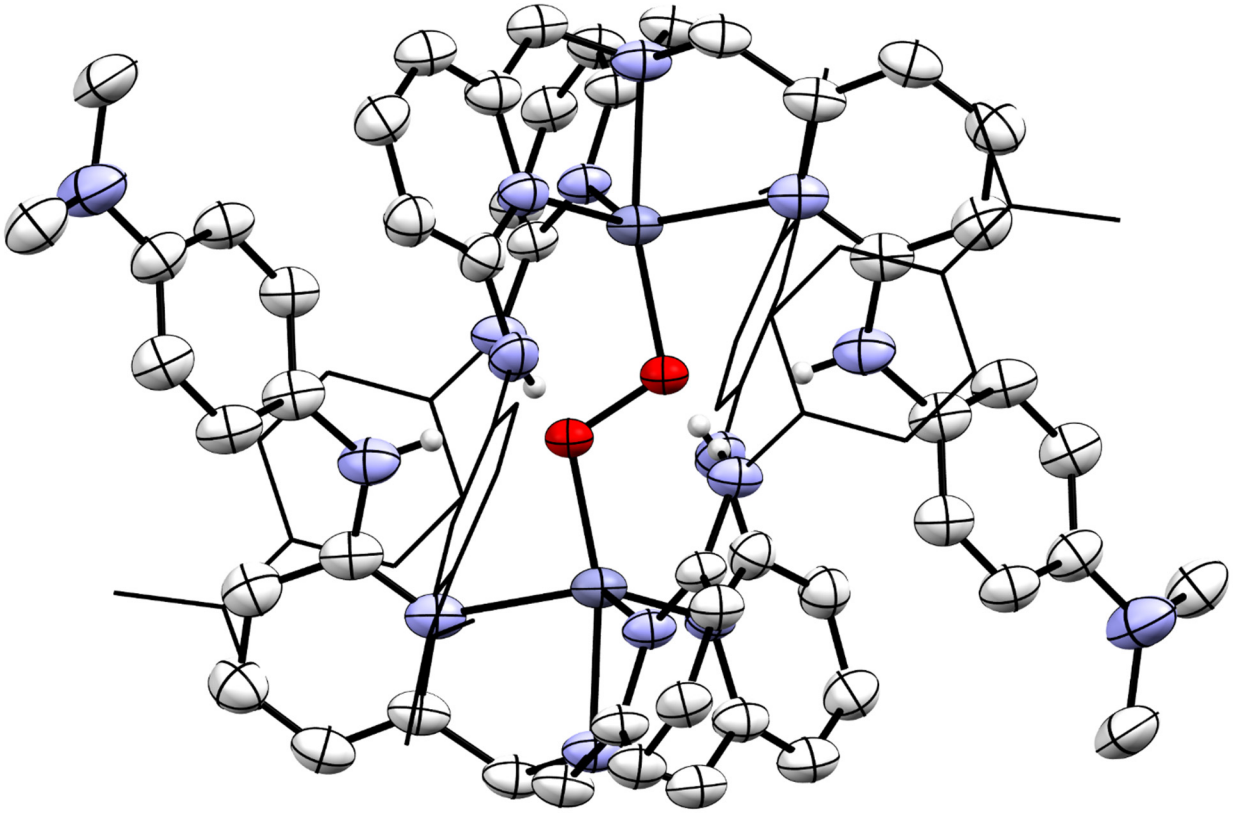

Figure S70 Molecular structure of the cationic portion of $[L^{NMe2}{}_2Zn_2O_2][OTf]_2$ displayed with 50% probability ellipsoids. Select hydrogen atoms are omitted and select phenyl substituents are displayed in wireframe for clarity. Disordered solvates and the minor O_2^{2-} moiety are also omitted for clarity.

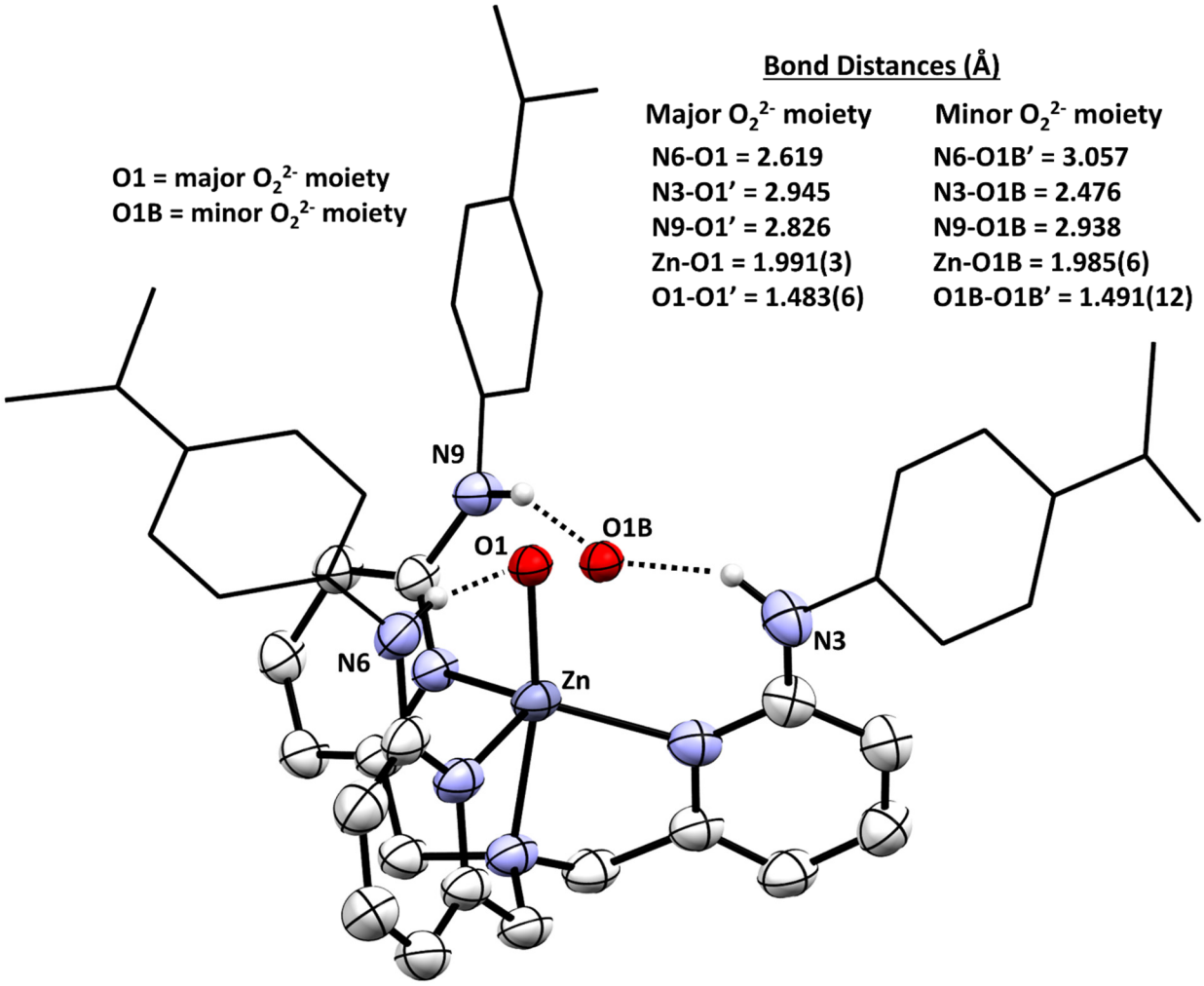

Figure S71 Depiction of the asymmetric unit of $[L^{NMe2}{}_2Zn_2O_2][OTf]_2$ to emphasize differences in hydrogen bonding between the major and minor O_2^{2-} moieties. Relevant bond distances for the disordered O_2^{2-} unit are listed.

Description of hydrogen bonding interactions for minor O_2^{2-} moiety

The O_2^{2-} is disordered over two positions (O1 and O1B). There are six hydrogen bonding interactions to the O1B-O1B' fragment (minor moiety). For each '(L^R)Zn' fragment, two –NHAr groups engage in hydrogen bonding with the proximal oxygen (N3-O1B = 2.476; N9-O1B = 2.938 Å) while one –NHAr group engages the distal oxygen (N6-O1B' = 3.057 Å). The Zn-O distances and O-O distances are equivalent between the two moieties.

Compound: $(L^H)Zn(N_3)_2$

Local Name: ed451h

Table S6. Crystallographic parameters for $(L^H)Zn(N_3)_2$

Crystal data	
Chemical formula	$C_{36}H_{33}N_{12.72}O_{0.42}Zn$
M_r	715.93
Crystal system, space group	Monoclinic, $P2_1/n$
Temperature (K)	85
a, b, c (Å)	10.1301 (1), 23.9224 (2), 13.8970 (1)
β (°)	98.932 (1)
V (Å^3)	3326.91 (5)
Z	4
Radiation type	Cu $K\alpha$
μ (mm^{-1})	1.43
Crystal size (mm)	0.12 × 0.12 × 0.08
Data collection	
Diffractometer	Dtrek-*CrysAlis PRO*-abstract goniometer imported rigaku-*D*TREK* images
Absorption correction	Multi-scan *CrysAlis PRO* 1.171.38.41 (Rigaku Oxford Diffraction, 2015) Empirical absorption correction using spherical harmonics, implemented in SCALE3 ABSPACK scaling algorithm.
T_{min}, T_{max}	0.754, 1.000
No. of measured, independent and observed [$I > 2s(I)$] reflections	50416, 6175, 6103
R_{int}	0.060
$(\sin \theta/\lambda)_{max}$ (Å^{-1})	0.607
Refinement	
$R[F^2 > 2\sigma(F^2)]$, $wR(F^2)$, S	0.055, 0.135, 1.10
No. of reflections	6175
No. of parameters	499
No. of restraints	85
H-atom treatment	H atoms treated by a mixture of independent and constrained refinement
$\Delta\rho_{max}$, $\Delta\rho_{min}$ (e Å^{-3})	1.19, -0.90

Computer programs: *CrysAlis PRO* 1.171.38.41 (Rigaku OD, 2015), *SHELXS97* (Sheldrick, 2008), *SHELXL2018*/1 (Sheldrick, 2015, 2018), SHELXLE Rev882 (Hübschle *et al.*, 2011).

Refinement details:

One of the azide groups is disordered with small amounts of a nitrate ion. The N-O distances were restrained to be similar and the NO_3 moiety to be planar. U^{ij} components of ADPs for disordered atoms closer to each other than 2.0 Å were restrained to be similar. Subject to these conditions the occupancy ratio refined to 0.860(5) to 0.140(5). We have been unable to identify the source of the nitrate contaminant that is observed in the molecular structure.

Alternate refinement of occupational disorder: The NO_3^- ion can alternately be modeled as a HCO_3^-. Subject to the modeling conditions described above, the occupancy ratio refined to 0.860(5) to 0.140(5) in favor of N_3^- (note the occupancy is the same as in the NO_3^- case). The R1 of the model does not change between the two scenarios (R1 = 5.49 for NO_3^-; 5.48 for HCO_3^-). A bicarbonate impurity can be rationalized by trace OH^- and atmospheric CO_2.

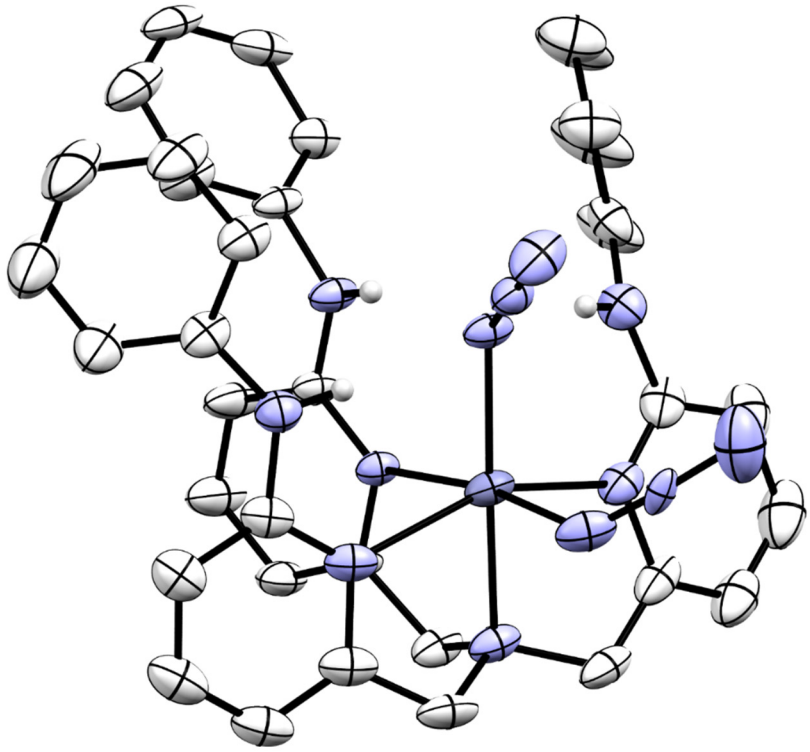

Figure S72 Molecular structure of $(L^H)Zn(N_3)_2$ displayed with 50% probability ellipsoids. Select hydrogen atoms are omitted as well as partially occupied nitrate anion (see refinement details).

Compound: $(L^{CF3})Zn(N_3)_2$

Local Name: jk3171

Table S7. Crystallographic parameters for $(L^{CF3})Zn(N_3)_2$

Crystal data	
Chemical formula	$2(C_{39}H_{30}F_9N_{12.81}O_{0.29}Zn)\cdot C_2H_3N$
M_r	1879.11
Crystal system, space group	Monoclinic, *C*2/*c*
Temperature (K)	150
a, *b*, *c* (Å)	25.6729 (16), 16.2244 (12), 19.9405 (18)
β (°)	98.007 (3)
V (Å^3)	8224.8 (11)
Z	4
Radiation type	Mo *K*α
μ (mm^{-1})	0.69
Crystal size (mm)	0.16 × 0.14 × 0.04
Data collection	
Diffractometer	Bruker AXS D8 Quest CMOS diffractometer
Absorption correction	Multi-scan *SADABS* 2016/2: Krause, L., Herbst-Irmer, R., Sheldrick G.M. & Stalke D., J. Appl. Cryst. 48 (2015) 3-10
T_{min}, T_{max}	0.479, 0.746
No. of measured, independent and observed [$I > 2s(I)$] reflections	49855, 10109, 5721
R_{int}	0.129
$(\sin\theta/\lambda)_{max}$ (Å^{-1})	0.670
Refinement	
$R[F^2 > 2\sigma(F^2)]$, $wR(F^2)$, *S*	0.065, 0.191, 1.02
No. of reflections	10109
No. of parameters	732
No. of restraints	721
H-atom treatment	H-atom parameters constrained
	$w = 1/[s^2(F_o^2) + (0.0669P)^2 + 13.1095P]$ where $P = (F_o^2 + 2F_c^2)/3$
$\Delta\rho_{max}$, $\Delta\rho_{min}$ (e Å^{-3})	0.70, -0.76

Computer programs: Apex3 v2016.9-0 (Bruker, 2016), *SAINT* V8.37A (Bruker, 2016), *SHELXS97* (Sheldrick, 2008), *SHELXL2018*/1 (Sheldrick, 2015, 2018), SHELXLE Rev882 (Hübschle *et al.*, 2011).

Refinement details:

One CF_3 group and one *p*-CF_3 phenyl group were refined as disordered. Their geometries were restrained to those of the third not disordered equivalent substituent. One of the disordered phenyl rings was constrained to resemble an ideal hexagon, with C-C distances of 1.39 Å. U^{ij} components of ADPs for disordered atoms closer to each other than 2.0 Å were restrained to be similar. Subject to these conditions the occupancy ratio refined to 0.757(7) to 0.243(7) for the *p*-CF_3 phenyl group, and to 0.633(7) to 0.367(7) for the CF_3 group.

An acetonitrile molecule is 1:1 disordered around a two-fold axis. Its atoms were subjected to a rigid bond restraint (RIGU).

One of the azide groups is disordered with small amounts of a nitrate ion. The N-O distances were restrained to be similar and the NO_3 moiety to be planar. U^{ij} components of ADPs for disordered atoms closer to each other than 2.0 Å were restrained to be similar. Subject to these conditions the occupancy ratio refined to 0.904(4) to 0.096(4). We have been unable to identify the source of the nitrate contaminant that is observed in the molecular structure.

Alternate refinement of occupational disorder: The NO_3^- ion can alternately be modeled as a HCO_3^-. Subject to the modeling conditions described above, the occupancy ratio refined to 0.905(4) to 0.095(4) in favor of N_3^- (note the occupancy is the same as in the NO_3^- case). The R1 of the model does not change between the two scenarios (R1 = 6.45 for NO_3^-; 6.46 for HCO_3^-). A bicarbonate impurity can be rationalized by trace OH^- and atmospheric CO_2.

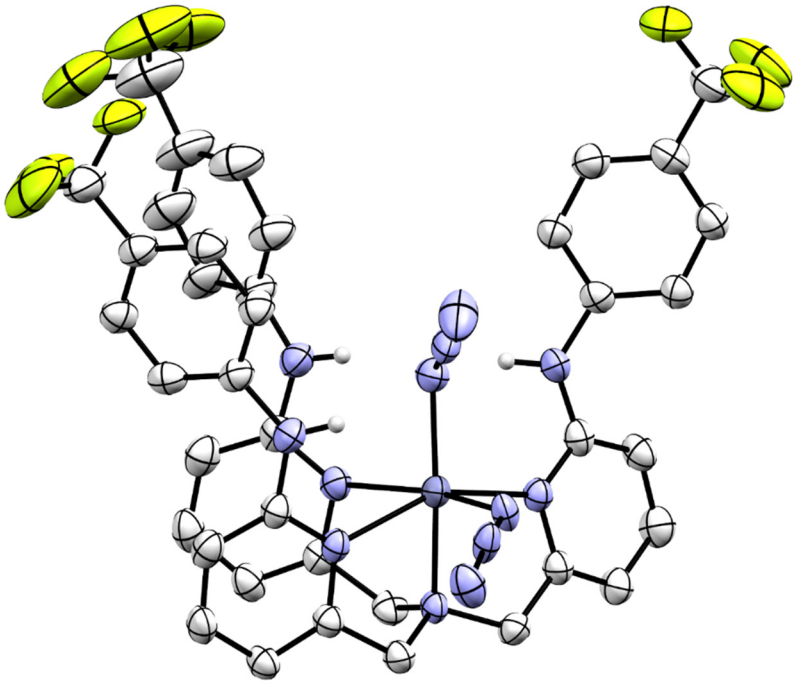

Figure S73 Molecular structure of $(L^{CF3})Zn(N_3)_2$ displayed with 50% probability ellipsoids. Select hydrogen atoms are omitted as well as a partially occupied nitrate anion (see refinement details).

Compound: $L^{OMe}Zn(N_3)_2$

Local Name: jk3119

Table S8. Crystallographic parameters for $L^{OMe}Zn(N_3)_2$

Crystal data	
Chemical formula	$C_{39}H_{39}N_{13}O_3Zn \cdot C_2H_3N$
M_r	844.25
Crystal system, space group	Monoclinic, $P2_1/n$
Temperature (K)	150
a, b, c (Å)	9.3139 (3), 16.7896 (6), 25.5526 (9)
β (°)	93.9525 (15)
V (Å^3)	3986.3 (2)
Z	4
Radiation type	Mo $K\alpha$
μ (mm^{-1})	0.68
Crystal size (mm)	0.55 × 0.22 × 0.18
Data collection	
Diffractometer	Bruker AXS D8 Quest CMOS diffractometer
Absorption correction	Multi-scan *SADABS* 2016/2: Krause, L., Herbst-Irmer, R., Sheldrick G.M. & Stalke D., J. Appl. Cryst. 48 (2015) 3-10
T_{min}, T_{max}	0.626, 0.747
No. of measured, independent and observed [$I > 2s(I)$] reflections	50414, 14890, 10260
R_{int}	0.049
$(\sin \theta/\lambda)_{max}$ (Å^{-1})	0.771
Refinement	
$R[F^2 > 2\sigma(F^2)]$, $wR(F^2)$, S	0.044, 0.118, 1.03
No. of reflections	14890
No. of parameters	619
No. of restraints	275
H-atom treatment	H atoms treated by a mixture of independent and constrained refinement
$\Delta\rho_{max}$, $\Delta\rho_{min}$ (e Å^{-3})	0.76, -0.88

Computer programs: Apex3 v2016.9-0 (Bruker, 2016), *SAINT* V8.37A (Bruker, 2016), *SHELXS97* (Sheldrick, 2008), *SHELXL2018*/1 (Sheldrick, 2015, 2018), SHELXLE Rev882 (Hübschle *et al.*, 2011).

Refinement details:

An anisyl substituent is disordered by rotation of the methoxy group. The two disordered moieties were restrained to have similar geometries. U^{ij} components of ADPs for disordered atoms closer to each other than 2.0 Å were restrained to be similar. Subject to these conditions the occupancy ratio refined to 0.550(4) to 0.450(4).

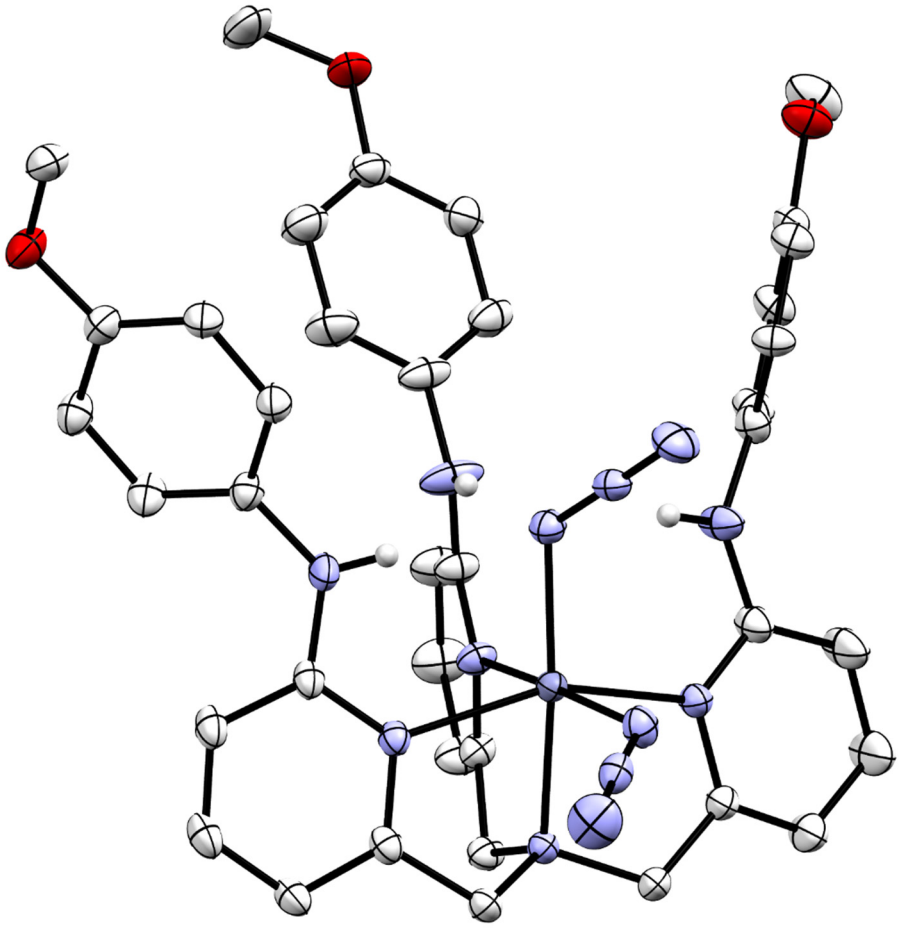

Figure S74 Molecular structure of $(L^{OMe})Zn(N_3)_2$ displayed with 50% probability ellipsoids. Select hydrogen atoms are omitted.

Compound: $L^{NMe2}Zn(N_3)_2$

Local Name: jk3120

Table S9. Crystallographic parameters for $L^{NMe2}Zn(N_3)_2$

Crystal data	
Chemical formula	$C_{42}H_{48}N_{16}O_{0.81}Zn \cdot 0.812(C_4H_{10}O) \cdot 0.376(C_2H_3N)$
M_r	917.97
Crystal system, space group	Monoclinic, $P2_1/n$
Temperature (K)	150
a, b, c (Å)	17.5214 (13), 10.7394 (8), 24.7785 (15)
β (°)	90.811 (3)
V (Å^3)	4662.1 (6)
Z	4
Radiation type	Mo $K\alpha$
μ (mm^{-1})	0.58
Crystal size (mm)	0.27 × 0.15 × 0.07
Data collection	
Diffractometer	Bruker AXS D8 Quest CMOS diffractometer
Absorption correction	Multi-scan *SADABS* 2016/2: Krause, L., Herbst-Irmer, R., Sheldrick G.M. & Stalke D., J. Appl. Cryst. 48 (2015) 3-10
T_{min}, T_{max}	0.656, 0.746
No. of measured, independent and observed [$I > 2s(I)$] reflections	49997, 12078, 9205
R_{int}	0.065
$(\sin \theta/\lambda)_{max}$ (Å^{-1})	0.715
Refinement	
$R[F^2 > 2\sigma(F^2)]$, $wR(F^2)$, S	0.040, 0.106, 1.04
No. of reflections	12078
No. of parameters	698
No. of restraints	296
H-atom treatment	H atoms treated by a mixture of independent and constrained refinement
$\Delta\rho_{max}$, $\Delta\rho_{min}$ (e Å^{-3})	0.67, -0.45

Computer programs: Apex3 v2016.9-0 (Bruker, 2016), *SAINT* V8.37A (Bruker, 2016), *SHELXS97* (Sheldrick, 2008), *SHELXL2018*/1 (Sheldrick, 2015, 2018), SHELXLE Rev882 (Hübschle *et al.*, 2011).

Refinement details:

A solvate pocket is occupied by either one molecule of diethyl ether, or two molecules of acetonitrile. The diethyl ether is disordered over two slightly shifted positions. The two disordered moieties were restrained to have similar geometries. The acetonitrile bond distances and angles were restrained to expected values. U^{ij} components of ADPs for all disordered atoms closer to each other than 2.0 Å were restrained to be similar. Subject to these conditions the occupancy rates refined to 0.571(3) and 0.241(3) for the two ether moieties, and to two times 0.188(2) for the acetonitrile molecules.

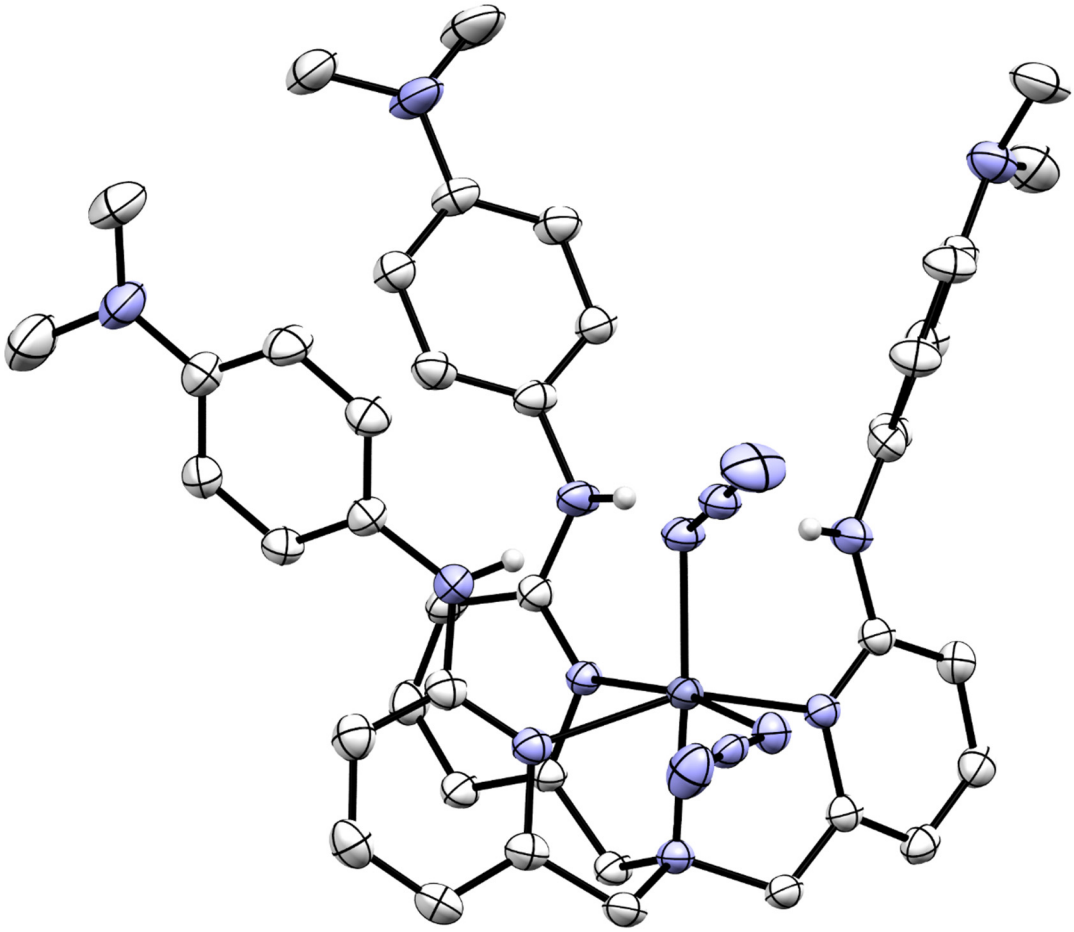

Figure S75 Molecular structure of $(L^{NMe2})Zn(N_3)_2$ displayed with 50% probability ellipsoids. Select hydrogen atoms are omitted.

Compound: (TPA)Zn$(N_3)_2$

Local Name: jk3156

Table S10. Crystallographic parameters for (TPA)Zn$(N_3)_2$

Crystal data	
Chemical formula	$C_{18}H_{18}N_{10}Zn$
M_r	439.79
Crystal system, space group	Monoclinic, $P2_1/n$
Temperature (K)	150
a, b, c (Å)	8.8065 (4), 14.9343 (6), 14.7137 (6)
β (°)	90.2374 (15)
V (Å^3)	1935.11 (14)
Z	4
Radiation type	Cu Ka
μ (mm^{-1})	2.00
Crystal size (mm)	0.21 × 0.19 × 0.07
Data collection	
Diffractometer	Bruker AXS D8 Quest CMOS diffractometer
Absorption correction	Multi-scan *SADABS* 2016/2: Krause, L., Herbst-Irmer, R., Sheldrick G.M. & Stalke D., J. Appl. Cryst. 48 (2015) 3-10
T_{min}, T_{max}	0.354, 0.526
No. of measured, independent and observed [I > 2s(I)] reflections	16920, 3994, 3659
R_{int}	0.077
(sin θ/λ)$_{max}$ (Å^{-1})	0.639
Refinement	
$R[F^2 > 2\sigma(F^2)]$, $wR(F^2)$, S	0.052, 0.138, 1.05
No. of reflections	3994
No. of parameters	262
H-atom treatment	H-atom parameters constrained
$\Delta\rho_{max}$, $\Delta\rho_{min}$ (e Å^{-3})	0.79, -1.02

Computer programs: Apex3 v2016.9-0 (Bruker, 2016), *SAINT* V8.37A (Bruker, 2016), *SHELXS97* (Sheldrick, 2008), *SHELXL2018*/1 (Sheldrick, 2015, 2018), SHELXLE Rev882 (Hübschle *et al.*, 2011).

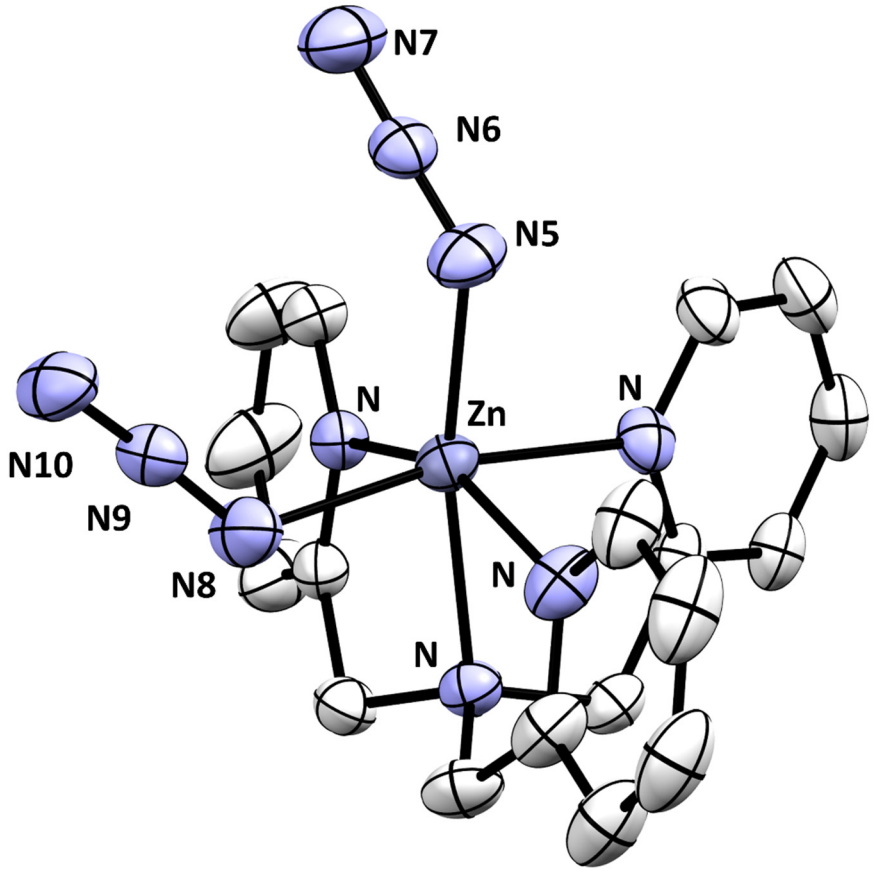

Figure S76 Molecular structure of (TPA)Zn(N_3)$_2$ displayed with 50% probability ellipsoids. Hydrogen atoms are omitted for clarity.

Compound: [(TPA)Zn(N_3)][ClO_4]

Local Name: jk3117

Table S11. Crystallographic parameters for [(TPA)Zn(N_3)][ClO_4]

Crystal data	
Chemical formula	$C_{18}H_{18}N_7Zn{\cdot}ClO_4$
M_r	497.21
Crystal system, space group	Monoclinic, $P2_1/c$
Temperature (K)	150
a, b, c (Å)	15.2872 (7), 9.1683 (5), 14.9606 (7)
β (°)	94.6552 (17)
V (Å^3)	2089.93 (18)
Z	4
Radiation type	Mo $K\alpha$
μ (mm^{-1})	1.34
Crystal size (mm)	0.55 × 0.29 × 0.08
Data collection	
Diffractometer	Bruker AXS D8 Quest CMOS diffractometer
Absorption correction	Multi-scan *SADABS* 2016/2: Krause, L., Herbst-Irmer, R., Sheldrick G.M. & Stalke D., J. Appl. Cryst. 48 (2015) 3-10
T_{min}, T_{max}	0.537, 0.747
No. of measured, independent and observed [$I > 2s(I)$] reflections	40126, 9018, 7048
R_{int}	0.044
$(\sin\theta/\lambda)_{max}$ (Å^{-1})	0.808
Refinement	
$R[F^2 > 2\sigma(F^2)]$, $wR(F^2)$, S	0.044, 0.118, 1.07
No. of reflections	9018
No. of parameters	281
H-atom treatment	H-atom parameters constrained
$\Delta\rho_{max}$, $\Delta\rho_{min}$ (e Å^{-3})	1.64, -0.96

Computer programs: Apex3 v2016.9-0 (Bruker, 2016), *SAINT* V8.37A (Bruker, 2016), *SHELXS97* (Sheldrick, 2008), *SHELXL2018*/1 (Sheldrick, 2015, 2018), SHELXLE Rev882 (Hübschle *et al.*, 2011).

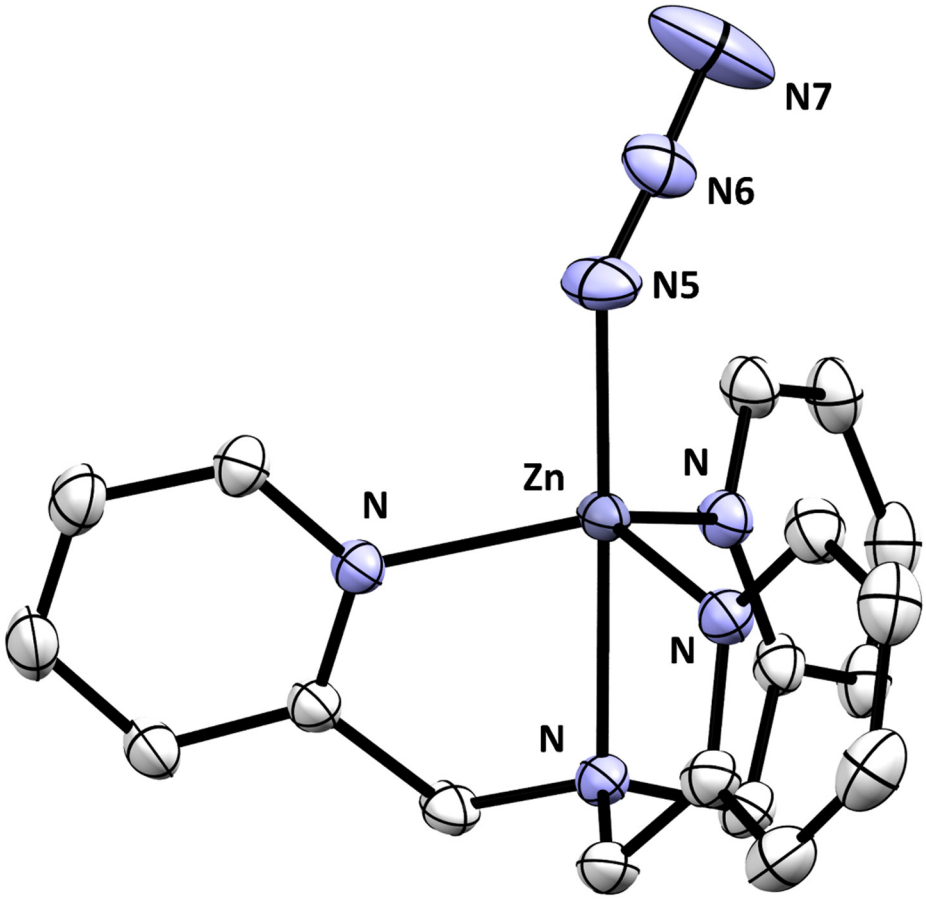

Figure S77 Molecular structure of $[(TPA)Zn(N_3)][ClO_4]$ displayed with 50% probability ellipsoids. The perchlorate anion is omitted for clarity. Selected bond distances (Å) and angles (°): $Zn\text{-}N_{pyridine}$ = 2.0722(14), 2.0858(15), and 2.0642(14); $Zn\text{-}N_{anchor}$ = 2.2208(13); Zn-N5 = 2.0051(15); N5-N6 = 1.167(2); N6-N7 = 1.146(3); Zn-N5-N6 = 131.75(14).

Compound: $L^{H}Zn(OH)(OTf)$

Local Name: ed415

Table S12. Crystallographic parameters for $L^{H}Zn(OH)(OTf)$

Crystal data	
Chemical formula	$2(C_{37}H_{34}F_3N_7O_4SZn)\cdot C_2H_3N$
M_r	1631.33
Crystal system, space group	Orthorhombic, $Pna2_1$
Temperature (K)	85
a, b, c (Å)	35.9729 (6), 8.6719 (2), 23.2969 (3)
V (Å^3)	7267.5 (2)
Z	4
Radiation type	Cu $K\alpha$
μ (mm^{-1})	2.06
Crystal size (mm)	0.23 × 0.01 × 0.01
Data collection	
Diffractometer	Dtrek-*CrysAlis PRO*-abstract goniometer imported rigaku-*D*TREK* images
Absorption correction	Multi-scan *CrysAlis PRO* 1.171.38.41 (Rigaku Oxford Diffraction, 2015) Empirical absorption correction using spherical harmonics, implemented in SCALE3 ABSPACK scaling algorithm.
T_{min}, T_{max}	0.656, 1.000
No. of measured, independent and observed [$I > 2s(I)$] reflections	106634, 13472, 12173
R_{int}	0.097
$(\sin\theta/\lambda)_{max}$ (Å^{-1})	0.608
Refinement	
$R[F^2 > 2\sigma(F^2)]$, $wR(F^2)$, S	0.072, 0.196, 1.06
No. of reflections	13472
No. of parameters	986
No. of restraints	2
H-atom treatment	H-atom parameters constrained
$\Delta\rho_{max}$, $\Delta\rho_{min}$ (e Å^{-3})	2.12, -1.02
Absolute structure	Refined as an inversion twin.
Absolute structure parameter	0.33 (3)

Computer programs: *CrysAlis PRO* 1.171.38.41 (Rigaku OD, 2015), *SHELXS97* (Sheldrick, 2008), *SHELXL2018*/1 (Sheldrick, 2015, 2018), SHELXLE Rev882 (Hübschle *et al.*, 2011).

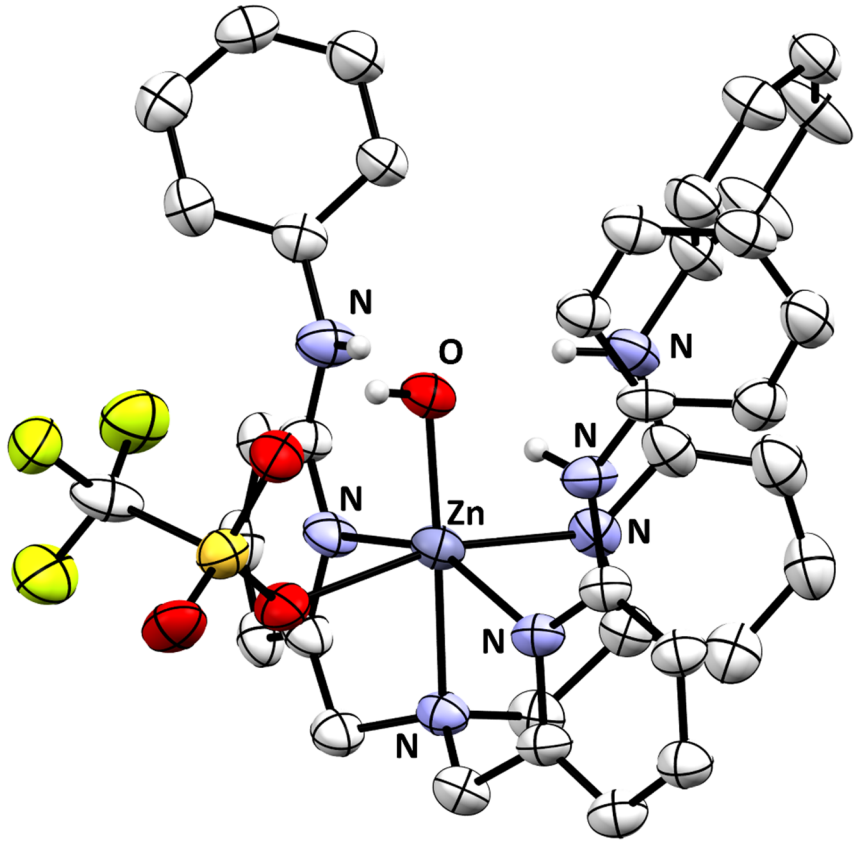

Figure S78 Molecular structure of $L^{H}Zn(OH)(OTf)$ displayed with 50% probability ellipsoids. Selected bond distances (Å): Zn-$N_{pyridine}$ = 2.169(7), 2.202(7), and 2.205(7); Zn-N_{anchor} = 2.176(6); Zn-OH = 1.976(6); Zn-OTf = 2.404(6).

Compound:[(L^H)ZnCl][ClO_4]

Local Name: jk3146

Table S13. Crystallographic parameters for [(L^H)ZnCl][ClO_4]

Crystal data	
Chemical formula	$C_{36}H_{33}ClN_7Zn{\cdot}ClO_4{\cdot}2.5(C_2H_4Cl_2)$
M_r	1011.34
Crystal system, space group	Triclinic, $P\bar{1}$
Temperature (K)	150
a, *b*, *c* (Å)	13.083 (2), 16.323 (3), 22.431 (4)
α, β, γ (°)	69.675 (4), 85.118 (7), 82.517 (4)
V (Å^3)	4449.8 (14)
Z	4
Radiation type	Mo *K*α
μ (mm^{-1})	1.02
Crystal size (mm)	0.55 × 0.17 × 0.03
Data collection	
Diffractometer	Bruker AXS D8 Quest CMOS diffractometer
Absorption correction	Multi-scan *SADABS* 2016/2: Krause, L., Herbst-Irmer, R., Sheldrick G.M. & Stalke D., J. Appl. Cryst. 48 (2015) 3-10
T_{min}, T_{max}	0.103, 0.970
No. of measured, independent and observed [$I > 2s(I)$] reflections	47836, 14561, 9924
R_{int}	0.098
$(\sin\theta/\lambda)_{max}$ (Å^{-1})	0.581
Refinement	
$R[F^2 > 2\sigma(F^2)]$, $wR(F^2)$, *S*	0.106, 0.330, 1.05
No. of reflections	14561
No. of parameters	1390
No. of restraints	1283
H-atom treatment	H-atom parameters constrained
$\Delta\rho_{max}$, $\Delta\rho_{min}$ (e Å^{-3})	2.72, -0.74

Computer programs: Apex3 v2016.9-0 (Bruker, 2016), *SAINT* V8.37A (Bruker, 2016), *SHELXS97* (Sheldrick, 2008), *SHELXL2018*/1 (Sheldrick, 2015, 2017), SHELXLE Rev882 (Hübschle *et al.*, 2011).

Refinement details:

A perchlorate anion is disordered in place. The two disordered moieties were restrained to have similar geometries as another not disordered perchlorate. U^{ij} components of ADPs for disordered atoms closer to each other than 2.0 Å were restrained to be similar. Subject to these conditions the occupancy ratio refined to 0.592(10) to 0.408(10).

Several 1,2-dichloroethane molecules are disordered. One was refined as not disordered. Three as two-fold disordered (one of them around or slightly offset an inversion center), and one as three fold disordered slightly offset an inversion center, and one four-fold disordered with one of the three moieties incompatible with its symmetry created counterpart created by an inversion center. All 1,2-dichloroethane molecules were restrained to have similar geometries, and some C-Cl and C-C distances were in addition restrained to be similar to each other (disorder around inversion centers). U^{ij} components of ADPs for disordered atoms closer to each other than 2.0 Å were restrained to be similar. Subject to these conditions the occupancy rates refined to 0.808(7) and 0.192(7) (Cl5, Cl6 vs. Cl5B, Cl6B), 0.1367(13) (Cl7), 0.1011(8) (Cl8), 0.525(9) (Cl9, Cl10), 0.376(7) (Cl11, Cl12), 0.211(9) (Cl13, Cl14), 0.304(3) (Cl15, Cl16), 0.311(3) (Cl17, Cl18), 0.286(3) (Cl19, Cl20), 0.099(3) (Cl21, Cl22), 0.577(18) (Cl23), 0.124(7) (Cl24, Cl25), and 0.475(9) (Cl26, Cl27).

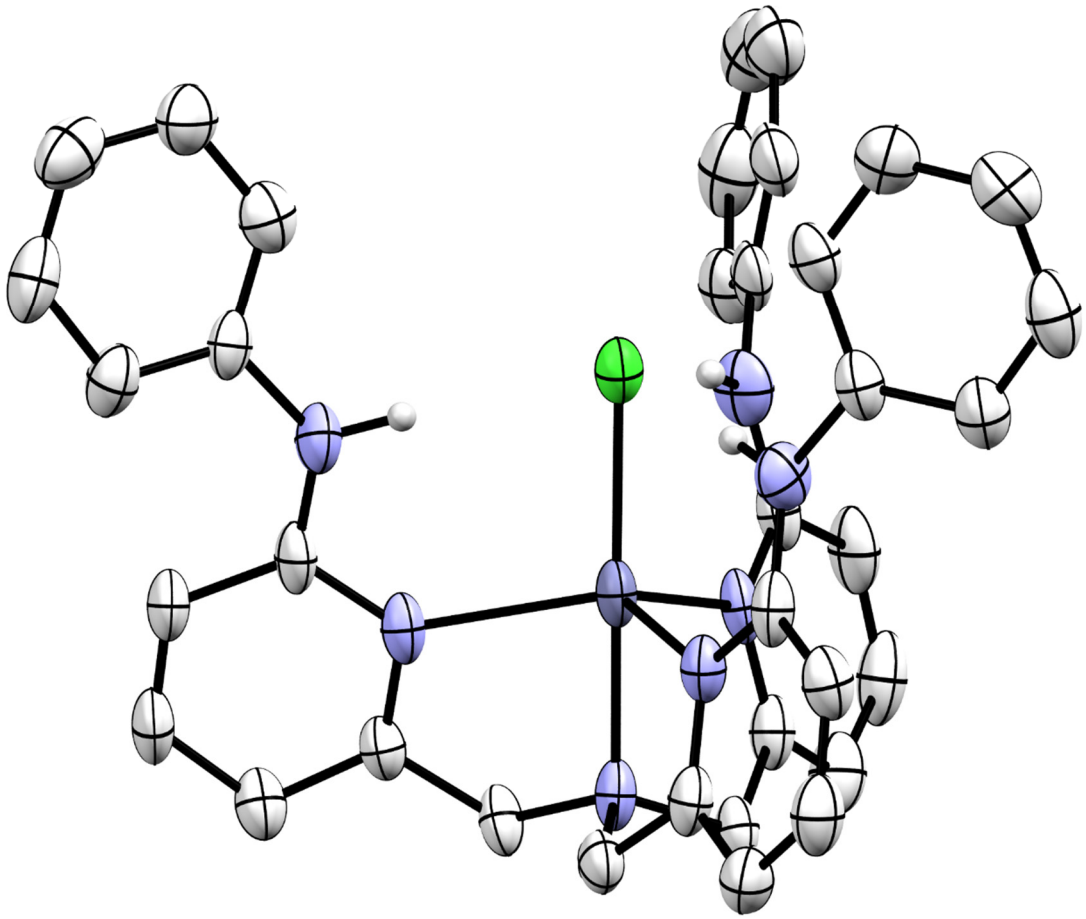

Figure S79 Molecular structure of $[L^{H}ZnCl][ClO_4]$ displayed with 50% probability ellipsoids. Select hydrogen atoms, perchlorate anions, cocrystallized 1,2-dichloroethane solvates, and second asymmetric cation in the unit cell have been omitted.

Table S14. Experimentally determined bond distances and angles of zinc peroxide complexes

Bond (Å) or Angle (°)	$[L^{CF3}{}_2Zn_2O_2]^{2+}$ (X1 = O)	$[L^{H}{}_2Zn_2O_2]^{2+}$ (X1 = O)	$[L^{OMe}{}_2Zn_2O_2]^{2+}$ (X1 = O)	$[L^{NMe2}{}_2Zn_2O_2]^{2+}$ (X1 = O)
Zn1-O1	1.9507(16)	1.9656(7)	1.9724(16)	1.991(3)
Zn1-$N_{pyridine}$	2.1406(18)	2.1122(9)	2.1289(19)	2.148(2)
Zn1-$N_{pyridine}$	2.1514(19)	2.1669(9)	2.1497(19)	2.156(3)
Zn1-$N_{pyridine}$	2.305(2)	2.2597(9)	2.227(2)	2.185(3)
Zn1-N_{anchor}	2.0997(19)	2.1216(9)	2.129(2)	2.131(3)
O1-O1'	1.524(3)	1.4954(13)	1.518(3)	1.483(6)
Zn1-Zn1'	4.719	4.745	4.784	4.742
Zn1-O1-O1'	113.41(14)	114.21(7)	114.76(14)	112.1(3)
τ_5	0.75	0.83	0.83	0.77

Table S15. Experimentally determined bond distances and angles of zinc azide complexes

Bond (Å) or Angle (°)	$L^{CF3}Zn(N_3)_2$	$L^{H}Zn(N_3)_2$	$L^{OMe}Zn(N_3)_2$	$L^{NMe2}Zn(N_3)_2$	$(TPA)Zn(N_3)_2$
Zn-$N_{3(axial)}$	2.055(3)	2.1037(15)	2.0790(13)	2.0741(15)	2.035(2)
Zn- $N_{3(equitorial}$)	2.063(3)	2.1010(15)	2.1056(14)	2.1357(15)	2.114(2)
Zn-$N_{pyridine}$	2.309(3)	2.2581(13)	2.2083(12)	2.1956(14)	2.2115(19)
Zn-$N_{pyridine}$	2.365(3)	2.2447(12)	2.2474(12)	2.2538(15)	2.202(2)
Zn-$N_{pyridine}$	2.292(3)	2.2457(14)	2.3052(13)	2.2629(14)	2.153(2)
Zn-N_{anchor}	2.146(3)	2.1573(13)	2.1547(13)	2.1602(14)	2.2358(18)
Zn-N-$N_{(axial)}$	122.7(3)	126.72(13)	123.81(11)	121.36(12)	128.54(18)
Zn-N-$N_{(equitorial)}$	127.1(3)	117.86(11)	130.69(11)	121.35(12)	126.44(19)

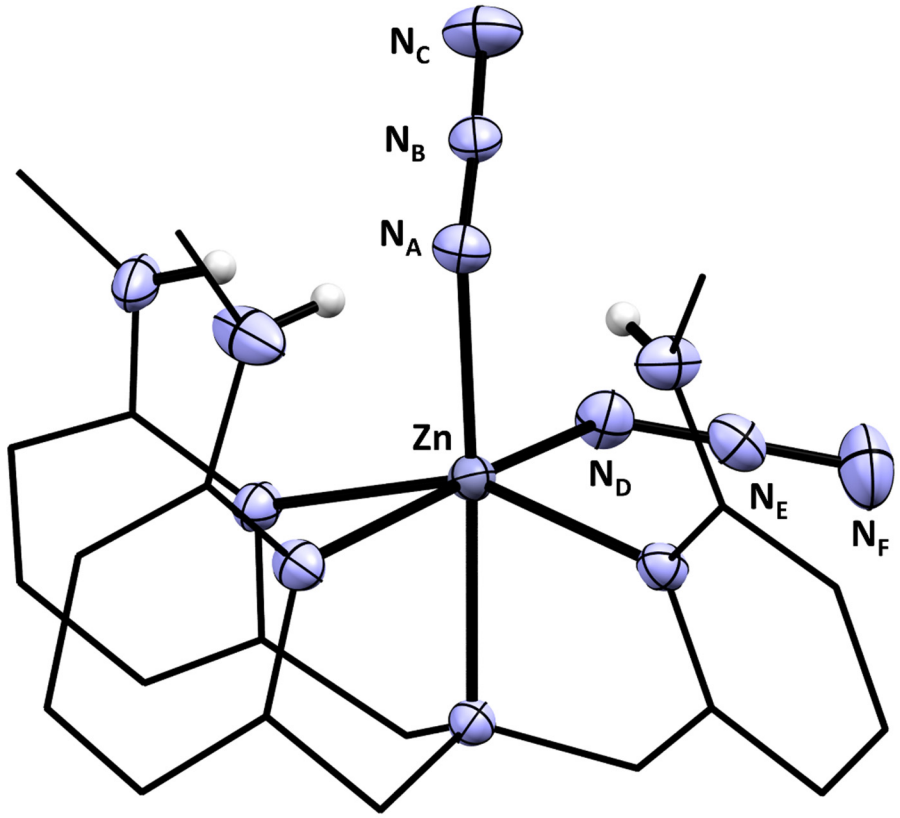

Table S16. Experimentally determined bond distances and angles of zinc azide complexes

Bond (Å)	$L^{CF3}Zn(N_3)_2$	$L^{H}Zn(N_3)_2$	$L^{OMe}Zn(N_3)_2$	$L^{NMe2}Zn(N_3)_2$	$(TPA)Zn(N_3)_2$
$Zn\text{-}N_A$	2.055(3)	2.1037(15)	2.0790(13)	2.0741(15)	2.035(2)
$Zn\text{-}N_D$	2.063(3)	2.1010(15)	2.1056(14)	2.1357(15)	2.114(2)
$N_A\text{-}N_B$	1.207(5)	1.190(2)	1.1978(19)	1.198(2)	1.185(3)
$N_B\text{-}N_C$	1.147(5)	1.165(2)	1.150(2)	1.149(2)	1.156(3)
$N_D\text{-}N_E$	1.230(6)	1.096(2)	1.180(2)	1.163(2)	1.185(3)
$N_E\text{-}N_F$	1.138(6)	1.212(2)	1.170(2)	1.176(2)	1.151(3)

Computational Details.

All calculations were performed using Gaussian 09[11] and visualized in GaussView. Head-Gordon's long range-corrected functional (ωB97XD)[12] was used with the Pople basis set 6-31G(d,p)[13] to calculate C, H, and N atoms and the Ahlrich basis set def2-TZVP[14] to calculate Zn atoms. Spin-restricted structures were freely optimized in C_1 symmetry from coordinates generated from the X-ray structure using a polarizable continuum model (PCM) of CH_2Cl_2. Calculated vibrational spectra were used to verify that the optimized structures were minima on the potential energy surface by the absence of imaginary frequencies and to assign the experimental azide IR bands.

Table S17. DFT-calculated IR bands of (TPA)Zn$(N_3)_2$

IR Band	Axial N_3	Equitorial N_3	Δ (axial – equatorial)
Calculated, cm^{-1}	2221.20	2196.03	25.17
Experimental, cm^{-1}	2057.7	2032.8	24.9

References:

[1] Dahl, E. W.; Dong, H. T.; Szymczak, N. K. *Chem. Commun.* **2018**, *54*, 892-895.
[2] Tyeklár, Z.; Jacobson, R. R.; Wei, N.; Murthy, N. N.; Zubieta, J.; Karlin, K. D. *J. Am. Chem. Soc.* **1993**, *115*, 2677-2689.
[3] Chuang, C.-L.; dos Santos, O.; Xu, X; Canary, J. W. *Inorg. Chem.* **1997**, *36*, 1967-1972.
[4] Bruker Advanced X-ray Solution, Apex3 v2016.9-0, (2016).
[5] Van der Sluis, P.; Spek, A. L. *Acta Crystallogr., Sect. A.* **1990**, *46*, 194-201.
[6] Bruker Advanced X-ray Solutions, Saint v8.34A, (2014).
[7] Sheldrick, G. M. *Acta Crystallogr., Sect. A.* **2008**, *64*, 112-122.
[8] Murthy, N. N.; Karlin, K. D. *J. Chem. Soc., Chem. Commun.* **1993**, 1236-1238.
[9] Lin, C.-C.; McCrory, C. C. L. *ACS Catal.* **2017**, *7*, 443-451.
[10] McCrory, C. C. L.; Jung, S.; Ferrer, I. M.; Chatman, S. M.; Peter, J. C.; Jaramillo, T. F. *J. Am. Chem. Soc.* **2015**, *137*, 4347-4357.
[11] Gaussian 09, Revision D.01, M. J. Frisch, G. W. Trucks, H. B. Schlegel, G. E. Scuseria, M. A. Robb, J. R. Cheeseman, G. Scalmani, V. Barone, B. Mennucci, G. A. Petersson, H. Nakatsuji, M. Caricato, X. Li, H. P. Hratchian, A. F. Izmaylov, J. Bloino, G. Zheng, J. L. Sonnenberg, M. Hada, M. Ehara, K. Toyota, R. Fukuda, J. Hasegawa, M. Ishida, T. Nakajima, Y. Honda, O. Kitao, H. Nakai, T. Vreven, J. A. Montgomery, Jr., J. E. Peralta, F. Ogliaro, M. Bearpark, J. J. Heyd, E. Brothers, K. N. Kudin, V. N. Staroverov, R. Kobayashi, J. Normand, K. Raghavachari, A. Rendell, J. C. Burant, S. S. Iyengar, J. Tomasi, M. Cossi, N. Rega, J. M. Millam, M. Klene, J. E. Knox, J. B. Cross, V. Bakken, C. Adamo, J. Jaramillo, R. Gomperts, R. E. Stratmann, O. Yazyev, A. J. Austin, R. Cammi, C. Pomelli, J. W. Ochterski, R. L. Martin, K. Morokuma, V. G. Zakrzewski, G. A. Voth, P. Salvador, J. J. Dannenberg, S. Dapprich, A. D. Daniels, Ö. Farkas, J. B. Foresman, J. V. Ortiz, J. Cioslowski, and D. J. Fox, Gaussian, Inc., Wallingford CT, 2009.
[12] Chai, J.-D.; Head-Gordon, M, *Phys. Chem. Chem. Phys.* **2008**, *10*, 6615.
[13] Ditchfield, R; Hehre, W. J.; Pople, J. A. *J. Chem. Phys.* **1971**, *54*, 724.
[14] Weigend, F.; Ahlrichs, R. *Phys. Chem. Chem. Phys.* **2005**, *7*, 3297.